REACTIVE ABSORPTION OF CARBON DIOXIDE INTO PROMOTED POTASSIUM CARBONATE SOLVENTS

HENDY THEE

Submitted in total fulfilment of the requirements of the degree of Doctor of Philosophy.

August 2013

Department of Chemical and Biomolecular Engineering
The University of Melbourne
Australia

DEDICATION

This thesis is dedicated to my parents, Mr. Thee Haryono Kurniawan and Mrs. Ong July.

ABSTRACT

The increase in the carbon dioxide (CO_2) emissions to our atmosphere is the major contributor to global climate change. A number of methods for reducing greenhouse gases have been proposed including carbon capture and sequestration (CCS). To date, reactive absorption of CO_2 into amine solvents is undoubtedly the most widely used technology for CO_2 capture.

Much research has been devoted to developing alternatives to amine solvents. One of the many potential solvent candidates is potassium carbonate (K_2CO_3). Although potassium carbonate is associated with lower cost, less toxicity and is less prone to degradation effects when compared to the current industrial benchmark solvent, monoethanolamine (MEA), it has a low rate of reaction resulting in poor mass transfer performance. Developing a non-toxic and affordable promoter will facilitate the use of potassium carbonate solvent systems for CO_2 capture.

Using a well-characterized wetted wall column (WWC), the reaction kinetics of CO_2 into unpromoted and borate-promoted potassium carbonate (K_2CO_3) solutions have been studied. Results presented here show that, at 80 °C, the addition of small amounts of boric acid (0.2 M, 0.6 M and 1.5 M) accelerates the overall absorption process of CO_2 in carbonate solvents by 3 %, 10 % and 29 % respectively. The Arrhenius expression for the reactions CO_2 + OH^- and CO_2 + $B(OH)_4^-$ are k_{OH} [M^{-1} s^{-1}] = $2.53\times10^{11}\exp(-4311/T\,[K])$ and k_{borate} [M^{-1} s^{-1}] = $5.5\times10^{11}\exp(-6927/T\,[K])$; and the activation energies are 35.8 kJ mol^{-1} and 57.6 kJ mol^{-1} respectively.

The reaction kinetics of CO_2 absorption into a potassium carbonate solution promoted with monoethanolamine (MEA) have also been evaluated under conditions resembling those found at industrial CO_2 capture plants. Results presented here show that at 63 °C the addition of MEA in small quantities, 1.1 M (5 wt%) and 2.2 M (10 wt%), accelerates the overall rate of absorption of CO_2 in a 30 wt% potassium carbonate solvent by a factor of 16 and 45 respectively. The Arrhenius expression for the reaction between CO_2 and MEA is k_{MEA} [M^{-1} s^{-1}] = $4.24\times10^{9}\exp(-3825/T\,[K])$ where the activation energy is

31.8 kJ mol^{-1}. Experimental results have been incorporated into an existing Aspen Plus™ model using the E-NRTL thermodynamic package. The resulting model replicates pilot plant data and simulates industrial capture processes employing K_2CO_3 and MEA as the capture agent.

In addition, the absorption kinetics of carbon dioxide (CO_2) into amino acid promoted potassium carbonate solutions has been studied. Experiments were conducted at concentrations up to 2.0 M and temperatures from 40 – 82 °C. Results presented here show that the addition of 1.0 M glycine, sarcosine and proline accelerates the overall rate of absorption of CO_2 into a 30 wt% K_2CO_3 solvent by a factor of 22, 45 and 14 respectively at 60 °C. The Arrhenius expressions for the reaction between CO_2 and aforementioned amino acids are $k_{2\text{-Gly}}$ [M^{-1} s^{-1}] = $1.22\times10^{12}\exp(-5434/T\ [K])$, $k_{2\text{-Sar}}$ [M^{-1} s^{-1}] = $6.24\times10^{10}\exp(-1699/T\ [K])$ and $k_{2\text{-Pro}}$ [M^{-1} s^{-1}] = $1.02\times10^{11}\exp(-2168/T\ [K])$ where the activation energies are 45.2 kJ mol^{-1}, 14.1 kJ mol^{-1} and 18.0 kJ mol^{-1} respectively. The reaction order with respect to glycine is found to be 1, while the reaction order with respect to sarcosine and proline is observed to be in the range of 1.3 – 1.6 and 1.2 – 1.3 respectively.

The effect of adding small amounts of commercial carbonic anhydrase enzyme, namely Novozymes NS81239, on the absorption of CO_2 into a 30 wt% potassium carbonate has been investigated. Results demonstrated that at 40 °C, the addition of this enzyme (300 mg L^{-1}, 600 mg L^{-1} and 1300 mg L^{-1}) enhances the pseudo-first-order rate constant and thus, the overall absorption process of CO_2 into potassium carbonate solvents by 14 %, 20 % and 34 %. However, a further increase in the concentration to 6600 mg L^{-1} appears to be ineffective as it presents no greater catalytic effect than that from 1300 mg L^{-1} [NCA]. It is also found that at a constant enzyme concentration, the overall absorption of CO_2 into carbonate solvents increases with temperature ranging from 40 °C to 60 °C. Above this range, an increase in temperature proves to be counter-productive.

Results from this study have implications for the operation of carbonate based solvent systems for carbon capture processes, and more specifically will allow more accurate design of absorber units.

DECLARATION

This is to certify that:

i.) the thesis comprises only my original work towards the PhD except where indicated in the acknowledgements.

ii.) due acknowledgement has been made in the text to all other material used.

iii.) the thesis is less than 100,000 words in length, exclusive of tables, graphs, and bibliographies.

Hendy Thee

August 2013.

PUBLICATIONS

JOURNAL PUBLICATIONS

H. Thee, K. Smith, G. da Silva, S.E. Kentish, G.W. Stevens, 2012. Carbon dioxide absorption into unpromoted and borate-catalyzed potassium carbonate solutions. *Chemical Engineering Journal,* vol. 181-182, pp. 694-701. (Section 4.2.3 and Chapter 5)

H. Thee, Y.A. Suryaputradinata, K. Mumford, K. Smith, G. da Silva, S. Kentish, G. Stevens, 2012. A Kinetic and Process Modeling Study of CO_2 Capture with MEA-Promoted Potassium Carbonate Solutions. *Chemical Engineering Journal*, vol. 210, pp. 271-279. (Chapter 6)

H. Thee, N.J. Nicholas, K. Smith, G. da Silva, S. Kentish, G. Stevens, 2014. A kinetic study of CO_2 capture with potassium carbonate solutions promoted with various amino acids: Glycine, sarcosine and proline. *International Journal of Greenhouse Gas Control*, vol. 20, pp. 212-222. (Chapter 7)

D. Guo, H. Thee, G. da Silva, J. Chen, W. Fei, S.E. Kentish, G.W. Stevens, 2011. Borate-Catalyzed Carbon Dioxide Hydration via the Carbonic Anhydrase Mechanism. *Environmental Science and Technology*, vol. 45 (11), pp. 4802-4807.

D. Guo, H. Thee, C.Y. Tan, J. Chen, W. Fei, S.E. Kentish, G.W. Stevens, G. da Silva, 2013. Amino Acids as Carbon Capture Solvents: Chemical Kinetics and Mechanism of the Glycine + CO_2 Reaction, *Energy & Fuels*, vol. 27 (7), pp. 3898-3904.

CONFERENCE PUBLICATIONS

H. Thee, K. Smith, G. da Silva, S.E. Kentish, G.W. Stevens, 2010. CO_2 Absorption by Borate-Promoted Potassium Carbonate under Pre-Combustion CO_2 Capture Conditions. *Poster presented at the Australian Institute of Energy - Melbourne Branch Postgraduate Student Energy Awards*, Melbourne, Australia, 6-7 October.

H. Thee, K. Smith, G. da Silva, S.E. Kentish, G.W. Stevens, 2010. CO_2 Absorption by Borate-Promoted Potassium Carbonate under Pre-Combustion CO_2 Capture Conditions. *Poster presented at the CO2CRC Research Symposium*, Melbourne, Australia, 1-3 December 2010.

K. Mumford, K. Smith, S. Shen, C. Anderson, Y.A. Suryaputradinata, W. Tao, K. Endo, H. Thee, S.E. Kentish, G.W. Stevens, 2010. Results from the Solvent Pilot Plant for Post-Combustion Capture at Hazelwood Power Station. *Oral presentation given at the CO2CRC Research Symposium 2010*, Melbourne, Australia, 1-3 December.

C. Anderson, K. Smith, K. Mumford, K. Endo, W. Tao, H. Thee, Y.A. Suryaputradinata, A. Qader, S.E. Kentish, G.W. Stevens, 2010. Results from the Solvent Pilot Plant for Pre-Combustion Capture. *Oral presentation given at the CO2CRC Research Symposium*, Melbourne, Australia, 1-3 December.

H. Thee, K. Smith, G. da Silva, S.E. Kentish, G.W. Stevens, 2011. CO_2 Absorption into Promoted Potassium Carbonate Solvents. *Oral presentation given at the Clean Energy and Global Change for the Future*, Tsinghua University, Beijing, China, 12-14 October.

H. Thee, K. Smith, G. da Silva, S.E. Kentish, G.W. Stevens, 2011. Making Carbon Capture Cheap and Environmentally Friendly. *Poster presented at the Clean Energy and Global Change for the Future*, Tsinghua University, Beijing, China, 12-14 October.

H. Thee, K. Smith, C.Y. Tan, G. da Silva, S.E. Kentish, G.W. Stevens, 2011. Enhancing the performance of potassium carbonate solvent for CO_2 absorption using rate promoters. *Poster presented at the CO2CRC Research Symposium 2011*, Adelaide, South Australia, 29 November - 1 December.

H. Thee, G. da Silva, S.E. Kentish, G.W. Stevens, 2012. A Kinetic and Process Modeling Study of CO_2 Capture with MEA-Promoted Potassium Carbonate Solutions. *Poster Presented at the AIE - Postgraduate Student Energy Awards*, 10-11 October.

K. Mumford, J. Gouw, I. Indrawan, A. Rabindran, H. Thee, G. da Silva, D. Quyn, G.W. Stevens, 2012. Development of novel solvent systems. *Poster presented at the CO2CRC Research Symposium 2012*, 25-31 November.

H. Thee, N. Nicholas, G. da Silva, S.E. Kentish, G.W. Stevens, 2012. Enhancing the performance of potassium carbonate solvents for CO_2 absorption using rate promoters. *Poster presented at the CO2CRC Research Symposium 2012*, Coolum, Queensland, 27-29 November.

ACKNOWLEDGEMENTS

I would firstly like to express my gratitude to my supervisors, Professor Geoff Stevens, Professor Sandra Kentish and Dr. Gabriel da Silva for their support, guidance and teaching. Their great expertise, wide knowledge in research and engineering fields and time for discussion have made a significant contribution to the completion of this thesis. Their patience and faith in me throughout the duration of my doctorate study are greatly appreciated.

I would like to thank the Cooperative Research Centre for Greenhouse Gas Technologies (CO2CRC) and Particulate Fluids Processing Centre (PFPC) for giving me the opportunity and funding to complete my PhD study.

I would like to acknowledge Dr Kathryn Smith's teaching, encouragement, support, and time to review my publications throughout the duration of my PhD and Dr. Ujjal Ghosh's teaching in the early stages of my PhD candidature. The work of my research project student, Benedikt Bauer, has contributed to the success of the thesis' experimental validation. Thanks to Dr. Michael Simioni and Dr. Colin Scholes for organizing all the coffee breaks on Fridays, your good humour and witty jokes surely helped vent out the stress from works and are much appreciated.

I would like to thank Kevin Smeaton and Justin Fox from the Engineering Workshop for helping me to design, build, maintain and repair my experimental equipment.

I would like to thank my colleagues, Yohanes Adi Suryaputradinata, Adrian Widjaya, Dr. Kohei Endo, Dr. Nathan Nicholas, Dr. George Chen, Wendy Tao, Alita Aguiar, Dr Andrew Lee, Dr. Kathryn Mumford, Hirra Azher, Andri Halim, Dr Guo, Indrawan, Jeffrey Guow, Josephine Lim and many others whose companionship made my PhD life much more enjoyable.

I would like to thank my wife, Amanda Bunjamin, for her support and never-ending faith in my ability to complete my PhD.

No words can describe how grateful I am to my late parents, Mr. Thee Haryono Kurniawan and Mrs. Ong July, for their love, patience and kindness towards me, and for the financial support invested in me. I am eternally thankful to them.

TABLE OF CONTENTS

LIST OF FIGURES

LIST OF TABLES

CHAPTER 1 - INTRODUCTION

Emission and Remediation of Greenhouse Gases

It has become apparent that the release of carbon dioxide (CO_2) into the atmosphere traps heat emitted from the sun. The more CO_2 there is, the hotter and wetter the earth's climate becomes. Observations suggest that the atmospheric concentration of carbon dioxide has been escalating over the past century when compared to the steady level of the 18th century, before the industrial revolution. The 2005 concentration of CO_2 was reported at 379 parts per million (ppm), while more recent (2013) measurements at a US government agency lab in Hawaii showed that the concentration has topped 400 ppm for the first time since three to five million years ago - before modern humans existed. This was 43% higher than that of the pre-industrial era [1]. Consequently, the average land surface temperature was reported to have increased by 0.4 - 0.6 °C in the last century, while the mean global temperature is now increasing at an unprecedented rate [2]. This is almost entirely caused by the emissions of man-made greenhouse gases for which fossil fuels contribute over three quarters of the total emissions [3].

The use of energy was reported to be the largest source of greenhouse gas emission amongst other anthropogenic sources [1]. As represented in Figure 1-1, energy is responsible for over 80% of the manmade greenhouse gases in Annex-1 or industrialized countries including Australia, New Zealand, Canada, France, Germany, United Kingdom, United States and others as listed in a report by International Energy Agency (IEA) [1]. Agriculture has a smaller contribution, generating mostly CH_4 and N_2O from livestock and rice cultivation, while industrial processes unrelated to energy have approximately the same contribution as agriculture, producing mainly N_2O and fluorinated gases [1].

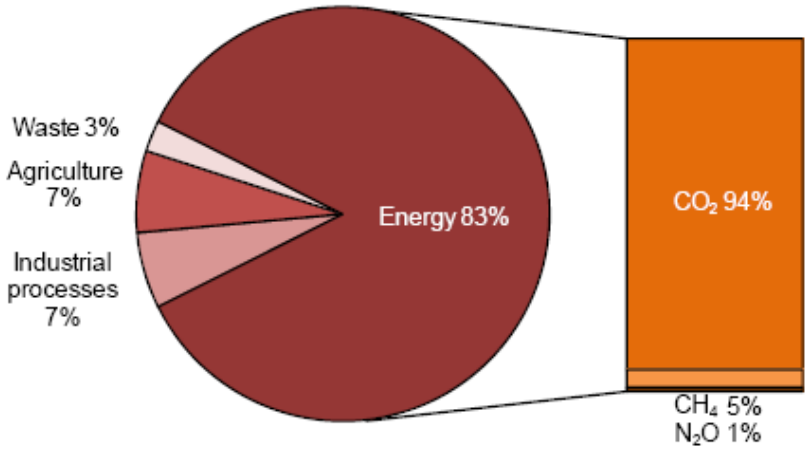

Figure 1-1 Shares of anthropogenic greenhouse gas emissions in Annex-1 or industrialized countries in 2006. Reprinted from [1].

The direct combustions of both fossil and non-fossil fuels dominate the energy sector. As depicted in Figure 1-2, global total energy supply (TPES) had more than a twofold increase between 1971 and 2007. Although the use of non-fossil fuel energy has slightly increased, fossil fuels have been the major source of energy supply over the past 35 years. In 2007, fossil fuels contributed approximately 82% of the global TPES.

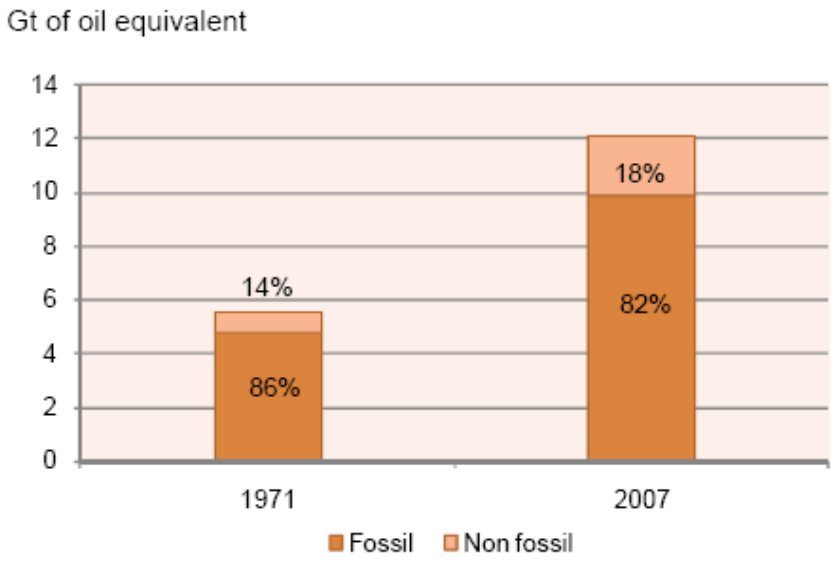

Figure 1-2 World primary energy supply. Reprinted from [1].

Much relying on fossil fuels, the increasing world energy demand is obviously a key factor in the observed upward trends in the world's carbon dioxide emissions. As seen in Figure 1-3, annual carbon dioxide emissions from fuel combustion have been increasing significantly from near zero before the industrial revolution in 1870's to 29 $GtCO_2$ in 2007.

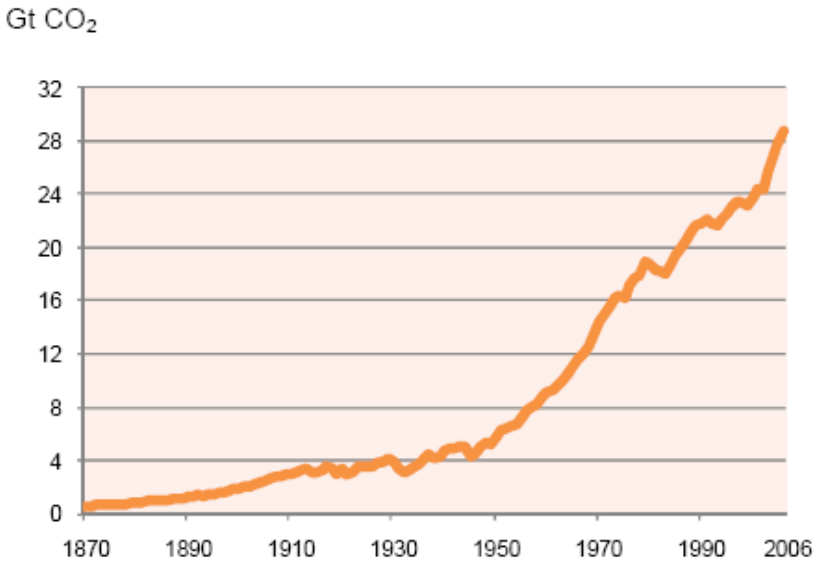

Figure 1-3 CO_2 emissions from fossil fuel combustion. Reprinted from [1].

The World Energy Outlook projects that world energy supply will rise by 40% between 2007 and 2030 [4]. With fossil fuels remaining at around 80%, carbon dioxide emissions from both fossil and non-fossil fuel combustion are consequently expected to continue their growth reaching 40.2 $GtCO_2$ by 2030. Such a trend is in accordance with the worst case scenario presented in the IPCC report, which forecasts the earth's average temperature to increase between 2.4 and 6.4 °C by 2100 [5].

Statistically, coal has been a major source of electricity in comparison to other fossil fuel sources [6]. Coal combustion is a well developed technology to produce electricity. As of 2005, it was responsible for up to 90% of the power generated in Australia [7]. The availability of coal as a natural resource is abundant. This makes coal an affordable and reliable source of energy. As depicted in Figure 1-4, the use of coal as an energy source has been increasing

since 1950. It is evident that coal has been and will continue to be one of the major sources of fuel for electricity generation.

In comparing coal to natural gas and petroleum, IEA suggested that natural gas-fired plants are the most efficient (55-60%) and have the lowest carbon dioxide emission, producing 0.45 kg CO_2/kWh [8]. On the other hand, petroleum fuels produce 0.80 kg CO_2/kWh. Coal-fired power plants generate the most carbon dioxide, approximately 0.96 kg CO_2/kWh, and are only 40-50% efficient.

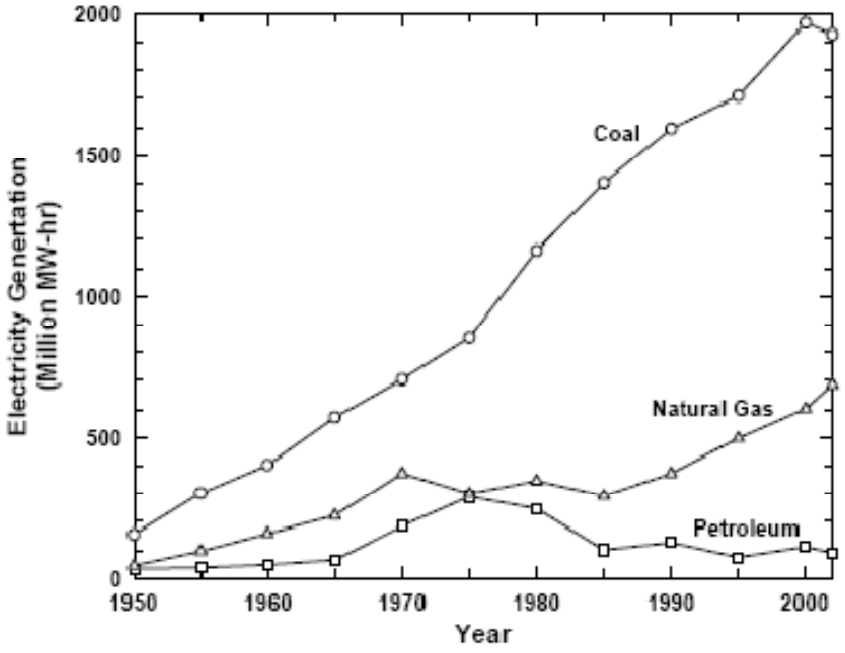

Figure 1-4 Electricity generation from fossil fuels from 1950 to 2002. Reprinted from [6].

It is obvious that the application for carbon dioxide capture and storage (CCS) should be targeted to coal-fired power plants. Developing an affordable capture technology for coal-fired power plants is critical for the reduction in world's CO_2 emissions. Thus, this thesis focuses on the application of carbon capture targeted to conditions seen at coal-fired power plants.

Carbon Capture and Storage (CCS)

A number of technologies have been developed for carbon dioxide removal from flue gases. These technologies include membranes, adsorption, cryogenics, and absorption into a chemical solvent [2]. Despite the small footprint membrane technology has offered, high selectivity combined with high throughput of CO_2 is principally difficult to achieve, particularly at an industrial scale of CO_2 capture from coal-fired power plants. Similarly, the main drawback of the adsorption process is that it has a poor CO_2 capacity and CO_2 selectivity. Cryogenic separation necessitates a process for water removal and a large amount of energy is required for refrigeration, which often makes this process prohibitive due to high costs. So far, CO_2 capture by a solvent absorption process provides the most mature and economical option for separating CO_2 from bulk gas streams [8].

As shown in Figure 1-5, these CO_2 capture processes can be integrated into industrial processes and fossil fuel energy sectors as follows: pre-combustion, post-combustion, and oxyfuel.

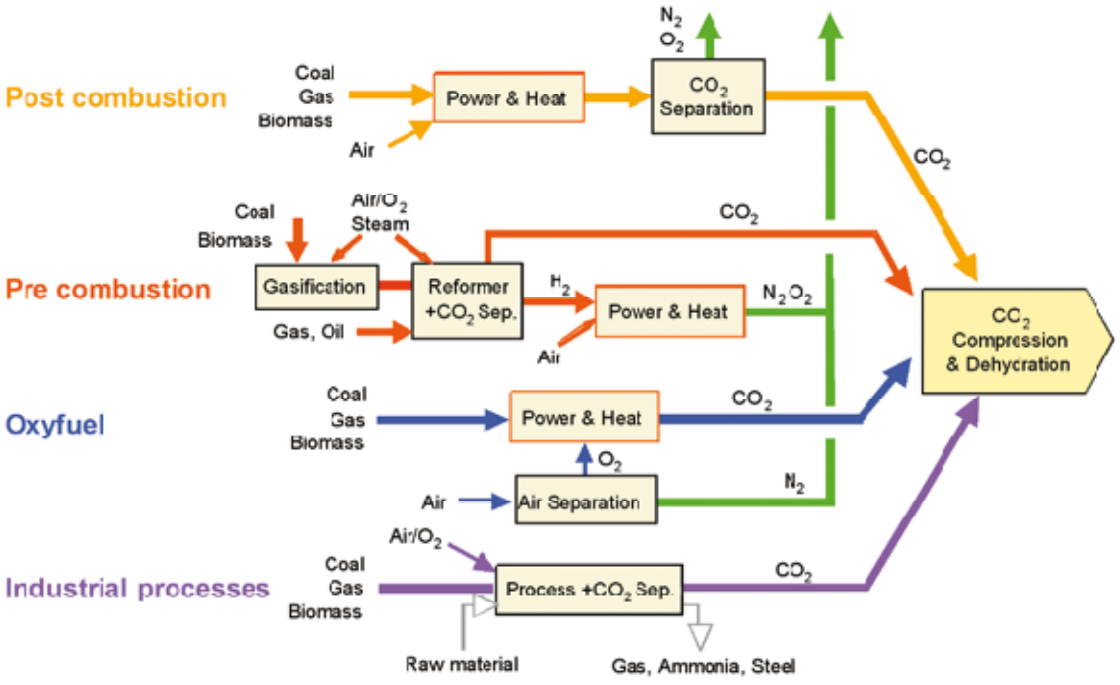

Figure 1-5 Carbon dioxide capture systems. Taken from [2].

Post combustion capture processes are usually retrofitted to the existing infrastructure. On the other hand, pre-combustion capture processes generate a syngas from which CO_2 can be removed before further processing for liquid fuel production or electricity generation. Oxyfuel is a rather new process in which the need for CO_2 separation is eliminated although it requires an oxygen/nitrogen separation which is usually more expensive due to the similarity of oxygen and nitrogen chemical properties.

There are several industrial applications involving process streams where the opportunity to capture CO_2 can be exploited. These processes include steel production, natural gas sweetening, cement production, and ammonia production. Due to the scope of this project, industrial processes will not be discussed any further, but they are seen as a potential for further study.

It is important to note that a significant cost will be associated with the transportation and storage of CO_2 following the removal of carbon dioxide from flue gases. Due to the scope of this project, this thesis will focus only on the capture process of CO_2 using solvent absorption technology.

CHAPTER 2 - LITERATURE REVIEW

2.1 Overview of Solvent Technology

2.1.1 Absorber and Desorber Configuration

The basic principle behind solvent absorption is the transfer of a gas such as carbon dioxide (CO_2) from the waste gas stream to a liquid solvent in a gas-liquid contactor known as an absorber. The loaded solvent is then regenerated in a similar contactor known as a desorber or regenerator.

Figure 2-1 shows a basic configuration of a solvent absorption system for CO_2 capture. The CO_2 is removed from the flue gas and the treated flue gas leaves from the top of the absorber. A CO_2-lean solvent enters the top of the absorber allowing a counter-current contact with the flue gas in the absorber which is normally a packed column. The rich solvent exits from the base of the absorber where it flows to a heater, which pre-heats the solvent before entering the absorber. The rich solvent is then pumped to the top of the desorber or regenerator which is also typically a packed column. A high temperature as well as a low pressure is applied as a driving force for the release of CO_2 from the solvent. This cycling process ensures the conservation of the solvent.

Various conditions are encountered in CO_2 removal process and specific to the application of the process. These conditions are tabulated and shown in Table 2-1 [9]. Concentrated CO_2 streams and high total pressures are generally encountered in natural gas treating and ammonia syngas processing. The inlet concentrations of carbon dioxide are normally in the range of 2 - 3 vol% for natural gas treating process and 10 - 15 vol% for coal-fired power plants, while the inlet pressure is approximately atmospheric for both. Outlet CO_2 concentrations of the treated gas are specific to the process requirements. However, the treating should target at least 90% CO_2 removal and 95% purity [10].

While this work mainly focuses on reactive absorption processes in alkaline solution, both reactive absorption in alkaline solution and absorption in a physical solvent are suitable process techniques for treating gas streams containing acid gases such as carbon dioxide and hydrogen sulfide. However, it is important to note that physical absorption processes are economically

feasible only when the acid gas partial pressure is high (> 14 bar) as the capacity of physical solvents is a function of partial pressure. Physical solvents physically dissolve acid gases without any chemical reaction. These gases are then released without the application of heat instead by reducing the pressure. Conversely, a reactive absorption requires the presence of chemical reaction in the solution which has the effect of enhancing the liquid phase mass transfer. In reactive absorption, stripping occurs by reversing this chemical reaction, typically through the application of heat.

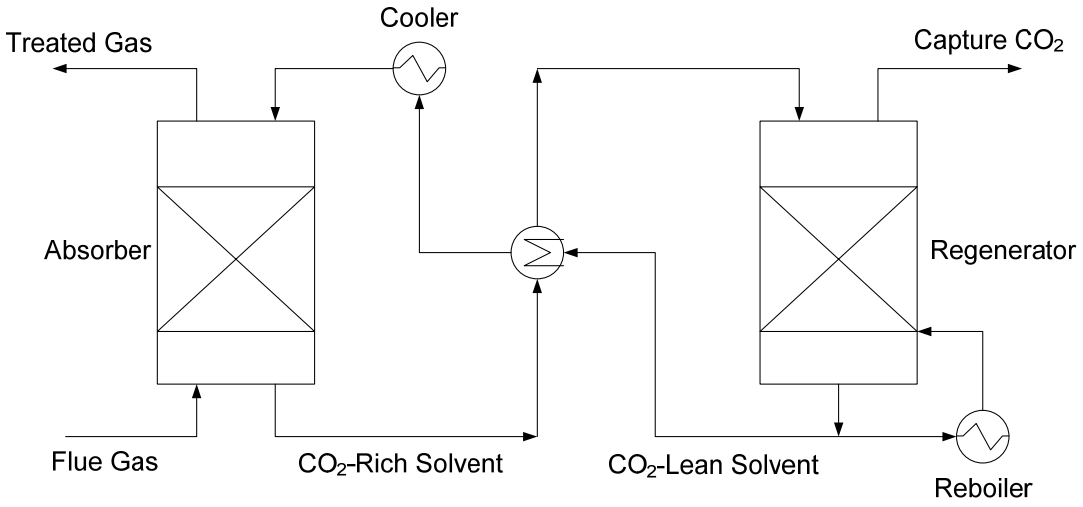

Figure 2-1 Basic configuration of a solvent absorption system for CO_2 capture.

Table 2-1 CO_2 capture process conditions normally encountered in the absorber [9].

Process	**Inlet CO_2 (vol%)**	**Outlet CO_2 (vol%)**	**P_{TOT} (atm)**
Natural gas treatment	0 - 50	1 - 2	10 - 70
Ammonia	17 - 19	0.01 - 0.2	30
Coal power plant	10 - 15	1 - 1.5	1 - 1.3
Natural gas power plant	2 - 3	0.2 - 0.3	1 - 1.3

2.1.2 Solvent Screening based on Cost

CCS has been proposed as a solution that justifies not only immediate reduction in carbon dioxide emissions but also the world's need for cheap and reliable sources of energy. However, the cost for implementing CCS technology

is still prohibitive. Past studies estimate that the integration of CO_2 capture increases the wholesale price of electricity generation from coal-fired power plants by up to 80% [11]. Each element of this cost must be well comprehended and reduced in order to implement CCS technology.

It has been reported that the capture and compression cost alone contributes up to 80% of the total CCS cost with the remaining cost due to sequestration and transportation [12]. This estimation is based on the cost of CO_2 capture using an industrial benchmark solvent, a 30 wt% monoethanolamine (MEA) solvent. However, the overall cost varies depending on many factors such as: site specifications, quality of the waste gas, and technology utilized. It becomes self-explanatory that the greatest opportunity for reducing both capital and operating costs associated with CCS technology is associated with improving the capture process.

Almost half of the cost of CO_2 capture is associated with solvent regeneration [12]. The regeneration energy is often determined by the solvent characteristics such as: CO_2 loading capacity, heat of absorption and rate of absorption.

The CO_2 loading capacity is a measure of the amount of CO_2 that can be absorbed per unit of solvent. The loading capacity is related to the vapour-liquid equilibrium characteristics of the solvent. An increase in solvent capacity leads to more CO_2 being absorbed and desorbed for the same amount of solvent. This subsequently leads to a more efficient process.

A past study by Oyenaken and Rochelle [27] shows that the heat of absorption plays an equally important role to that of the solvent capacity in determining the regeneration energy. At a fixed solvent capacity, solvents with a higher heat of absorption demand less energy to regenerate. Similarly, at a fixed heat of absorption, solvents with a higher capacity require less energy.

The rate of absorption is another key factor in determining both capital and operating costs of the capture process. A faster rate of absorption leads to a reduced column height, saving capital costs associated with building of the contactor. Additionally, the absorber can be operated closer to equilibrium resulting in more efficient process. Depending on the chemistry of reactive

absorption, an improved heat of desorption can lead to a decrease in the rate of absorption.

A solvent with these attributes can result in significant reduction in operating and capital cost of carbon capture process. In addition to being environmentally benign, the screening of the potential solvents must be based upon the aforementioned properties.

2.1.3 Mass Transfer of Fast Chemical Reaction

The analysis of mass transfer in this study is based on the assumption that the gas, such as CO_2, is soluble in the liquid but any reactants or products present in the solvent will not enter the gas. Flux, N_{CO2} [mol m^{-2} s^{-1}], can be calculated as follows:

$$N_{\mathrm{CO_2}} = -D_{\mathrm{CO_2}} \frac{\partial[\mathrm{CO_2}]}{\partial x}$$

Equation 2-1

As depicted in Figure 2-2, mass transfer coefficients are a proportionality of flux to a concentration driving force across gas and liquid films and can consequently be defined as:

$$N_{\mathrm{CO_2}} = \begin{cases} K_{\mathrm{G}}\left(P_{\mathrm{CO_2}} - P^*_{\mathrm{CO_2}}\right) \\ k_{\mathrm{g}}\left(P_{\mathrm{CO_2}} - P_{\mathrm{CO_2},i}\right) \\ k_{\mathrm{l}}^{\circ}\left([\mathrm{CO_2}]_i - [\mathrm{CO_2}]_b\right) \text{ or } \dfrac{k_{\mathrm{l}}^{\circ}}{H}\left(P_{\mathrm{CO_2},i} - P^*_{\mathrm{CO_2}}\right) \end{cases}$$

Equation 2-2

K_{G} [mol Pa^{-1} m^{-2} s^{-1}] is the overall gas phase mass transfer coefficient, k_{g} [mol Pa^{-1} m^{-2} s^{-1}] is the gas film mass transfer coefficient, and k_{l}° [m s^{-1}] represents the liquid mass transfer coefficient. $P_{\mathrm{CO_2}}$ [Pa] is the average bulk partial pressure, $P^*_{CO_2}$ [Pa] is the equilibrium partial pressure of CO_2, and $P_{\mathrm{CO_2,i}}$ [Pa] is the partial pressure of CO_2 at the gas-liquid interface. H [Pa m^3 mol^{-1}] represents the Henry's Law constant of CO_2 in the solvent.

In addition, Equation 2-1 shows that mass transfer coefficients are functions of the diffusivities of CO_2 in the solvent, D_{CO_2} [m^2 s^{-1}].

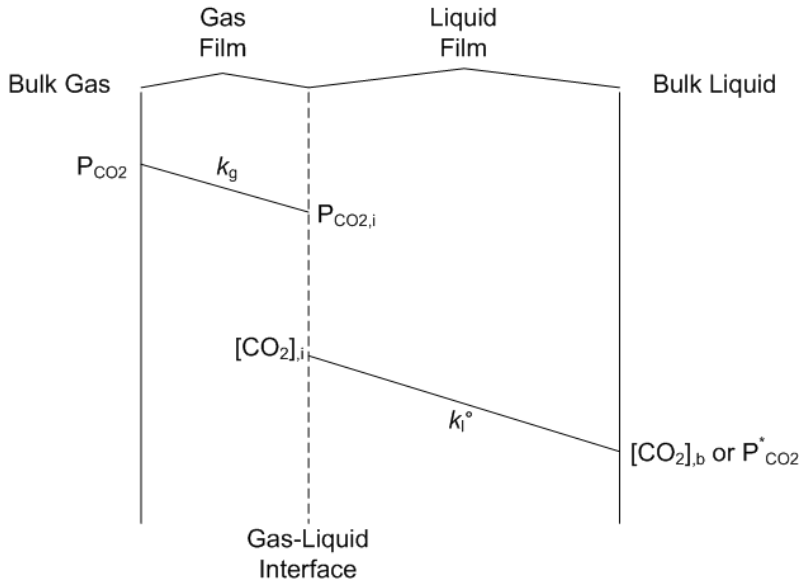

Figure 2-2 Physical mass transfer of CO_2 from bulk gas to bulk liquid. Adapted from [13].

In a non-reactive gas liquid system, the overall mass transfer coefficient consists of two resistances in series: the gas film and the liquid film. Thus, the overall resistance is the sum of the gas resistance and the liquid film resistance, as shown in the following equation:

$$\frac{1}{K_G} = \frac{1}{k_g} + \frac{H}{k_l^\circ}$$

Equation 2-3

The addition of chemical reaction leads to an increase in the rate of absorption and lowers the equilibrium partial pressure. This analysis considers the second order reaction shown in Equation 2-4. The rate of reaction r_{CO2} ($d[CO_2]/dt$) [mol s^{-1}] is given by Equation 2-5 (NB: in this work all species are aqueous unless otherwise stated).

$$CO_2 + OH^- \leftrightarrow HCO_3^-$$

Equation 2-4

$$r_{CO2} = -k_{OH}[CO_2][OH^-]$$

Equation 2-5

With chemical reactions occurring in the liquid, there are three factors to consider: what happens in the gas film, in the liquid film and in the body of the liquid. Figure 2-3 [13] illustrates simultaneous mass transfer with chemical reactions; with subscript 'A' being the CO_2 species while subscript 'B' being the OH^- species.

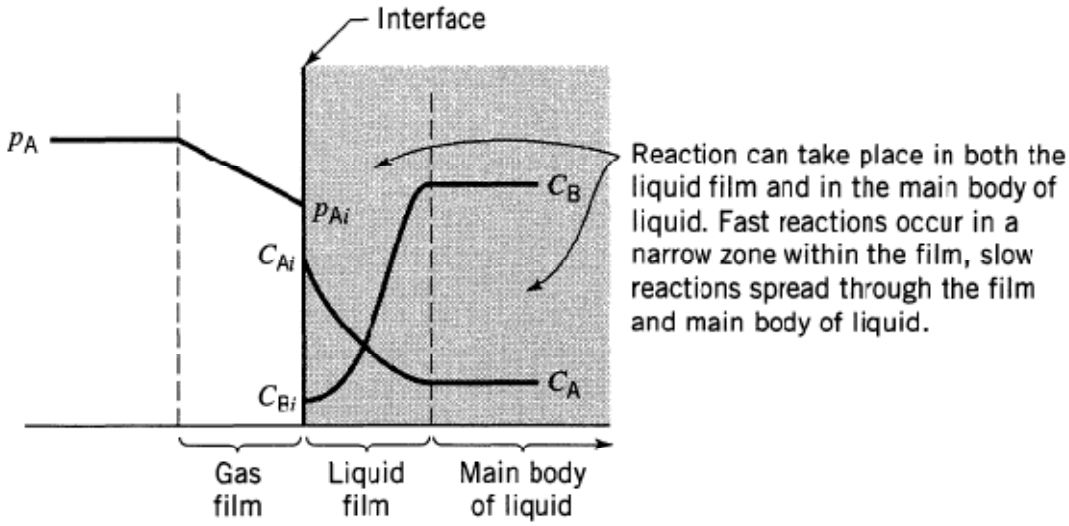

Figure 2-3 Mass transfer with chemical reactions. Taken from [13].

This increase in the absorption rate due to chemical reaction is often described using an enhancement factor, *E*. The value of *E* is always greater than or equal to one. Levenspiel [13] formulated a general rate equation with chemical reactions as follows:

$$N_{CO_2} = \frac{1}{\frac{1}{k_g} + \frac{H}{k_1^{\circ} E}} (P_{CO_2} - P_{CO_2}^{*})$$

Equation 2-6

The enhancement factor, which accounts for the reaction of CO_2, is defined as the ratio of flux of CO_2 with chemical reaction to the flux of CO_2 by physical absorption. Figure 2-4 shows that E is dependent on two quantities; the enhancement factor for an infinitely fast reaction, E_i and the Hatta number, M_H. The Hatta number is a dimensionless number that compares the rate of absorption of solute (*i.e.* CO_2) in a reactive system to the rate of absorption of the same solute in the case of physical absorption. The Hatta number is actually the criterion for whether the reaction occurs completely in the liquid bulk or completely in the liquid film. Generally, at increasing values of the Hatta number, the chemical reaction is approaching the gas-liquid interface and the enhancement factor is limited by the value given by E_i.

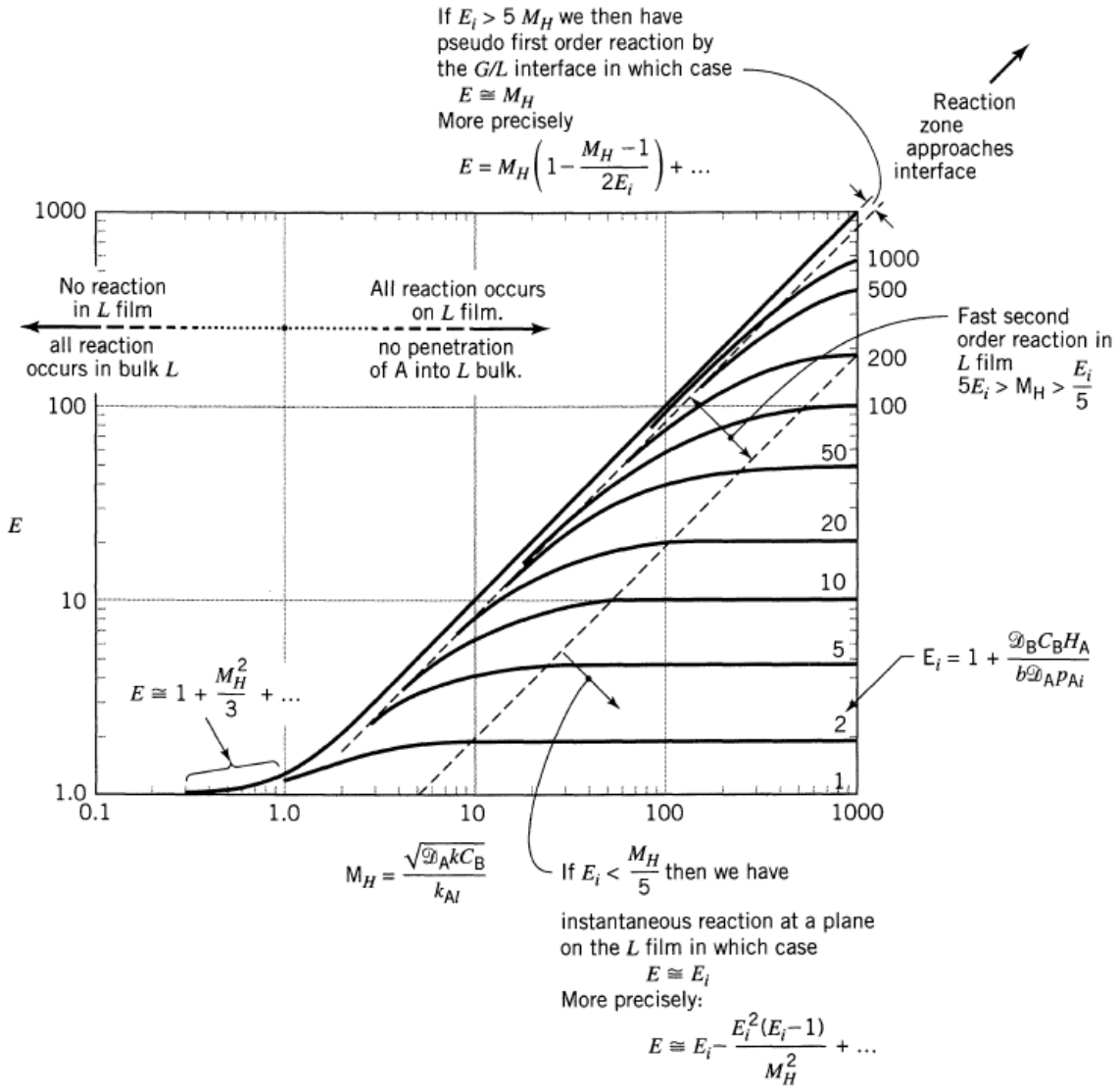

Figure 2-4 Enhancement factor for fluid-fluid reactions as a function of M_H and E_i. Taken from [13].

The reaction of CO_2 with hydroxide ions is regarded as a fast but not 'instantaneous' reaction and the reactant, [OH^-], present in the liquid is in excess. As depicted in Figure 2-5, most species 'A' or aqueous CO_2 reacts with reactant 'B' or OH^- ions in a thin layer near the gas-liquid interface.

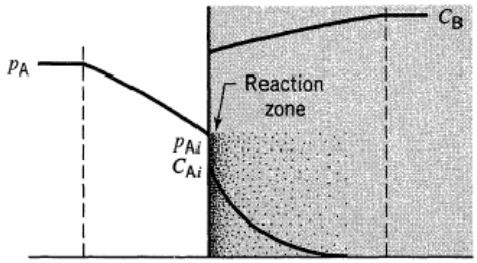

Figure 2-5 Fast chemical reaction with an excessive concentration of reactant 'B' or OH^- and a limited concentration of species 'A' or CO_2 in this case. Taken from [13].

When the concentration of OH^- does not drop appreciably within the film, it can be regarded as constant throughout, and the second order reaction simplifies to the more easily solved pseudo first order rate expression. Danckwerts [14] also showed that for some gas-liquid systems a surface renewal model was better than the model described in Equation 2-6. Danckwerts [14] also assumed that the gas mass transfer resistance could be neglected. The term P_{CO2}^* in Equation 2-6 is also often neglected as experiments are done at high partial pressures of CO_2 (*i.e.* $P_{CO2} >> P_{CO2}^*$). In this case, the rate of absorption of CO_2, R (mol s^{-1}), can be given by [14]:

$$\left(\frac{R}{m_{CO2}c_{CO2}V_l}\right)^2 = (k_l^o a)^2 + k_1 D_{CO2} a^2$$

Equation 2-7

Where m_{CO2} is the ratio of solubility in the liquid phase and in the gas phase, C_{CO2} is the concentration in the gas phase and V_l is the liquid phase volume. The pseudo first order rate coefficient is k_1 while a is the interfacial area in m^2/m^3.

Manipulation of this expression leads to:

$$N_{CO_2} = \frac{\sqrt{\left(k_l^\circ\right)^2 + D_{CO2}k_1}}{H} P_{CO_2}$$

Equation 2-8

where N_{co2} is the molar flux in mol m^{-2} s^{-1}. For simple reaction with a base, OH^-, the pseudo first order rate constant k_1 (s^{-1}) is defined as:

$$k_1 = k_{OH}[OH^-]$$

Equation 2-9

The addition of a promoter will increase the apparent rate of reaction, and assuming a second order reaction between CO_2 and promoter, Equation 2-9 becomes:

$$k_1 = k_{OH}[OH^-] + k_{Prom}[Prom]$$

Equation 2-10

2.2 Solvents for CO_2 Absorption

2.2.1 Alkanolamine Solvents

The most commonly used solvents for CO_2 capture are amine solvents [16]. The variety of amine solvents is effectively endless, but some of the more commonly used amines are outlined in Table 2-2.

Table 2-2 Common amines used in gas treating process [9].

Class	Name	Structure
Primary Amine	Monoethanolamine (MEA)	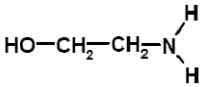
	Diglycolamine (DGA)	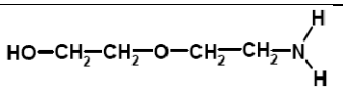
Secondary Amine	Diethanolamine (DEA)	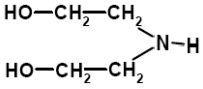
	Diisopropanolamine (DIPA)	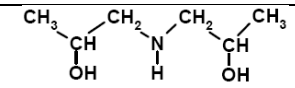
Tertiary Amine	Triethanolamine (TEA)	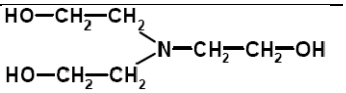
	N-methyldiethanolamine (MDEA)	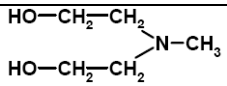
Hindered Amine	2-amino-2-methyl-1-propanol (AMP)	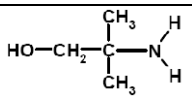

Primary and Secondary Amines

The capacity for amine solvents to react with carbon dioxide is due to the reactivity of the amine group. As shown in Equation 2-11 and Equation 2-12, the reaction of CO_2 with primary or secondary amines generates an amine carbamate via an exothermic pathway. Caplow [17] suggested a reaction mechanism for carbamate formation through a zwitterionic intermediate, a net-neutral molecule with localized positive and negative electrical charges. This zwitterion mechanism is a two-step process in which the CO_2 reacts with the amine to form an intermediate followed by a proton removal by bases (H_2O, OH^- or the amine itself) present in the solution. It is important to note that when the base (B) is dominated by amine itself, the loading capacity is limited to 0.5 mol CO_2 per mol of amine.

$$CO_2 + NHR_1R_2 \underset{k_r}{\overset{k_f}{\rightleftharpoons}} {}^{+}NHR_1R_2COO^{-}$$

Equation 2-11

$$^{+}NHR_1R_2COO^{-} + B \xrightarrow{k_b} NR_1R_2COO^{-} + BH^{+}$$

Equation 2-12

Based on Equation 2-11, the rate of reaction of CO_2 can be described as:

$$r_{CO_2} = -k_f[CO_2][\text{Amine}] + k_r[\text{zwitterion}]$$

Equation 2-13

The change in concentration of zwitterion (Equation 2-11 and Equation 2-12) can be described as:

$$-\frac{d[\text{zwitterion}]}{dt} = k_f[CO_2][\text{Amine}] - k_r[\text{zwitterion}] - \sum k_b[B][\text{zwitterion}]$$

Equation 2-14

Assuming quasi pseudo state conditions for the concentration of the zwitterion, Equation 2-13 becomes [18]:

$$r_{CO_2} = -\sum k_b[B][\text{zwitterion}]$$

Equation 2-15

And manipulation of Equation 2-14 gives:

$$[\text{zwitterion}] = \frac{k_f[CO_2][\text{Amine}]}{k_r + \sum k_b[B]}$$

Equation 2-16

Substituting Equation 2-16 into Equation 2-15, the rate of reaction of CO_2 can be expressed as follows:

$$r_{CO_2} = -\frac{k_f[CO_2][\text{Amine}]}{1 + \frac{k_r}{\sum k_b[B]}}$$

Equation 2-17

Past studies indicate that the reaction of CO_2 with primary amines is often first order with respect to the concentration of the amine [9, 19-22]. This suggests that the rate limiting step is the zwitterion formation (Equation 2-11) such that $1 >> k_r/\sum k_b[B]$ and thus, Equation 2-17 reduces to a simple second order kinetic relationship as follows:

$$r_{CO_2} = -k_f[CO_2][\text{Amine}]$$

Equation 2-18

Alternatively, if it is assumed that the proton removal by a base is rate limiting, such that $1 << k_r/\sum k_b[B]$, Equation 2-17 reduces to:

$$r_{CO_2} = -\sum k_b \frac{k_f}{k_r}[CO_2][\text{Amine}][B]$$

Equation 2-19

The standard absorption process commonly considered for a post-combustion CO_2 capture process uses a 30 wt% or 7 M aqueous solution of MEA. The availability of a lone pair of electrons in the basic amine group of an MEA molecule makes it very reactive towards carbon dioxide. As shown in Equation 2-11 and Equation 2-12, a MEA molecule reacts with carbon dioxide to form an amine carbamate and a proton. At 50 °C, this reaction proceeds very efficiently releasing a heat load of approximately 72 kJ per mole of CO_2 absorbed (30 wt% MEA) [23].

The solvent is regenerated by heating the loaded solution to around 120 °C. A thermal energy of 165 kJ per mol of CO_2 desorbed is required for the regeneration [24]. A significant increase in the thermal energy is required for the desorption of CO_2, when compared to the exothermic heat of absorption, due to the extra energy required to heat water sensibly to approximately 120 °C and to generate steam to drive desorption.

To increase reaction rates, researchers have looked into the use of MEA solvents combined with the use tertiary alkanolamine solvents such as MDEA

[25], cyclic diamines such as piperazine (PZ), sterically hindered amines like AMP [23] and blends of various alkanolamines [26]. Table 2-3 shows some past studies in which MEA-promoted systems have been investigated.

Table 2-3 Typical experimental conditions in which the use of MEA has been studied [24].

Solvent	**Concentration of Solvent (MEA Concentration)**	**Temperature range**	**Reference**
MDEA	27 wt% (3 wt%) 25 wt% (5 wt%) 23 wt% (7 wt%)	25-60 °C	[25]
PZ	2.0 M (30 wt%)	96 °C	[27]
TEA	0.1-0.5 M (0.1-0.5 M)	30-40 °C	[28]

Carbon dioxide absorption using primary and secondary amines may encounter many operational issues including high energy consumption. One of the main challenges with the use of amine solvents is its susceptibility to oxidative degradation due to exposure of the solvent to oxygen found in most flue gas streams. Researchers [29] found that primary amines such as MEA degrade faster than their secondary and tertiary counterparts such as DEA and MDEA.

Degradation products of amine solvents include glycine, ammonia, carboxylic acids, pyridines, amines, substituted amides, substituted alkanols, substituted alkanones, substituted azetidines, substituted aldehydes and polymers of high molecular weight [24, 30]. Formic acid and 2-butanamine [31] are among the most concerning toxic by-products which prompt the use of alternative solvents. The formation of degradation products also results in reduced solvent capacity and thus, the overall plant efficiency. Indeed, it has been found that the use of MEA for a carbon capture process from coal-fired power plants could lead to an increase of human toxicity (an index that reflects the potential harm of a unit of chemical released to the environment and is often used in life cycle analysis) potential of more than 150% [32].

Tertiary Amines

Equation 2-20 describes a single step reaction mechanism of tertiary amines with CO_2. This reaction generates a protonated amine and bicarbonate ion instead of an amine carbamate as observed in the reaction of primary and secondary amines with CO_2. Although the absorption rate is slower and consumes water, this reaction results in high CO_2 loading capacity and has low heat of absorption [33].

$$CO_2 + NR_1R_2R_3 + H_2O \leftrightarrow {}^{+}NHR_1R_2R_3 + HCO_3^{-}$$

Equation 2-20

The rate of this reaction can be expressed as a second order reaction shown in Equation 2-18.

TEA and MDEA have been studied for removal of acidic gases such as CO_2 and H_2S. As tertiary amines lack the N-H bond required to form a carbamate, this reduces the reaction rate by encouraging CO_2 hydrolysis to form bicarbonate and a protonated amine.

Unlike primary and secondary amines (see Equation 2-11 and Equation 2-12), tertiary amines are not limited to a solvent loading of 0.5 mole CO_2 per mole of amine. These solvents readily approach a maximum loading of 1 mole CO_2 per mole of amine, significantly increasing the solvent capacity [25].

Investigations of MDEA and TEA kinetics includes work that has been performed by Blauwhoff *et al.* [34], Versteeg and van Swaaij [33], Rinker *et al.* [35], Sada *et al.* [36], Donaldson and Nguyen [37], Crooks and Donnellan [38], and Littel *et al.* [39]. At room temperature, the average second-order rate constant is 4 M^{-1} s^{-1} for MDEA and 2 M^{-1} s^{-1} for TEA. In comparison to MDEA, MEA (primary amine) and DEA (secondary amine) have a rate constant three orders of magnitude higher [22] at the same temperature.

Hindered Amines

Researchers [9, 40] defined hindered amine as a primary amine in which the amino acid group is attached to a tertiary carbon, or a secondary amine in which the amino group is attached to a secondary or tertiary carbon. It can also

be interpreted as one where the carbamate reaction is restricted by the bulkiness of the atoms surrounding the amine group. Hindered amines have been used in several industrial processes for CO_2 and H_2S removal.

The reaction of CO_2 with hindered amines is similar to that of tertiary amines. The CO_2 initially reacts to form an unstable carbamate:

$$CO_2 + Am + H_2O \leftrightarrow AmCOO^- + H_3O^+$$

Equation 2-21

Owing to steric hindrance, this reaction is slow and hence is the main contributor to the overall reaction rate. Following this reaction, the carbamate reacts rapidly with water to form a bicarbonate ion via an equilibrium reaction as shown in Equation 2-22.

$$AmCOO^- + H_2O \leftrightarrow AmH^+ + HCO_3^-$$

Equation 2-22

From Equation 2-21 and Equation 2-22, the loading capacity of hindered amines approaches 1 mol of CO_2 per mol of amine.

In summary, the formation of bicarbonate shown in Equation 2-22 results in high CO_2 loading capacity, however the kinetics are slow due to the low concentrations of carbamate species formed in the solution.

Yih and Shen [41], Alper [42], and Sharma [43] studied at the kinetics of CO_2 absorption into AMP and found that the overall second order rate constant ranges from 500 - 1000 M^{-1} s^{-1} at room temperature.

2.2.2 Amino Acid Based Solvents

Amino acid based solvents have a number of advantages over amine solutions. They are highly resistant to oxidative degradation and have very low volatilities and minimal toxicity [44, 45]. Amino acids have been commercially used in acidic gas removal processes, including glycine in the Giammarco-Vetrocoke process [46, 47], alanine and diethyl or dimethyl glycine in the BASF

Alkazid solvent [46, 48], and precipitating amino acids in the DECAB process [49].

Amino acids have the same functional group as amines, and thus may possess a similar reactivity towards CO_2 [44, 50]. That being said, the presence of the same functional groups to alkanolamines does propose a number of significant problems including limited solvent capacity and high heats of regeneration [51]. Table 2-4 shows past studies on the use of amino acid salts as an alternative for alkanolamine solvents. The reaction pathways follow those of the relevant amine group (primary, secondary or tertiary).

Table 2-4 Kinetic and solubility studies and modelling on a number of amino acids used for carbon capture.

Potassium salts of:	**Basis of Study**	**Concentration Range**	**Temperature Range**	**P_{CO2} (kPa)**	**Reference**
Glycine	• Solubility	0.1 - 3 M	20 - 78 °C	< 60	[52]
	• Modelling	0.1 - 3 M	25 °C	-	[53]
Threonine	• Solubility	1 M	40 °C	< 60	[52]
Taurine	• Solubility • Modelling	0.5 - 4 M	25 - 40 °C	0.1 - 6	[54, 55]
Alanine	• Rate kinetics	0.5 M - 3 M	25 °C	0 - 8	[56]
Aminohexanoic acid					
L-Arginine					
L-Aspartic Acid					
L-Glutamic Acid					
L-Methionine					
L-Phenylalanine					
L-Proline					
Sarcosine					
Sodium Glycinate	• Solubility	10 - 30 wt%	30 - 50 °C	0.1 - 200	[57]

n.b. Sodium glycinate is the only species in this table that is not a potassium salt.

2.2.3 Potassium Carbonate Solvents

Potassium carbonate (K_2CO_3) is an alternative solvent that may potentially overcome some of the issues associated with amine solvents. The major benefit is the ability to run the absorption process at high temperatures resulting in a more efficient and economical regeneration process. Potassium carbonate is also associated with lower toxicity and better resistance to degradation than commonly seen with amine solvents at high temperatures and in the presence of oxygen and other minor flue gas components such as SO_x and NO_x [58-60].

The absorption of carbon dioxide in this case occurs by:

$$CO_2 + CO_3^{2-} + H_2O \leftrightarrow 2\ HCO_3^-$$

Equation 2-23

The reaction is usually described in terms of two parallel, reversible reactions described in Equation 2-4 and Equation 2-24.

$$HCO_3^- + OH^- \leftrightarrow CO_3^{2-} + H_2O$$

Equation 2-24

Since the reaction rate is limited by the reaction of CO_2 with hydroxide (i.e. Equation 2-4), it can be represented as a second order rate expression as shown in Equation 2-5.

Additionally, aqueous carbon dioxide may react with water to form bicarbonate as shown in Equation 2-25. The contribution of this reaction to the overall absorption of CO_2 is usually assumed to be negligible in basic solutions.

$$CO_2 + H_2O \leftrightarrow HCO_3^- + H^+$$

Equation 2-25

The use of potassium carbonate as an absorption solvent has emerged since the early 20th century [61]. In the 1950's, Benson and field established the Benfield process which employed hot potassium carbonate as a CO_2 absorption solvent. This process was run at high partial pressures of CO_2 and temperatures with a purpose to enhance the mass transfer and thus, reduce the gas purification costs [62-64]. During 1970's, this process was further developed by adding a small amount of a rate promoter, DEA which significantly reduced the capital and operating costs of the process and generated higher treated gas purity [61].

Researchers found that carbon dioxide capture systems employing hot carbonate solvents require less heat integration between the absorber and the

regenerator as heats of absorptions are 37% that of amine systems [24, 62]. With regeneration energy constituting almost half of the total capture cost [12], it is obvious that a significant reduction in this energy demand can increase the overall efficiency of the plant.

As coal gasification is normally run at an elevated pressure, temperature and high concentration of carbon dioxide (30 - 35 vol%) [63], coal gasification is an example of a process which would greatly benefit from the integration of a carbon capture solvent system employing hot carbonate solvents. At an elevated pressure, the CO_2 absorption can be run at a temperature equivalent or above the atmospheric boiling temperature of carbonate solvents. This significantly reduces the heating load of the regenerator.

Potassium carbonate based absorption processes are lower cost, less toxic, and less prone to degradation effects that are commonly seen with MEA at high temperatures and in the presence of oxygen and other minor flue gas components. Potassium carbonate acquires the ability to absorb not only CO_2 but also other polluting gases found in standard flue gases such as sulfur oxides (SO_x) and nitrogen oxides (NO_x). In addition, when compared to amine solvents, potassium carbonate solvents have very low volatility which results in much reduced solvent loss to atmosphere.

Despite the aforementioned advantages, performance reductions caused by the exposure of carbonate solvents to flue gas impurities such as sulphur and nitrogen oxides may be inevitable. Additionally, potassium carbonate systems are prone to precipitation at high solvent loadings.

2.2.4 Promoters

The major challenge associated with potassium carbonate is its low rate of reaction resulting in poor mass transfer performance. Previous studies indicate that the transfer of carbon dioxide into potassium carbonate solvents at a room temperature approximately equals that of physical solvents such as water, indicating negligible rate enhancement due to chemical reaction [65, 66]. At 45 °C, the rate enhancement due to the reaction shown in Equation 2-4 becomes apparent leading to a substantial increase in the mass transfer rate when compared to physical solvents. However, the mass transfer rate is still far

below that of amine solvents such as MEA, DEA and piperazine, even at a temperature as high as a typical absorber operating temperature of 120 °C [65, 66].

One approach to improving solvent performance is to blend potassium carbonate with promoters. Factors that are considered in screening a promoter include:

- Promoters should possess a high CO_2 absorption rate
- They should be economically affordable for mass production
- They should have a low vapour pressure to suppress the loss of promoter through evaporation
- They should be environmentally benign, non-corrosive and resistant to degradation by solvent exposure to high temperature, oxygen, gas impurities such as SO_x and NO_x
- They should be a lewis base that cannot be too strong or too weak.

A recent study by Cullinane and Rochelle [67] suggests that when such a promoter is used, potassium carbonate solvent is an energy efficient CO_2 absorbent and acquires several advantages over amine solvents such as MEA. Bishnoi et al [68] determined through experimental kinetic studies that carbonate systems when promoted by piperazine (PZ) have rate constants which surpass that of amine solvents. Past studies on a number rate promoters typically used in carbonate systems are summarized in Table 2-5.

Table 2-5 Most commonly used rate promoters for carbonate solvent systems.

Promoter	Promoter concentration	K_2CO_3 concentration	Temperature range	P_{CO2} (kPa)	Reference
Diethanolamine (DEA)	1 - 3wt%	30 wt%	100 °C	N/A*	[69]
	2 M	1 M	18 °C	100	[70]
Triethanolamine (TEA)	1 - 3wt%	30 wt%	100 °C	N/A*	[69]
Monoethanolamine (MEA)	1 - 3wt%	30 wt%	100 °C	N/A*	[69]
	2 M	1 M	18 °C	100	[70]
Piperazine (PZ)	0.45- 3.6 M	0 - 3.1 M	25 - 110 °C	0 - 48	[71]
Diisopropanolamine (DIPA)	0.6 M	2 M	90 °C	30	[72]
2-amino-2-methyl-1-propanol (AMP)	unknown				
Boric acid, $B(OH)_3$	1 - 5 wt%	30 wt%	50 - 80 °C	unknown	[73]

*Note that Results for DEA, TEA and MEA presented in this table were obtained from desorption experiments and thus, partial pressure of CO_2 is not relevant.

Amine-Promoted K_2CO_3 Solvents

Usually primary or secondary amines are used as rate promoters while tertiary amines (where the zwitterions can no longer deprotonate) do not show a significant rate increasing effect [22, 74]. However, data at high temperatures and a thorough kinetic study of amine-promoted potassium carbonate solvent systems are very rare. This work (Chapter 6) is aimed at filling those gaps for MEA-promoted potassium carbonate systems.

Researchers have considered two different chemical mechanisms to describe the catalytic effect of rate promoters in the carbonate system. A shuttle mechanism was proposed to describe the catalytic activity of primary and secondary amine promoters at low temperatures [65]. In this mechanism, the promoter acts as a carrier to provide another pathway for the transport of the absorbed CO_2 from the gas-liquid interface to the bulk liquid. However, a more recent publication by Savage *et al.* [15, 75] indicated that the catalytic activity of amine in carbonate solutions can be better described by a homogeneous catalysis mechanism. The amine promoter in this mechanism acts as a homogenous catalyst for the reaction shown in Equation 2-4 by first forming an intermediate with the absorbed CO_2 via Equation 2-11. This process is followed by a very fast second step reaction in which the intermediate is deprotonated to produce the final product (Equation 2-12). In the homogenous catalysis mechanism, both reactions take place at the gas-liquid interface.

K_2CO_3 Solvents Promoted by Boric Acid

The use of boric acid is carbonate solvents is attractive as it is economically affordable, readily available for mass production and not expected to interact with gas impurities such as SOx and NOx.

An effective promoter for CO_2 absorption can be viewed as a Lewis base that cannot be too strong or too weak [66]. This facilitates the reaction with CO_2 which is a weak acid. When the pH is elevated to around 10, boric acid predominantly exists as borate $B(OH)_4^-$ [76], which satisfies these criteria as a good promoter for CO_2 absorption.

Figure 2-6 outlines the reaction mechanism of borate with CO_2. It can be seen from this figure, carbon dioxide molecules that reacts with borate, ultimately detach themselves from the borate compounds which subsequently leave them in the bicarbonate form.

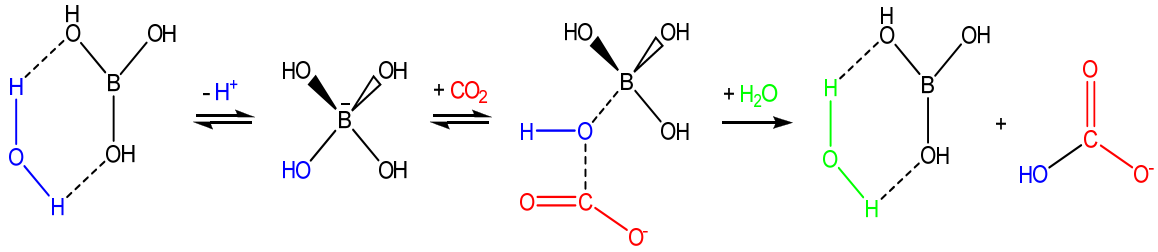

Figure 2-6 Catalytic mechanism of the absorption of CO_2 by boric acid [77].

Table 2-6 outlines some prior work on boric acid as a catalyst in CO_2 hydration. Although general studies on boric acid can be found in literature, very few of them actually cover the reaction kinetic of boric acid with carbon dioxide. Guo *et al.* [77] and Ghosh *et al.* [73] carried out an experimental kinetic study on the reaction of boric acid with carbon dioxide. Although only Ghosh *et al.* [73] performed the experiments at temperatures and concentrations relevant to the industrial CO_2 capture process, his results are only as good as a performance indicator. One of the objectives of this work is to extend his kinetic study of boric acid up to a point where the results can be used for simulation purposes and thus, allow accurate design of the absorber unit for carbon capture processes employing borate-promoted potassium carbonate solvents.

Table 2-6 Past studies on boric acid as a catalyst for CO_2 hydration.

Author (Year)	Basis of Study	Boric acid concentration	K_2CO_3 concentration	Temperature range	Reference
Eickmeyer (1974)	Industrial application	1 - 10 wt%	15 - 40 wt%	-	[78]
Supap *et al.* (2006)	Oxidative degradation	24 mM	N/A	55 - 120 °C	[58]
Ahmadi *et al.* (2008)	Simulation	1.25 M	3 M	60 - 120 °C	[79]
Ghosh *et al.* (2009)	Kinetic	1 - 5 wt%	30 wt%	50 - 80 °C	[73]
Guo *et al.* (2011)	Kinetic	6.25 mM	N/A	100 °C	[77]
Endo *et al.* (2011)	VLE	0 - 5 wt%	30 wt%	50 - 70 °C	[80]

CHAPTER 3 - SCOPE OF THESIS

Responding to the research needs for developing carbonate solvent systems for carbon capture from stationery coal-fired power plants, this research strives to satisfy a number of important objectives.

Chapter 5 focuses on the reaction kinetics of CO_2 into unpromoted and borate-promoted potassium carbonate solutions. This chapter aims to investigate the effect of boric acid on CO_2 absorption in potassium carbonate solutions at high boron concentrations and temperatures, conditions normally encountered in industrial carbon capture systems. In addition, rate constants for the $CO_2 + OH^-$ reaction in unpromoted potassium carbonate solutions obtained in this study validates the experimental technique used in this study.

Chapter 6 characterizes the reaction between CO_2 and MEA within carbonate solutions and measures the activation energy under temperatures, pH levels and ionic strengths relevant to industrial carbon capture systems. Using this experimental data, a rate-based absorption model employing MEA/K_2CO_3 mixtures has been developed using Aspen Plus™ (version 7.3) and compared with both bench and pilot scale data.

Chapter 7 focuses on the use of potassium carbonate solutions promoted with various primary and secondary deprotonated amino acids, i.e. glycine, sarcosine and proline, while Chapter 8 focuses on the use of carbonic anhydrase as a promoter in carbonate solutions.

These results provide valuable information for the operation of promoted potassium carbonate solvent systems for carbon capture processes, and more specifically will allow more accurate design of absorber units.

The scope of the proposed work encompasses conditions that would be encountered in industrial carbon capture systems. The temperature range of interest is from 25 °C - 80 °C, pH levels from 10 - 12 and ionic strength high (*i.e.* 30 - 40 wt% K_2CO_3). It should be noted that Chapters 4, 5 and 6 are of publication materials in Chemical Engineering Journal, while Chapters 7 and 8 are in the process to be published.

CHAPTER 4 - MATERIALS AND RESEARCH METHODOLOGY

This chapter summarizes the experimental methods and equipment used in this study for examining the performance of a number of promoters in the carbonate solutions. A wetted wall column was used to measure the absorption rates of CO_2 into carbonate solvents. Proton and carbon-13 nuclear magnetic resonance (NMR) spectroscopy was used to determine the concentration of amino acids in the carbonate solvents.

4.1 Materials

All chemicals employed in this study were of analytical reagent grade and used as supplied without further purification. Potassium Carbonate (≥ 99 %, Thasco Chemical Co. Ltd.) and potassium bicarbonate (≥ 99 %, Sigma-Alrich Australia) were weighed to prepare a chemical equivalent of a 30 wt% K_2CO_3 solution with an initial CO_2 loading of 0.15. This equated to a carbonate concentration of 2.4 M and bicarbonate concentration of 0.9 M. The promoters boric acid (≥ 99.5 %), MEA (≥ 99 %) and amino acids glycine (≥ 99 %), sarcosine (≥ 98 %) and L-proline (≥ 99 %) were purchased from Chem-Supply Australia, Science Supply Australia and Sigma-Aldrich Australia respectively (NB: in this work L-proline is referred as proline as the stereochemistry is not relevant). Potassium hydroxide (≥ 97 %) was purchase from Merck Australia and used for deprotonation of the amino acids.

Deuterium oxide (≥ 99 %), 3-(trimethylsilyl)propionic-2,2,3,3-d_4 acid sodium salt or TMS (≥ 98 %) and 1,4-dioxane (≥ 99 %) were purchased from Sigma-Aldrich Australia and used as an internal reference standard for nuclear magnetic resonance (NMR) measurements. CO_2/N_2 gas mixtures (10.2 % and 89.8 % CO_2 in N_2 obtained from BOC Gases Australia) were used for all experiments and for the calibration of a MGA3000C CO_2 gas analyser (ANRI Instrument and Control Pty. Ltd.).

An indicator and a buffer were acquired and used without further purification for stopped-flow experiments: 4-nitrophenol (≥ 99.5 %, Sigma-Aldrich Australia) and imidazole (≥ 99 %, Sigma-Aldrich Australia). Hydrochloric acid standard solution (1 M, Merck Australia) and sodium hydroxide (≥ 97.0 %, Chem-Supply Australia) solutions were used to adjust pH values. A carbonic

anhydrase enzyme was supplied by Novozymes Denmark with a product code 'NS81239'. The product contains approximately 3 g/L carbonic anhydrase enzyme protein and has an enzyme activity of 900 kWAU/mL. A CO_2/N_2 gas mixture (10.6 % CO_2 in N_2 obtained from BOC Gas Australia) was used to prepare aqueous CO_2 solutions. All reagents used in this study as well as its purity, supplier, purpose and chapters involved are summarized in Table 4-1.

Table 4-1 Information (purity, supplier, purpose and chapters involved) on all reagents used in this work.

Reagents	**Purity**	**Supplier**	**Purpose**	**Chapter**
Potassium carbonate, K_2CO_3	≥ 99 %	Thasco Chemical CO. Ltd.	Solvent	5, 6, 7, 8
Potassium bicarbonate, $KHCO_3$	≥ 99 %	Sigma-Alrich Australia	Solvent	5, 6, 7, 8
Boric acid, $B(OH)_3$	≥ 99.5 %	Chem-Supply Australia	Promoter	5
Monoethanolamine (MEA)	≥ 99 %	Science Supply Australia	Promoter	6
Glycine	≥ 99 %	Sigma-Aldrich Australia	Promoter	7
Sarcosine	≥ 98 %	Sigma-Aldrich Australia	Promoter	7
Proline	≥ 99 %	Sigma-Aldrich Australia	Promoter	7
Carbonic anhydrase enzyme	38 g/L	Novozymes Denmark	Promoter	8
Potassium hydroxide, KOH	≥ 97 %	Merck Australia	Deprotonation of amino acids	7
Deuterium oxide, D_2O	≥ 99 %	Sigma-Aldrich Australia	NMR	7
TMS	≥ 98 %	Sigma-Aldrich Australia	NMR	7
1,4-dioxane	≥ 99 %	Sigma-Aldrich Australia	NMR	7
4-nitrophenol	≥ 99.5 %	Sigma-Aldrich Australia	Indicator	8
Imidazole	≥ 99 %	Sigma-Aldrich Australia	Buffer	8
Hydrochloric acid, HCl	1 M	Merck Australia	pH control	8
Sodium hydroxide, NaOH	≥ 97 %	Chem-Supply Australia	pH control	8
CO_2 in N_2 gas mixture	10.2 %	BOC Gas Australia	Wetted wall column experiments and gas analyser calibration	5, 6, 7, 8
	89.8 %			5, 6, 7, 8
	10.6 %		Stopped-flow experiments	8

4.2 Research Methodology

A range of equipment has been developed for the determination of accurate kinetic rate data for gas-liquid systems. The hydrodynamics, mass transfer resistances, and the interfacial area should be well characterized in such equipment. The most important ones include a laminar jet, a wetted wall column, a wetted sphere absorber and a stirred cell. Typical values of the liquid phase mass transfer coefficients ($k_l°$) and contact times are presented in Table 4-2 [81].

Table 4-2 Characteristics of different experimental apparatus for gas-liquid reactions [81].

Apparatus	Contact time (s)	$10^3 \times k_l°$ (m s^{-1})
Laminar jet	0.01 -0.1	0.16 - 1.6
Wetted wall column	0.1 -2	0.036 - 0.16
Wetted sphere absorber	0.1 -1	0.05 -0.16
Stirred cell	> 1	0.016 -0.1

It should be noted that for a well defined gas-liquid contact area, the liquid mass transfer coefficient is relatively low in the stirred cell which limits its applicability for fast reactions. Although the gas-liquid interfacial area and gas-liquid mass transfer coefficient can be widely varied and accurately estimated in a laminar jet, a wetted wall column and a wetted sphere absorber, the contact time of a laminar jet is rather short and therefore, the selection falls between the remaining two apparatuses. A wetted wall column is chosen as it is simpler and thus easier to model than a wetted sphere absorber.

4.2.1 Wetted Wall Column (WWC) Description

The wetted wall column, shown in Figure 4-1, consists of a stainless steel tube 115 mm long with a 13 mm outer diameter. The total contact area, 4840 mm^2, was calculated as the longitudinal area of the tube, 4590 mm^2, and the area of the top of the column, 250 mm^2, which was considered a hemisphere due to the shape of the liquid film. The column was enclosed by a thick-walled steel cylinder with an outside diameter of 25 mm to provide a gas-liquid contact

chamber. The hydraulic diameter of the enclosure is 13 mm, giving a cross sectional area for gas flow of 380 mm^2. The chamber was housed inside a second thick-walled steel chamber (102 mm outside diameter) that served as an insulating bath with circulating heat transfer liquid.

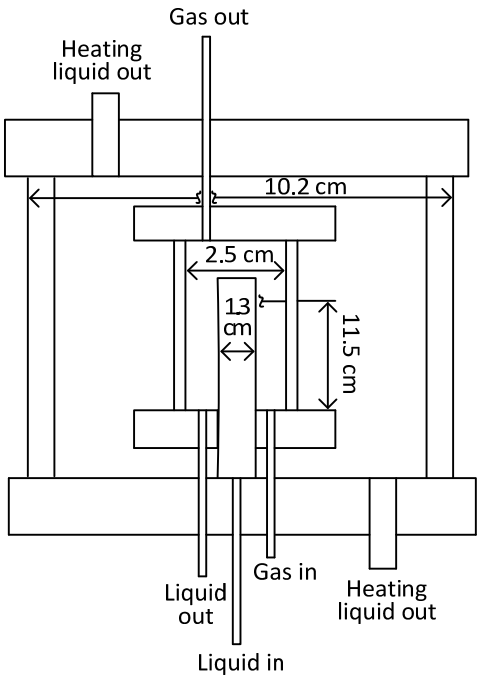

Figure 4-1 Dimension of wetted wall column used in this study.

The liquid solvent was contained in a stainless steel reservoir with a total volume of 3000 cm^3. The fluid was pumped from the reservoir to the gas-liquid contact chamber. The fluid flowed up through the middle of the column, overflowed at the top, and was evenly distributed on the outer surface of the column. The liquid was collected at the bottom of the column and pumped back to the solution reservoir by a positive displacement IDEX micropump (Process Pump Pty. Ltd.). A typical liquid flowrate used in this experiment was 100 mL/min.

The gas flowrate was manually controlled by an outlet needle valve and monitored using an Aalborg flowmeter (0 - 1000 mL/min) (Pryde Measurement Pty. Ltd.). The gas was saturated with water at the operating temperature of the column in a sealed vessel immersed in a heat bath in order to avoid the gas absorbing water further downstream. After saturation, the gas was introduced

to the bottom of the column through a ¼ inch tube. It subsequently flowed counter-currently past the liquid film. The gas exited the top of the column and was routed to a condenser, and subsequently, a cold trap which was submerged in an ice bath in order to remove any water from the gas stream before analysis. Pressure in the column was controlled by a needle valve on the gas outlet tubing. A process flow diagram of the full experimental setup is shown in Figure 4-2.

Liquid samples were analysed by acid titration prior to and after the experiment to determine solution pH and CO_2 loading which was defined as moles of CO_2 absorbed per mole of K_2CO_3. The concentration of HCO_3^- and CO_3^{2-} was determined using a Metrohm Titrando 809 autotitrator (Switzerland).

To measure the concentration of amino acid based promoters, liquid samples were analysed using proton and carbon-13 NMR spectroscopy. All NMR spectra were acquired on a Varian Unity Plus 400 MHz spectrometer at 25 °C and plotted using MestRe-C NMR Data Processing Software from MestreLab Research. TMS and D_2O were used as external and internal reference standards of the ^1H NMR respectively while 1,4-dioxane was used for ^{13}C NMR measurement.

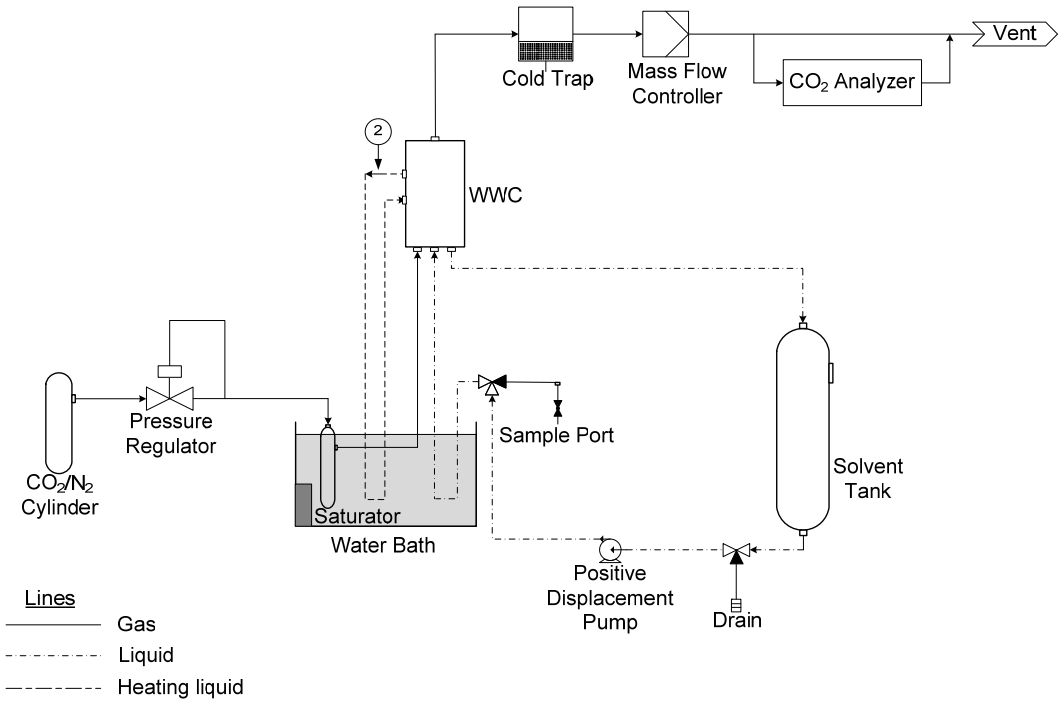

Figure 4-2 Process flow diagram of the wetted wall column.

Liquid Titration

Liquid samples were taken and analysed for the solution pH and CO_2 loading using an automated titrator (Metrohm Titrando 809, Switzerland). Sulphuric acid at 0.4 M (Univar, ≥ 98 % purity, Australia) was used to titrate the solution samples. A typical double endpoint titration result is shown in Figure 4-3.

4 mL of liquid samples contained in a 80 mL beakers were mixed with 40 mL of RO water. The samples were subsequently titrated against 0.4 M sulfuric acid solutions (Univar, ≥ 98 % purity, Australia).

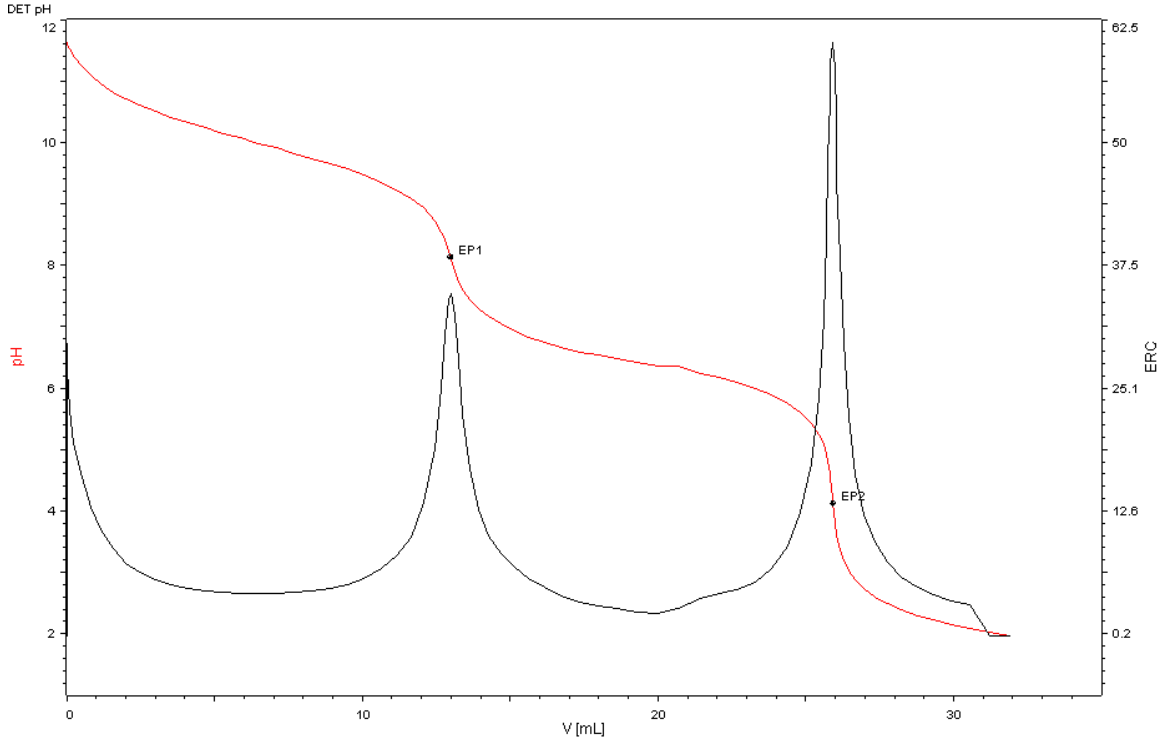

Figure 4-3 Typical double endpoint titration used to determine the concentration of K_2CO_3 and $KHCO_3$. The red graph indicates the pH of the solution and the black graph shows the gradient of the pH curve. The solution used for this demonstration contains 2.6 M of K_2CO_3 and 0 M of $KHCO_3$.

Figure 4-3 is an example of an output from the automatic titrator used for carbonate/bicarbonate solutions which have the capacity to buffer. The endpoints EP1 and EP2 can be described by Equation 4-1 and Equation 4-2 and have endpoint volumes V_1 and V_2.

$$2\ K_2CO_3 + H_2SO_4 \rightarrow K_2SO_4 + 2\ KHCO_3$$

Equation 4-1

$$2\ KHCO_3 + H_2SO_4 \rightarrow K_2SO_4 + 2\ CO_2 + 2\ H_2O$$

Equation 4-2

The concentrations of bicarbonate and carbonate are determined using the following two equations:

$$[CO_3^{2-}] = \frac{V_1 \times [H_2SO_4] \times 2}{V_{sample}}$$

Equation 4-3

$$[HCO_3^-] = \frac{(V_2 - 2V_1) \times [H_2SO_4] \times 2}{V_{sample}}$$

Equation 4-4

V_{sample} is defined as the size of the sample of solution taken (4 mL).

Gas Concentration Analysis

Concentrations of gas samples were measured using a multi-gas analyser (ADC, MGA3000, Australia). Specifications for operational parameters of the gas analyser can be found in the following table:

Table 4-3 Operating parameters for the multi-gas analyser used for CO_2 concentration measurements in this study.

Operating temperature	150 °C
Operating Pressure	Atmospheric
Flow rate	0.2 – 1 L/min
Repeatability	< 0.1 % fsd
Noise	< 0.1 % fsd
Cell response	4 s

The gas analyser was calibrated against CO_2/N_2 gas mixtures (10.2 % and 89.8 % CO_2 in N_2, BOC Gas Australia) weekly.

4.2.2 WWC Methodology

During each experiment, data points were collected at a steady-state flux with a bulk CO_2 partial pressure of 90 kPa and an initial solution loading of 0.15 (unless otherwise stated). Experiments were performed in which both concentration of the promoter and temperature were varied. Three repeat runs were carried out for each set of conditions. Standard deviations from the repeat runs were used to calculate the uncertainty intervals for the pseudo first order rate constant k_{obs} (s^{-1}) values, which are twice the standard error. As the change in CO_2 concentration over the WWC was relatively small compared to the total CO_2 concentration of the liquid, the equilibrium partial pressure of CO_2 was assumed constant for each experiment, and was obtained from Endo [80]. The effect of the addition of promoter on the equilibrium partial pressure of CO_2 was assumed to be negligible due to the high CO_2 partial pressure used in the investigation.

Experimental conditions were chosen such that the concentration of hydroxyl ions and promoter were always in large excess over dissolved carbon dioxide, resulting in pseudo-first-order kinetics. Hence, the gas absorption rate can be expressed as Equation 2-8.

In the absence of promoter, the apparent pseudo first order rate constant k_{obs} (s^{-1}) can then be expressed as Equation 2-9 (the pseudo first order rate constant k_1 is referred as k_{obs} from this point onwards for consistency purposes with the journal publications) and is related to the CO_2 reaction rate r_{CO2} (M s^{-1}) by:

$$r_{CO2} = -k_{obs}[CO_2]$$

Equation 4-5

The value of k_{OH} is determined in Chapter 5 and used in later chapters. The Henry's Law constant and the diffusivity constant of CO_2 in the promoted potassium carbonate solution were obtained from the literature [82-90]. Literature data were used to validate a correlation between the Henry's law constant in a potassium carbonate solution and ionic strength first reported by Astarita *et al.* [16] and used by Proll *et al.* [88]. The same method was used

when estimating the diffusivity constant of CO_2 in the potassium carbonate solutions. The physical liquid mass transfer coefficient was calculated using correlations developed by Pacheco [91] and Treybal [92].

4.2.3 WWC Characterization

Gas Mass Transfer Coefficient

The gas film mass transfer, k_g, in a WWC has been determined by Bishnoi [68] who performed an experiment on an absorption of sulfur dioxide into 0.1 M NaOH. His experimental results have been correlated with a predicted gas film mass transfer proposed by Hobler [93]. The Sherwood number is defined as:

$$Sh = 1.075\left(Re\ Sc\ \frac{d}{h}\right)^{0.85}$$

Equation 4-6

The Schmidt number is defined as:

$$Sc = \frac{\mu_g}{\rho_g D_{CO_2}}$$

Equation 4-7

where μ_g [pa s^{-1}] is the gas viscosity and ρ_g [kg m^{-3}] is the gas density. Also, h is the height of the WWC (115 mm) and d is the hydraulic diameter of the annulus (13 mm). The Reynolds number is:

$$Re = \frac{\rho_g v d}{\mu_g}$$

Equation 4-8

where v [m s^{-1}] is the linear velocity of the gas. The gas film mass transfer coefficient can be found from the following definition of the Sherwood number.

$$Sh = \frac{RTk_g d}{D_{CO_2}}$$

Equation 4-9

where T [K] is the temperature and R [J K^{-1} mol^{-1}] is the gas constant. This correlation is used in the present study for determining the gas phase mass transfer coefficient.

Liquid Mass Transfer Coefficient

Mshewa and Pacheco [91] determined the liquid film mass transfer coefficient, k_l^o, in a WWC via CO_2 desorption from physical solvents such as water and ethylene glycol. A correlation of k_l^o based on an experimental work performed by Vivian and Peaceman [94] was originally used by Mshewa. Pacheco then obtained additional data and expanded the correlation to accommodate different experimental conditions. In the current study, experimental measurements of CO_2 desorption from water were performed in order to verify and extend the experimental data obtained by Mshewa and Pacheco [91]. Pacheco's experimental data were obtained from experiments performed at 700 kPa and over a range of temperatures from 25 °C to 120 °C.

When CO_2 is absorbed (or desorbed) from a liquid flowing down the WWC, the following equation describes the mass balance at the liquid side:

$$V_L \frac{d[CO_2]_b^L}{dt} = k_l^\circ a\left([CO_2]_i^L - [CO_2]_b^L\right) = \frac{k_l^\circ a}{H}\left(P_{CO_2,i} - P_{CO_2}^*\right)$$

Equation 4-10

where V_L [m^3] is the volume of liquid circulating through the system, a [m^2] is the interfacial area for mass transfer in the WWC. Assuming that desorption of CO_2 from water is completely liquid film controlled, the partial pressure of CO_2 approaches that at the gas bulk, i.e. $P_{CO_2,i} \approx P_{CO_2,b}$. This assumption is validated as calculations demonstrate that the liquid film resistance contributes up to 97 % of the total resistance.

Considering the molar concentration of CO_2 in the gas is related to its partial pressure by:

$$[CO_2]_b^G = \frac{P_{CO_2,b}}{RT}$$

Equation 4-11

Equation 4-10 becomes:

$$V_L \frac{d[CO_2]_b^L}{dt} = \frac{k_l^\circ a}{H}\left(RT[CO_2]_b^G - RT[CO_2]_b^L\right)$$

Equation 4-12

The molar concentrations of CO_2 at the gas and liquid bulk can be related by the following mass balance equation:

$$k_l^\circ a\left([CO_2]_i^L - [CO_2]_b^L\right) = G\left([CO_2]^{G,in} - [CO_2]^{G,out}\right)$$

Equation 4-13

where G [m^3 s^{-1}] is the gas volumetric flow rate in the WWC and the superscripts 'G,in' and 'G,out' indicate the concentrations at the inlet and outlet of the WWC respectively. As CO_2 is desorbed using a pure nitrogen gas stream, $[CO_2]^{G,in}$ can be regarded as 0. Assuming the main contribution to the driving force at the gas side is given by the average of inlet and outlet CO_2 concentration, *i.e.* in Equation 4-12, $[CO_2]_b^G = 0.5[CO_2]^{G,out}$ and when Equation 4-13 is solved for $[CO_2]_b^L$, the following is obtained:

$$[CO_2]_b^L = \left(\frac{G}{k_l^\circ a} + \frac{RT}{2H}\right)[CO_2]^{G,out}$$

Equation 4-14

From Equation 2-5 and Equation 4-13, the following is obtained:

$$V_L \frac{d[CO_2]_b^L}{dt} = -G[CO_2]^{G,out}$$

Equation 4-15

which gives:

$$V_L \left(\frac{G}{k_l^\circ a} + \frac{RT}{2H}\right)\frac{d[CO_2]^{G,out}}{dt} = -G[CO_2]^{G,out}$$

Equation 4-16

Equation 4-16 can be integrated from the start of the desorption experiment ($t = 0$) to a given time t generating:

$$\log_e\left[\frac{[CO_2]^{G,out}(t)}{[CO_2]^{G,out}(t=0)}\right] = -\frac{G}{V_L\left(\frac{G}{k_l^\circ a} + \frac{RT}{2H}\right)}t$$

Equation 4-17

Equation 4-17 indicates that the physical mass transfer coefficient of CO_2 in the WWC can be determined by measuring the slope of the plot of $\log_e\left[[CO_2]^{G,out}(t)\right]$ against time.

Desorption experiments were performed by first introducing CO_2 to a beaker containing 1.5 L of water for approximately three hours. Pure nitrogen was then used to desorb the CO_2 from the liquid using the WWC and the outlet CO_2 gas concentration and flowrate were recorded. Absorption of CO_2 in water takes place through physical and chemical absorption. Chemical absorption is governed by the reaction shown in Equation 2-25. In agreement with work done by Versteeg [85], calculations show that only 1.7 % of the absorbed CO_2 is

present as carbonate and bicarbonate ions. This verifies that such chemical absorption is negligible and therefore, it is reasonable to assume that the release of CO_2 from water is completely governed by physical desorption.

Figure 4-4 represents a typical set of experimental data for a desorption experiment. A linear regression approximation is used to calculate the slope of the plot of $\log_e\left[[CO_2]^{G,out}(t)\right]$ against time during steady state desorption. The slope is then used to determine k_l°.

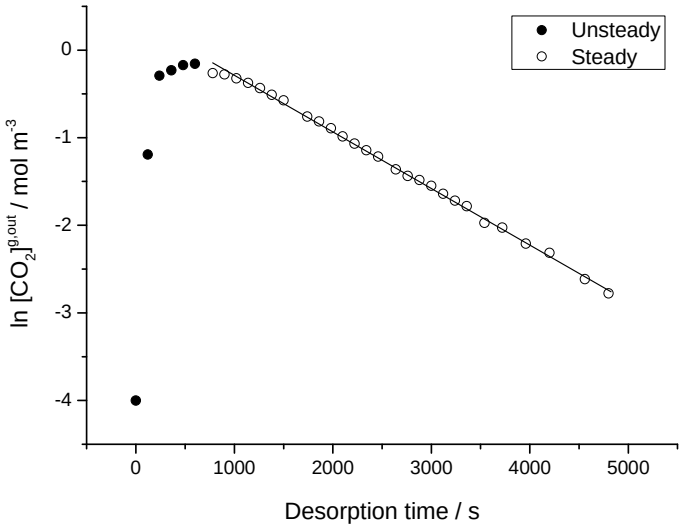

Figure 4-4 Desorption of CO_2 from water in the WWC at 60 °C and atmospheric pressure, $k_l°$ is determined to be 1.4×10^{-4} m s^{-1}.

The physical mass transfer coefficients for CO_2 in the WWC determined experimentally were compared with a fundamental model first developed by Emmert [95] and used by Pacheco [91]. This model is based on the solution of the equation of continuity for diffusion into a falling liquid film where convective transport is considered in the direction of the flow while diffusive transport is considered in the direction perpendicular to the liquid-gas interface. In the development of this model it is assumed that there is a parabolic velocity profile in the liquid phase and that the concentration of the diffusing species in the liquid-gas interface is uniform. Pacheco chose a form of the expression given by Hobler [91, 93]:

$$k_l^{\circ} = \frac{\dot{V}}{a}(1-\theta)$$

Equation 4-18

where $\dot{V}$ [$m^3\ s^{-1}$] is the volumetric flowrate of the liquid and θ represents a dimensionless driving force of the diffusing gas in the liquid film. θ is calculated as follows:

$$\theta = 1 - 3\sqrt{\frac{\eta}{\pi}}$$

Equation 4-19

A dimensionless penetration distance, η , is defined as:

$$\eta = \frac{D_{CO_2}\tau}{\partial^2}$$

Equation 4-20

τ [s] is the surface contact time, defined as:

$$\tau = \frac{h}{u_s}$$

Equation 4-21

The film thickness, δ [m], is given by:

$$\delta = \sqrt[3]{\frac{3\mu_l \dot{V}}{\rho_l g W}}$$

Equation 4-22

where μ_l [pa s] is the liquid viscosity, ρ_l [$kg\ m^{-3}$] is the liquid density, g [$m\ s^{-2}$] is the gravity constant and W [m] is the circumference of the column. A liquid surface velocity, u_s, is given by:

$$u_s = \frac{\rho_l g \partial^2}{2\mu_l}$$

Equation 4-23

Experimental results obtained from operating the current WWC over a range of operating conditions have been compared with this correlation developed by Pacheco [91] as well as a correlation developed by Treybal [92]. The good agreement between results (presented in Figure 4-5 and Figure 4-6) and theoretical predictions is considered to validate the WWC technique used to measure the reaction kinetics of unpromoted and promoted CO_2 absorption in potassium carbonate solutions. It is important to note that, at Reynolds number 66 shown in Figure 4-6, it is suspected that the liquid flowrate is not high enough to completely wet the column and therefore, the result at this particular point is seemingly deviated from the literature.

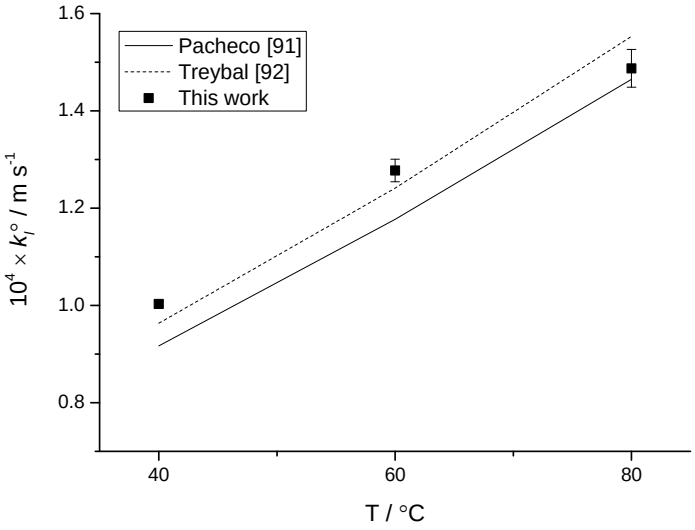

Figure 4-5 Effect of temperature on physical liquid mass transfer coefficient at atmospheric pressure and a constant Reynolds number (Re = 132).

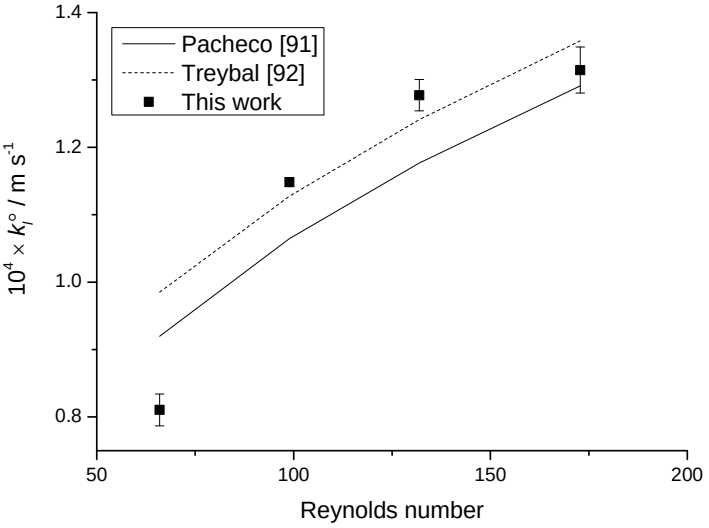

Figure 4-6 Effect of Reynolds number or liquid flowrate on the physical liquid mass transfer coefficient at 60 °C and atmospheric pressure.

4.3 Stopped-flow pH Indicator

The stopped-flow pH indicator technique was adapted from the work by Guo *et al.* [77] and used in this study to observe the reaction of CO_2 with the carbonic anhydrase enzyme supplied by Novozymes. Experiments were carried out by mixing a solution containing aqueous CO_2 with a pH-controlled reagent solution containing pH indicator (4-nitrophenol - 4.9×10^{-5} M), buffer (imidazole - 10 mM) and the enzyme (0.1, 0.5 and 1 v/v%) in a 1:1 ratio. Solutions containing CO_2 were prepared by bubbling CO_2/N_2 gas mixture through a gas absorption bottle equipped with a ring packing at a constant temperature of 25.3 °C for at least one hour before the experiment started. The flow of the gas mixture was continuous throughout the duration of the experiment. A gas tight syringe was used to transfer the CO_2 solutions to the stopped-flow apparatus. The concentration of CO_2 in the solution was determined from published solubility data [96], and was in the range of 1.6 to 2.1 mM. It is also important to note that the pH of the CO_2 solutions was adjusted to 7 by adding hydrochloric acid or sodium hydroxide. A Metrohm Titrando 809 autotitrator (Switzerland) was used to determine the reaction pH which occurs when the

CO_2 solution was mixed with the reagent solution. All concentrations quoted here refer to the reaction media after mixing.

Kinetic measurements reported in Chapter 8 were carried out by monitoring the indicator absorbance versus time using an Applied Photophysics SX.18MV-R Stopped-Flow Reaction Analyzer equipped with a 10-mm optical path length observation chamber. The reagent resevoirs and stopped-flow cell were temperature controlled to within ± 0.1 °C using Grant water bath. Before kinetic experiments, measurements of spectrophotometric properties were performed between 200 and 800 nm in the stopped-flow cell. Extinction coefficients for the base and acid forms of the pH indicator 4-nitrophenol at 400 nm are 200 M^{-1} cm^{-1} and 18100 M^{-1} cm^{-1}.

Eight repeat runs were performed at various enzyme concentrations, and values reported here represent averages. Reaction between the enzyme and CO_2 was typically complete within few seconds, and reaction rates corresponding to an approximately 10% initial conversion were obtained from the recorded absorbance traces by a signal exponential regression based on the Marquardt algorithm.

CHAPTER 5 - CO_2 ABSORPTION IN UNPROMOTED AND BORATE-CATALYZED POTASSIUM CARBONATE SOLUTIONS

5.1 Introduction

As described in Chapter 2, boric acid $B(OH)_3$ is one possible promoter for the carbonate solvent system. $B(OH)_3$ is attractive because it is relatively benign and economically affordable, and is not expected to interact with species such as sulphur dioxide or oxygen often present in the flue gas from power stations [80].

It has been reported that $B(OH)_3$ and $B(OH)_4^-$ are the predominant boron species at boron concentrations and pH range relevant to carbon capture systems [77, 97]. Using a stopped-flow indicator technique, results from previous work [77] in this laboratory showed that, at total boron concentrations from 4 to 12.5 mM and a temperature range 25 °C to 40 °C, $B(OH)_4^-$ catalyzes CO_2 hydration via the same fundamental mechanism as the enzyme carbonic anhydrase:

$$B(OH)_3 \cdot H_2O \leftrightarrow B(OH)_4^- + H^+$$

Equation 5-1

$$B(OH)_4^- + CO_2 \rightarrow B(OH)_4CO_2^-$$

Equation 5-2

$$B(OH)_4CO_2^- + H_2O \rightarrow B(OH)_3 \cdot H_2O + HCO_3^-$$

Equation 5-3

The apparent pseudo-first-order rate constant (k_{obs}, s^{-1}) can then be expressed as:

$$k_{obs} = k_{OH}[OH^-] + k_{borate}[B(OH)_4^-]$$

Equation 5-4

The aim of this study is to extend the work of Guo *et al.* [77] by investigating the effect of boric acid on CO_2 absorption in potassium carbonate

solutions at significantly higher boron concentrations and temperatures, which are closer to the conditions encountered in industrial carbon capture systems [80, 98].

5.2 Results

Rate constants (k_{OH}, M^{-1} s^{-1}) for the CO_2 + OH^- reaction in unpromoted carbonate systems were first investigated. The Arrhenius expression from 40 °C to 80 °C was found to be k_{OH} [M^{-1} s^{-1}] = $2.53\times10^{11}\exp(-4311/T\,[K])$ where the activation energy is 35.8 kJ mol^{-1}. The measured rate constant is similar to literature values (average deviation < 8 %) [15, 16, 99]. The good agreement between the present data (presented in Figure 5-1) and the empirical correlations is considered to validate the experimental procedure used in the present work.

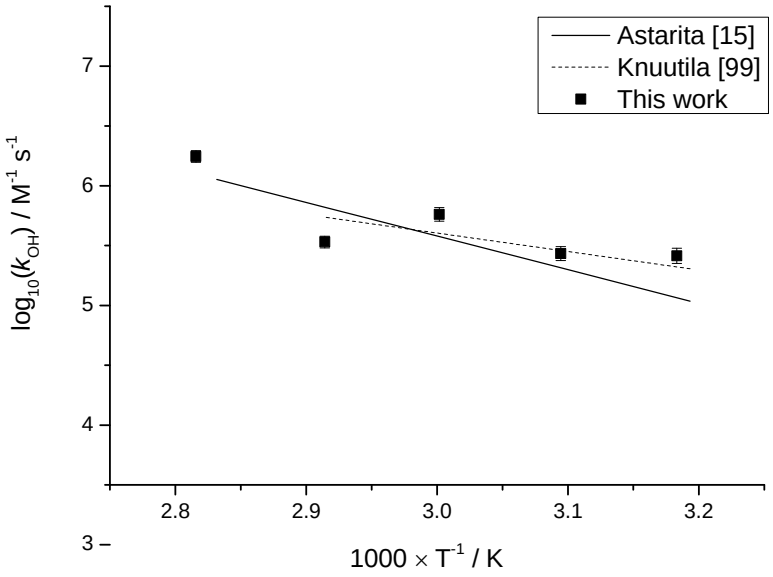

Figure 5-1 Arrhenius plot of $\log_{10}k_{OH}$ versus 1000/T including comparison with empirical correlations [15, 99].

At 80 °C the addition of 0.2 M, 0.6 M and 1.5 M boric acid into a 30 wt% potassium carbonate solution results in a drop in the pH from 10.1 to 9.8, 9.6 and 9.3 respectively. pKa values of boric acid are obtained from the literature

[100], and are used to calculate the distribution of $B(OH)_4^-$ against $B(OH)_3$. Figure 5-2 indicates that at around pH 9 - 10 $B(OH)_4^-$ is the dominant boron species, and is used to determine the concentration of active boron species.

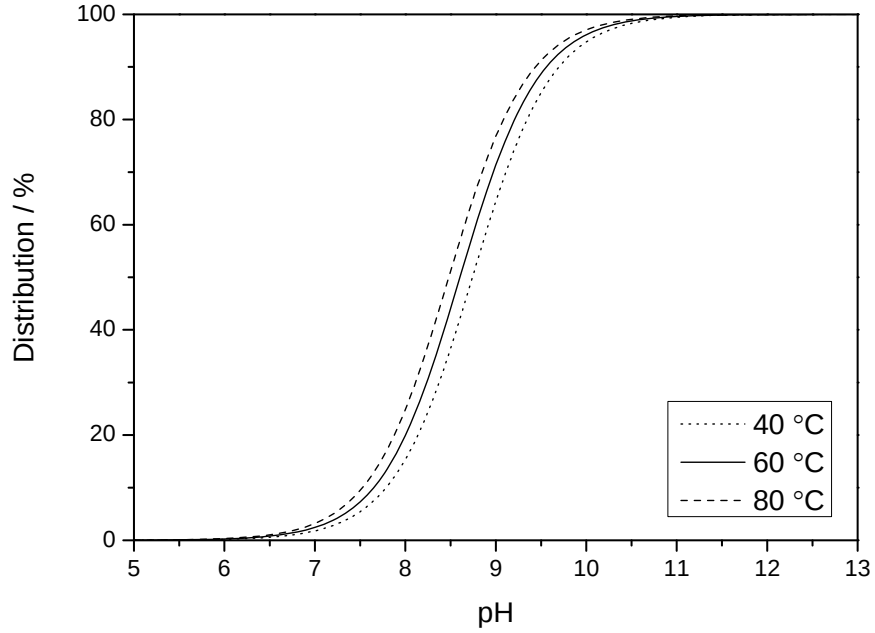

Figure 5-2 Distribution (%) of $B(OH)_4^-$ (against $B(OH)_3$) in borate solutions in the pH range 5 - 13 at 40 °C (dotted line), 60 °C (solid line) and 80 °C (dashed line).

Pseudo-first-order rate constants (k_{obs}, s^{-1}) for CO_2 reacting in unpromoted and borate-promoted potassium carbonate solutions at 40 °C, 60 °C and 80 °C are shown in Figure 5-3a. Results demonstrate that, at 80 °C, the addition of relatively small amounts of boric acid (0.2 M, 0.6 M and 1.5 M) accelerates the overall absorption process of CO_2 in carbonate solvents by 3 %, 10 % and 29 % respectively.

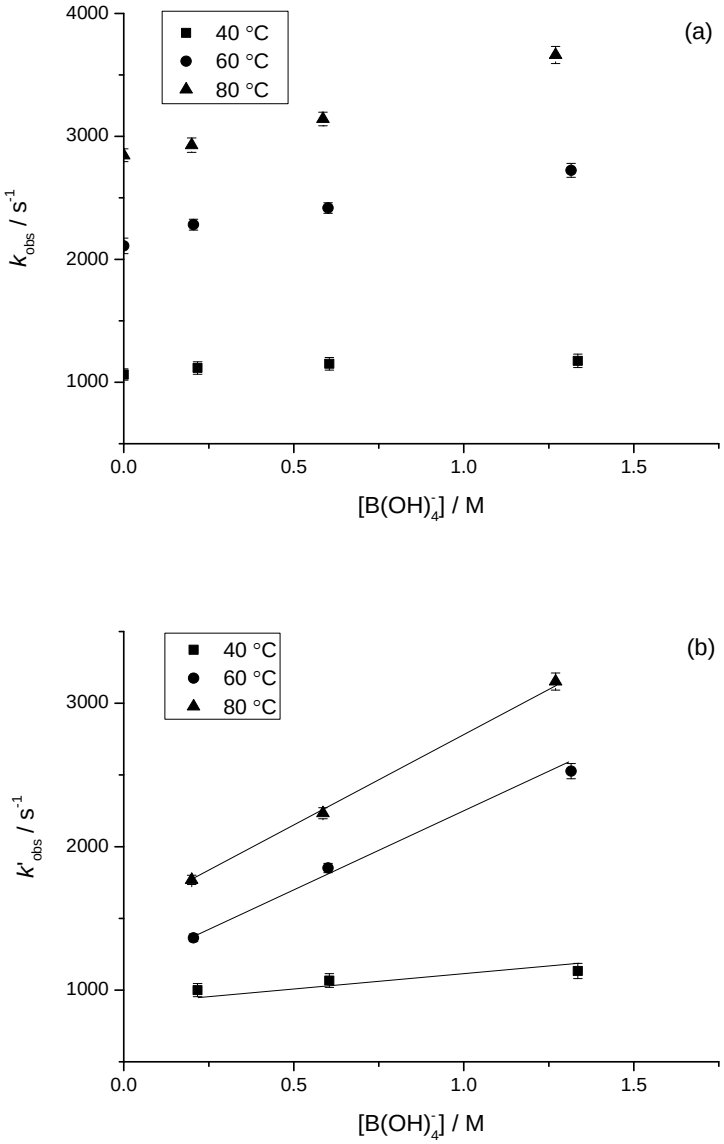

Figure 5-3 (A) Pseudo-first-order reaction rate k_{obs} versus concentration of promoter $[B(OH)_4^-]$ at 40 °C to 80 °C. **(B)** Plot of k'_{obs} (= k_{borate} $[B(OH)_4^-]$ = k_{obs} – $k_{OH}[OH^-]$) versus $[B(OH)_4^-]$ at 40 °C to 80 °C. The presence of tetrahydroxyborate ion, $B(OH)_4^-$, appears to improve the apparent rate constant (k_{obs}) especially at high temperatures. The reaction rate (k'_{obs}) increases linearly with $[B(OH)_4^-]$. The slopes of these lines represent the rate constants k_{borate}.

When the rate component attributed to reaction with OH^- is excluded (k'_{obs} = $k_{borate}[B(OH)_4^-]$ = k_{obs} - $k_{OH}[OH^-]$), non-zero rate constants are observed. This demonstrates the catalytic activity provided by the added boric acid. Figure

5-3b shows a linear relationship between k'_{obs} and $[B(OH)_4^-]$ suggesting that the catalyzed component is in a first-order relationship with $[B(OH)_4^-]$. The slope of these lines provides an estimation of the rate constant k_{borate} for the CO_2 + $B(OH)_4^-$ reaction. The Arrhenius expression from 40 °C to 80 °C was found to be k_{borate} [M^{-1} s^{-1}] = $5.5\times10^{11}\exp(-6927/T\,[K])$ where the activation energy is 57.6 kJ mol^{-1}. As illustrated in Figure 5-4, this finding is in good agreement with work by Guo *et al.* [77] which was done at low ionic strength conditions indicating that ionic strength may have little or no effect on the determination of k_{borate}.

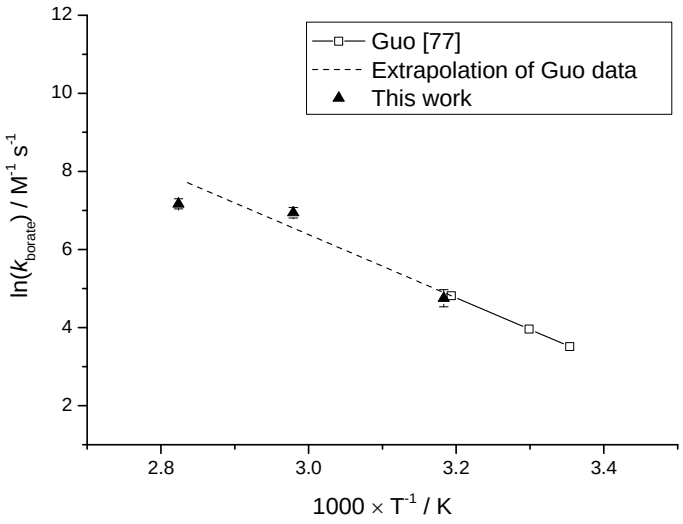

Figure 5-4 Arrhenius plot of $\ln k_{borate}$ versus $1000/T$ including comparison with previous study. Results from Guo *et al.* [77] which were conducted using stopped-flow equipment at much lower boron concentrations and temperatures. These results have been extrapolated and found to be consistent with the results presented here.

5.3 Discussion

Unloaded potassium carbonate solutions can have a pH of 12 where $[OH^-]$ becomes significant and thus the reaction CO_2 + OH^- governs the absorption process of CO_2 into potassium carbonate solutions. However, it is extremely difficult to maintain carbonate solvents at such high pH as the absorption of CO_2 releases protons and thus acidifies the solution. Figure 5-5 demonstrates a typical experimental plot of pH versus loading in a 30 wt% potassium carbonate solution at 60 °C. In a CO_2 capture plant, a 'lean' solvent

generally returned from a regenerator to an absorber is at around pH 10 or loading 0.2 [101, 102]. It is therefore apparent that under these conditions borate compounds can provide significant enhancement to the reaction rate.

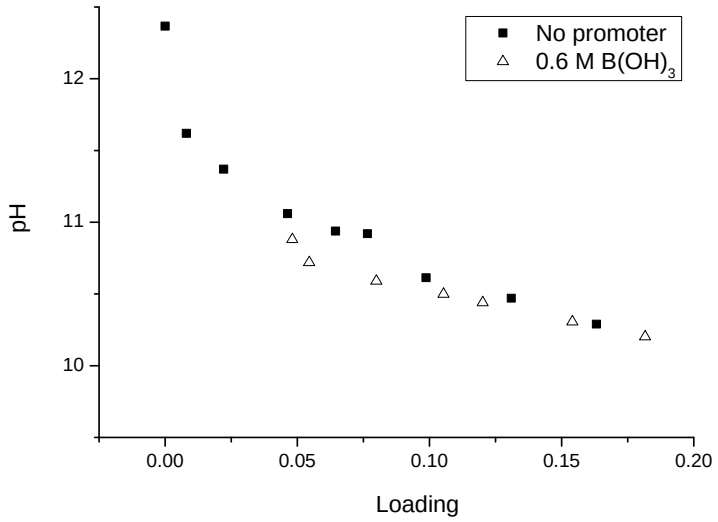

Figure 5-5 A typical experimental pH versus loading curve of unpromoted and borate-promoted potassium carbonate solvent at 60 °C.

Figure 5-6 shows that at 60 °C and pH 10, $B(OH)_4^-$ contributes up to almost 60 % of the reaction of CO_2 to form HCO_3^- and hence borate catalysis may prove to be useful for promoting carbonate systems.

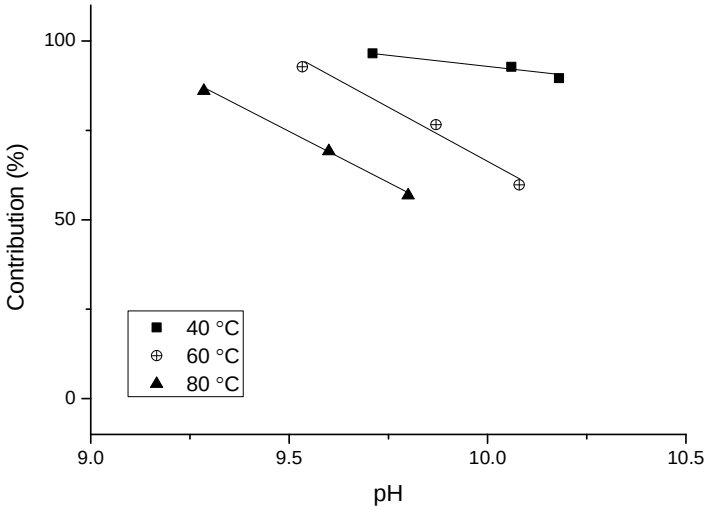

Figure 5-6 Contribution of borate catalysis in the pseudo-first-order rate constant (k_{obs}, s^{-1}). At pH 9 to 10 the contribution of reaction $CO_2 + B(OH)_4^-$ is significant.

5.4 Conclusions

A comprehensive kinetic study on the absorption of CO_2 into unpromoted and borate-promoted potassium carbonate solutions is presented in this work. Results indicate that an addition of a small amount of boric acid accelerates the apparent pseudo-first-order rate constant, and thus, the overall absorption of CO_2 into potassium carbonate solutions.

CHAPTER 6 - A KINETIC AND PROCESS MODELING STUDY OF CO_2 CAPTURE WITH MEA-PROMOTED POTASSIUM CARBONATE SOLUTIONS

6.1 Introduction

In comparison to the carbonate system, amines have a relatively high rate of reaction with dissolved carbon dioxide. However, their performance as solvents is limited by a high heat of absorption, along with issues associated with amine loss and degradation and corrosion [103]. One way to improve the overall solvent system performance for CO_2 capture is to blend a fast reacting amine, such as monoethanolamine (MEA), with a solvent that possesses a low heat of absorption, such as potassium carbonate (K_2CO_3), with the potential to take advantage of the benefits of both solvents.

The overall reactions between CO_2 and a primary amine RNH_2 can be derived from Equation 2-11 and Equation 2-12 as:

$$CO_2 + RNH_2 \leftrightarrow RNH_2^+COO^-$$

Equation 6-1

$$RNH_2^+COO^- + B \leftrightarrow RNHCOO^- + BH^+$$

Equation 6-2

The reaction shown in Equation 6-1 results in the formation of a zwitterion intermediate and is rate limiting, while the reaction shown in Equation 6-2 is the removal of a proton from the zwitterion by any base, B, to form the carbamate $RNHCOO^-$. At low CO_2 loadings the species water, hydroxide ions and MEA itself can act as bases [34]. In pure MEA solutions, the reaction rate is thus given by:

$$r_{CO2} = -k_{MEA}[CO_2][MEA]$$

Equation 6-3

The CO_2 absorption capacity of amine solvents is controlled by the consumption of the amine to form the carbamate. Furthermore, because of the

high exothermicity of Equation 6-2, the carbamate is also responsible for the high heat of absorption of amine solvents. These carbamates and their protonated counterparts can, however, undergo hydration reactions to regenerate the amine and produce a bicarbonate anion (Equation 6-4).

$$RNHCOO^- + H_2O \leftrightarrow RNH_2 + HCO_3^-$$

Equation 6-4

In this study, the reaction between CO_2 and MEA within carbonate solutions is characterized and its activation energy is measured under temperatures, pH levels and ionic strengths relevant to industrial carbon capture systems employing carbonate solutions. Under these experimental conditions the apparent rate constant k_{obs} can then be expressed as:

$$k_{obs} = k_{OH}[OH^-] + k_{MEA}[MEA]$$

Equation 6-5

Using this experimental kinetic data, a rate-based absorption model employing MEA/K_2CO_3 mixtures has been developed using Aspen Plus™ (version 7.3), which has been found to compare favorably with both bench and pilot scale data [104, 105]. The Aspen Plus™ simulation also provides excellent predictive capability and is a very useful design tool for studying process variables such as temperature, pressure, CO_2 loading and CO_2 removal rate.

6.2 Modeling

A simulation of a MEA-promoted potassium carbonate system was developed based on a default rate-based absorption model of CO_2 into MEA in Aspen Plus™ (Version 7.3). In this model, thermophysical property and reaction kinetic models were based on the work of Austgen *et al.* [106] and Hikita *et al.* [20]. A number of modifications have been incorporated into the default model in order to achieve agreement with pilot plant results [104] using a 32.5 wt% aqueous MEA solution. These modifications include updating the rate of chemical reactions from experimental data and literature values, and adding

binary interaction parameters between different components in the liquid phase. An open-loop absorption/desorption process flowsheet diagram obtained from the default rate-based absorption model from Aspen Plus™ is shown in Figure 6-1.

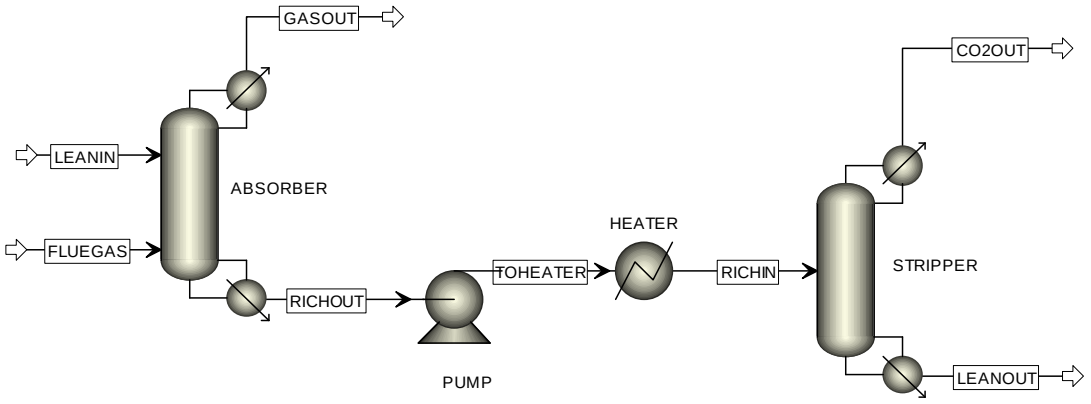

Figure 6-1 Open-loop absorption/desorption process flowsheet diagram within Aspen Plus™.

The aqueous phase reactions occurring within the CO_2-MEA-K_2CO_3-H_2O system can be classified into two categories: (1) those that are rate controlling and (2) those that are more rapid and thus can be assumed to rapidly reach equilibrium. The equilibrium equations include Equation 6-4 and the following equations:

$$RNH_3^+ + H_2O \leftrightarrow RNH_2 + H_3O^+$$

Equation 6-6

$$2\ H_2O \leftrightarrow H_3O^+ + OH^-$$

Equation 6-7

$$HCO_3^- + H_2O \leftrightarrow H_3O^+ + CO_3^{2-}$$

Equation 6-8

The equilibrium constants of these reactions are available in the literature and can be expressed as:

$$\ln K_{eq} = a_1 + {}^{a_2}/_{T} + a_3 \ln T + a_4 T$$

Equation 6-9

Coefficients a_1-a_4 are summarized in Table 6-1 for these equilibrium reactions together with the applicable temperatures and the relevant literature references [106-108].

Table 6-1 Temperature dependence of the equilibrium constants for reactions shown in Equation 6-4, Equation 6-6, Equation 6-7 and Equation 6-8.

Reaction	a_1	a_2	a_3	a_4	T (°C)	Source
Equation 6-4	-3.4	-5851	0	0	40-120	[106, 107]
Equation 6-6	140.9	-13446	-22.5	0	0-225	[108]
Equation 6-7	220.1	-12432	-35.5	0	0-225	[108]
Equation 6-8	6.7	-3091	0	0	40-120	[106, 107]

The rate controlling reactions are Equation 2-4 and Equation 6-1. The reaction rate constant (k) for these two equations is expressed in the form of an Arrhenius equation as follows:

$$k = Ae^{-[E_a/RT]}$$

Equation 6-10

Where R is the universal gas constant (kJ mol^{-1} K^{-1}) and T is temperature (K). Pre-exponential factors (A) and activation energies (E_a, kJ mol^{-1}) for each reaction are summarized in Table 6-2. Rate constants for Equation 2-4 were obtained from the previous chapter as well as prior work [74, 77] in a temperature range of 40 °C - 80 °C and from the work of Pinsent *et al.* [109] for 0 – 40 °C. The kinetic parameters for Equation 6-1 in a temperature range of 43 - 83 °C were taken from the work completed by Thee *et al.* [19]. The equilibrium constants used to calculate the kinetic parameters for the reverse of reactions

shown in Equation 2-4 and Equation 6-1 were obtained from the work done by Austgen *et al.* [106].

Table 6-2 Pre-exponential factors (*A*) and activation energies (E_a) for reactions shown in Equation 6.1-2 and Equation 6.1-4.

Reaction	Direction	A[a]	E_a (kJ mol^{-1})	Reaction order	T (°C)	Source
Equation 2-4	Forward	4.3×10^{13}	55.4	0	0-40	[109]
		2.5×10^{13}	35.8		40-80	[74, 77]
	Reverse	2.4×10^{17}	123.2	0	0-40	[109]
Equation 6-1	Forward	9.8×10^{10}	41.2	0	5.6-35.4	[20]
		2.6×10^{8}	25.3		43-83	This work
	Reverse	3.23×10^{19}	65.5	0	5.6-35.4	[20]

a. The unit of the pre-exponential factor, *A*, varies depending on the order of the reaction. If the reaction is first order, it has the unit s^{-1}. If the reaction is second order, it has the unit M^{-1} s^{-1}.

The CO_2-MEA-K_2CO_3-H_2O vapor-liquid equilibrium was described using an Electrolyte Non Random Two Liquid (E-NRTL) activity model. Binary electrolyte pair parameters were used to predict the activity coefficient of each component in the system. Aspen Plus™ default parameters for MEA and H_2O were used. These are obtained from the work of Austgen *et al.* [106] and have been shown to give an accurate prediction of VLE data for an MEA system [110, 111]. The parameters are claimed to be applicable at a temperature up to 120 °C and an MEA concentration up to 50 wt%. However, such default parameters provide a more limited prediction for carbonate species [80]. Cullinane and Rochelle developed alternate binary interaction parameters for the K_2CO_3-$KHCO_3$ system suitable for carbon capture processes [112]. In this investigation, a combination of the default parameters for MEA and the Cullinane parameters for K_2CO_3-$KHCO_3$ were used to simulate the CO_2-MEA-K_2CO_3-H_2O system.

6.3 Results and Discussion

6.3.1 Wetted Wall Column Kinetics

Figure 6-2 illustrates the effect of the addition of MEA on the pH of a 30 wt% potassium carbonate solution based on experimental results. At 43 °C the addition of 0.5 M, 1.1 M and 2.2 M MEA into the potassium carbonate solution results in an increase in the pH from 10.1 to 10.5, 11.0 and 11.8 respectively. These significant increases in the solvent pH increase the rate of reaction for $CO_2 + OH^-$ and hence the overall absorption rate of CO_2. Table 6-3 summarizes the speciation predicted by Aspen Plus™ under equivalent conditions including the concentration of free amine.

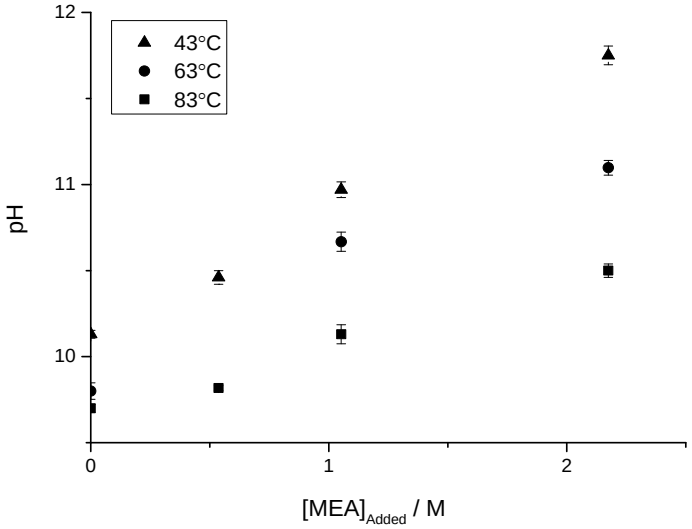

Figure 6-2 Temperature-dependent effect of addition of MEA on the pH of a loaded 30 wt% potassium carbonate solution.

Table 6-3 Speciation results for the wetted wall column experiment obtained from Aspen Plus™.

T (°C)	$[RNH_2]_{added}$	$[RNH_2]_{free}$	$[RNH_3^+]$	$[RNHCOO^-]$	$[HCO_3^-]$	$[CO_3^{2-}]$
43[b]	0.5	0.26	0.28	0.03	0.60	2.73
	1.1	0.58	0.41	0.06	0.46	2.85
	2.2	1.28	0.54	0.10	0.32	2.95
63[b]	0.5	0.34	0.21	0.04	0.72	2.62
	1.1	0.68	0.31	0.06	0.59	2.71
	2.2	1.38	0.43	0.11	0.46	2.80
83[b]	0.5	0.40	0.14	0.04	0.84	2.50
	1.1	0.77	0.22	0.07	0.75	2.56
	2.2	1.49	0.32	0.12	0.63	2.62
63[c]	0.5	0.22	0.32	0.04	1.38	2.28
	1.1	0.48	0.49	0.08	1.17	2.45
	2.2	1.07	0.69	0.16	0.91	2.63

a. The concentration unit of all species displayed in this table is kmol/m^3.
b. The initial concentration of bicarbonate and carbonate ion before the addition of MEA is 0.85 M and 2.42 M respectively (CO_2 loading = 0.15).
c. The initial concentration of bicarbonate and carbonate ion before the addition of MEA is 1.70 M and 1.99 M respectively (CO_2 loading = 0.30).
*Note that $[K^+]$ is not shown but allows charge balance.

Pseudo-first order rate constants (k_{obs}, s^{-1}) for CO_2 reacting in MEA-promoted potassium carbonate at 43 °C, 63 °C and 83 °C are shown in Figure 6-3a. Results demonstrate that, at 63 °C, the addition of MEA in relatively small amounts, 1.1 M (5 wt%) and 2.2 M (10 wt%), accelerates the pseudo-first order rate of absorption of CO_2 in a 30 wt% potassium carbonate solvents by a factor of 16 and 45 respectively. It was also found that an increase in temperature improves the overall absorption of CO_2. An increase in temperature from 43 °C to 63 °C and from 63 °C to 83 °C leads to an increase in the pseudo-first order rate of absorption of CO_2 in a 30 wt% potassium carbonate added with 1.1 M MEA by a factor of 2.3 and 2.5 respectively.

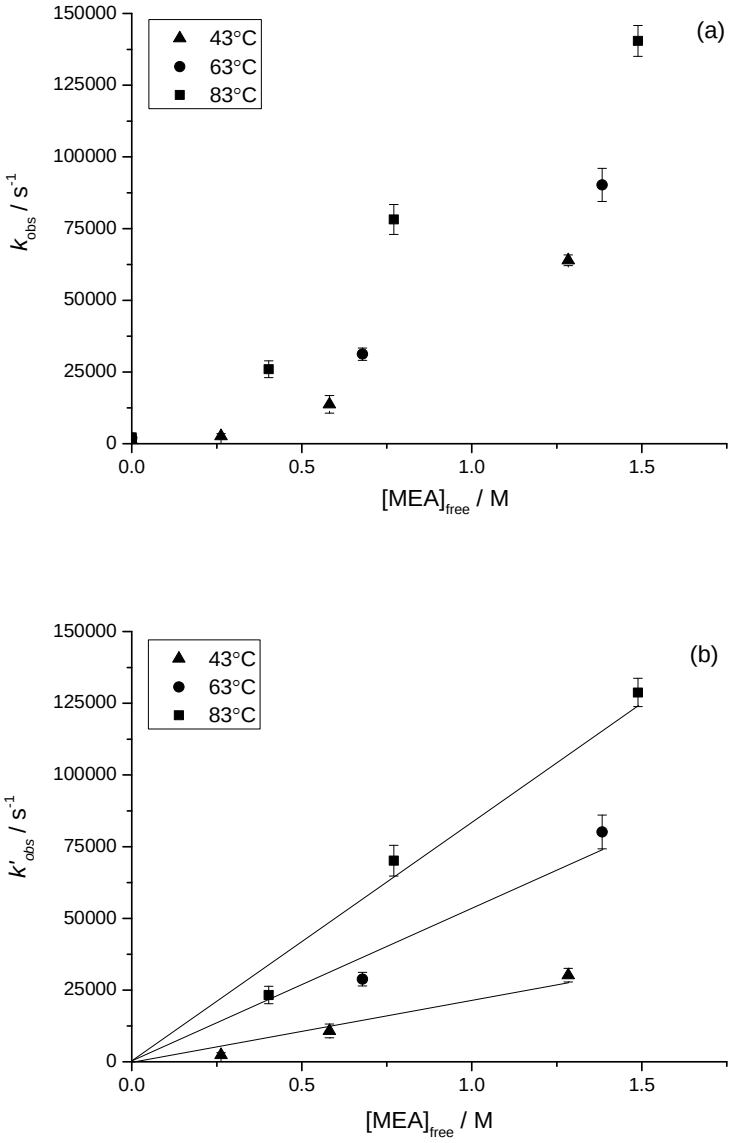

Figure 6-3 (A) Plot of pseudo-first-order reaction rate constant k_{obs} versus concentration of free amine $[MEA]_{free}$ at 43 °C to 83 °C. **(B)** Plot of k'_{obs} (= k_{MEA} [MEA] = $k_{obs} - k_{OH}$ $[OH^-]$) versus $[MEA]_{free}$ at 43 °C to 83 °C. The presence of MEA improves the apparent rate constant (k_{obs}) especially at high temperatures. The reaction rate (k'_{obs}) increases linearly with [MEA] indicating a first-order reaction rate. The slopes of these lines represent the rate constant k_{MEA}.

When the rate component due to CO_2 + OH^- is excluded (k'_{obs} = k_{MEA} [MEA] = $k_{obs} - k_{OH}$ $[OH^-]$), non-zero rate constants are observed, which can be attributed to the reaction of MEA with CO_2. Figure 6-3b shows a linear

relationship between k'_{obs} and [MEA] indicating that the assumption of pseudo-first-order kinetics is valid. The slopes of these lines provide values of the rate constant k_{MEA} (M^{-1} s^{-1}) for the CO_2 + MEA reaction. This finding is in agreement with the work of Aboudheir *et al.* [25, 113] who conducted their experiments over a range of MEA concentrations (0.19 M – 3.88 M) and a lower temperature range (20 °C – 40 °C), and concluded that the order of reaction can be approximated to 1 with respect to the concentration of MEA. The same conclusion was also drawn by Versteeg *et al.* [22] who summarized works from other researchers and found the data to be consistent over a range of MEA concentrations (0 M – 4.8 M) and a temperature range 0 °C – 40 °C.

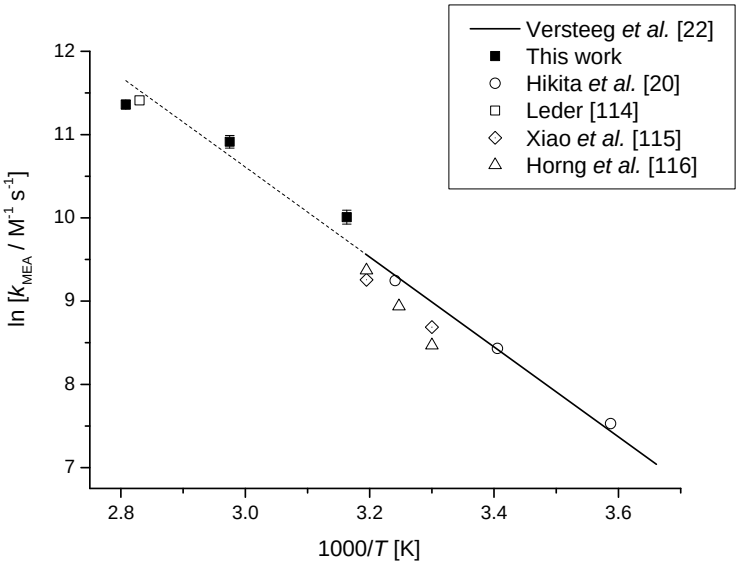

Figure 6-4 Arrhenius plot of lnk_{MEA} versus 1000/T for the reaction between MEA and CO_2 from this work compared with the extrapolated Arrhenius fit (dashed line) of a work by Versteeg *et al.* [22] and works by Hikita *et al.* [20], Leder [114], Xiao *et al.* [115], and Horng *et al.* [116].

For the MEA + CO_2 reaction the Arrhenius expression k_{MEA} [M^{-1} s^{-1}] = $4.24\times10^{9}\exp(-3825/T\ [K])$ from 43 °C to 83 °C is obtained, where the activation energy is 31.8 kJ mol^{-1}. Figure 6-4 shows that measured rate constants in this work are similar (deviation < 6 %) to the extrapolated data from work done in a lower temperature range (5.6 °C < T < 35.4 °C) and MEA concentration (0.0152

M < [MEA] < 0.177 M) by Hikita *et al.* [20]. Good agreement (deviation < 5 %) was also found between the experimental results obtained in this study and the model predictions provided by Versteeg *et al.* [22]. It is important to note that both work by Hikita *et al.* [20] and work by Versteeg *et al.* [22] were done in aqueous MEA without the presence of potassium carbonate. It was found that data from the present work are also in good agreement with the study conducted using a stirred vessel in the presence of potassium carbonate at a high temperature (i.e. 80 °C) by Leder [114]. Data from the present work were also compared with those from more recent work done at lower temperatures by Xiao *et al.* [115] and Horng *et al.* [116]. It is important to note that the data from previously mentioned authors are in good agreement with the model predictions provided by Versteeg *et al.* [22]. Indeed the Versteeg correlation provides the best overall fit to the data across the full temperature range.

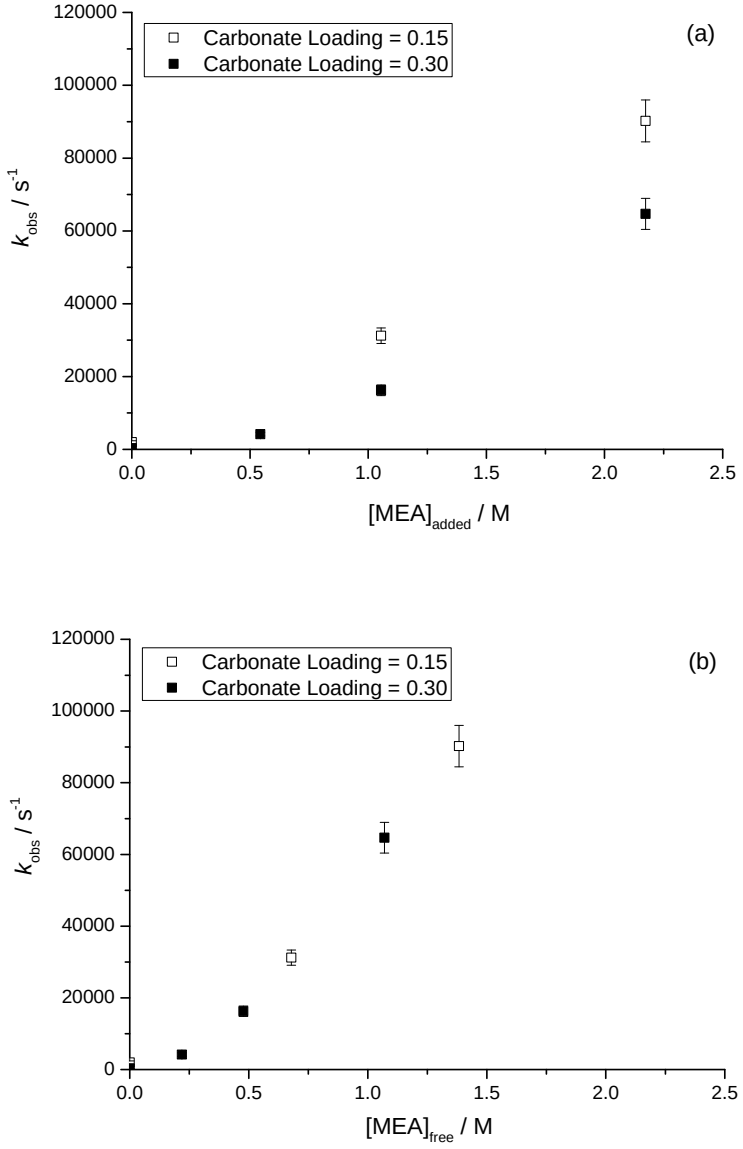

Figure 6-5 (A) Plot of k_{obs} versus concentration of MEA added to a 30 wt% potassium carbonate solution at different carbonate loadings at 63 °C. **(B)** Plot of k_{obs} versus concentration of free MEA at different carbonate loadings at 63 °C. An increase in carbonate loading decreases the concentration of free amine in the solution and thus, the overall absorption of CO_2 into MEA-promoted potassium carbonate.

The pseudo-first-order rate constant k_{obs} was found to decrease with increasing CO_2 loading in the liquid as shown in Figure 6-5. This can be explained mainly due to the decrease in free amine concentration and the pH or

hydroxyl ion concentration with increasing CO_2 loading. Excluding the rate component attributed to the reaction $CO_2 + OH^-$, Figure 6-6 shows the plot of k'_{obs} versus the concentration of free MEA. It can be deduced from this figure that loading does not affect the rate constant k'_{obs} when the concentration of active MEA is taken into account.

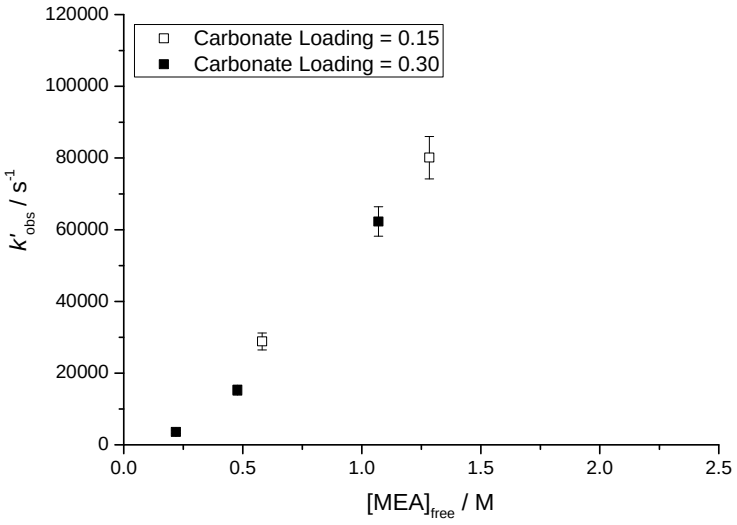

Figure 6-6 Plot of k'_{obs} versus concentration of free MEA at different carbonate loadings at 63 °C. Loading does not affect rate constant k'_{obs} when the concentration of active MEA is taken into account.

6.3.2 Aspen Plus™ Model Development and Validation

<u>CO_2-MEA-H_2O System</u>

The model was used to simulate a CO_2 capture pilot plant that employed a 32.5 wt% aqueous MEA solution as the capture agent. Flue gas and inlet solvent compositions as well as the absorber specification in the simulation were matched to the pilot plant [104]. The absorber had a total height of 11.1 m, an inside diameter of 42.7 cm and two 3.05 m packed beds with a collector plate. The packing selected for the simulation was IMTP No. 40, a random metal packing with a specific area calculated as 145 m^2/m^3. Mass transfer coefficients and interfacial area for IMTP No. 40 were predicted using the correlation presented by Onda *et al.* [117].

Simulation results as well as experimental performance data over 7 cases have been summarized in Table 6-4. Results show good agreement (deviation < 13%) between pilot plant data and simulation results.

Table 6-4 CO_2-MEA-H_2O simulations results compared to pilot plant data [104].

No	Lean loading	Gas composition	Gas rate	Liquid rate	CO_2 removal (%)	
	[CO_2]/[MEA]	CO_2 (mol %)	(m^3/min)	(L/min)	Experimental	Simulation
1	0.28	18.0	8.2	30.1	69	72
2	0.29	16.9	8.2	60.8	86	79
3	0.23	17.0	11.0	39.4	72	74
4	0.23	17.1	10.9	56.8	87	80
5	0.23	16.8	11.0	83.1	94	82
6	0.28	17.0	5.6	42.8	95	89
7	0.28	17.9	5.5	42.6	80	89
8	0.28	17.5	5.5	40.7	95	89
9	0.28	16.6	11.0	54.9	70	73

CO_2-K_2CO_3-H_2O System

The model was also used to simulate data collected from a CO_2 capture pilot plant operated at Hazelwood power station which employed a 30 wt% unpromoted potassium carbonate solvent [102, 118]. Inlet stream compositions and column specifications were again matched to the pilot plant. The simulation results presented in Table 6-5 were found to be in agreement with the pilot plant data (deviation < 20%). The gas and solvent temperatures in the absorber and regenerator obtained from the simulation are higher than the pilot plant data as the simulation does not directly account for heat loss from the vessels.

Table 6-5 CO_2-K_2CO_3-H_2O simulations results compared to pilot plant data at Hazelwood power station [102].

Unit	Stream	Parameter	Plant data	Simulation	Deviation (%)
Absorber	Gas-inlet	*T* (°C)	44.7	*Input*[a]	-
		P (kPag)	3.2	*Input*[a]	-
		Flowrate (kg h^{-1})	5602	*Input*[a]	-
	Gas-outlet	*T* (°C)	38.1	41.3	-8.4
		P (kPag)	0.3	0	-
		Flowrate (kg h^{-1})	4360	4383	-0.5
	Solvent-inlet	*T* (°C)	40.1	*Input*[a]	-
		Flowrate (kg h^{-1})	39870	*Input*[a]	-
	Solvent-outlet	*T* (°C)	43.6	54.2	-19.6
		Flowrate (kg h^{-1})	39940	41089	-2.9
Regenerator	Column	*T* (°C)	115	*Input*[a]	-
	Solvent-inlet	*T* (°C)	113	*Input*[a]	-
	Solvent-outlet	*T* (°C)	-	105.9	-
	Vapour-outlet	*T* (°C)	110.3	113.3	-2.7
		P (kPag)	48.1	49.1	-2.1
		Flowrate (kg h^{-1})	2000	*Input*[a]	-

a. Some of the pilot plant data were used as input data in the simulation model.

<u>CO_2-MEA-H_2O Simulation Compared to a Large Scale Industrial CO_2 Capture Plant</u>

The simulation model was also used to simulate an industrial scale CO_2 capture process from a 600 MWe bituminous coal fired power plant station [105]. The flowrate and composition of the flue gas from the power plant are used as inputs to the simulation model. A 30 wt% MEA solution is used to facilitate the absorption/desorption process in the capture plant. The simulation results presented in Table 6-6 are found to match (deviation < 5%) the pilot plant data.

Table 6-6 CO_2-MEA-H_2O simulations results compared to a large scale CO_2 capture plant using flue gas from a 600 MWe bituminous coal fired power plant station [105].

Unit	Stream	Parameter	Plant data	Simulation	Deviation (%)
Absorber	Gas-inlet	*T* (°C)	50	*Input*[a]	-
		P (kPa)	101.6	*Input*[a]	-
		Flowrate (kg h^{-1})	2.2×10^6	*Input*[a]	-
	Gas-outlet	CO_2 removal (%)	90	90	0
	Solvent-inlet	*T* (°C)	50	*Input*[a]	-
		P (kPa)	180	*Input*[a]	-
		Flowrate (kg h^{-1})	7.2×10^6	*Input*[a]	-
		CO_2 loading	0.24	*Input*[a]	-
	Solvent-outlet	*T* (°C)	51	49.5	+3
		P (kPa)	101.3	101.6	-0.3
		Flowrate (kg h^{-1})	7.4×10^6	7.5×10^6	-0.4
		CO_2 loading	0.48	0.48	+1
Regenerator	Column	*T* (°C)	108	103	+5
		P (kPa)	130	131	+1
		Thermal energy (GJ/ton CO_2)	4.2	4.5	+5

a. Some of the pilot plant data were used as input data in the simulation model.

Model Limitations

It is essential to note that the simulation model has a number of limitations. The approach used only accounts for the major reactions involving the components MEA, K_2CO_3 and H_2O. Reactions between MEA and flue gas impurities (such as SO_x and NO_x) which can form heat stable salts and subsequently reduce the capacity of the solvent to absorb CO_2 are not included due to the scope of this work. MEA degradation due to industrial conditions such as high temperatures has also not been taken into account in the simulation model due to limited knowledge on the complicated degradation pathways.

6.4 Conclusions

A comprehensive kinetic and process modeling study on the absorption of CO_2 into MEA-promoted potassium carbonate solutions has been presented in this work. Results show that the addition of MEA has significantly accelerated the apparent pseudo-first-order rate constant, and therefore, the overall absorption of CO_2 into potassium carbonate solutions is improved. Incorporating those experimental results into Aspen Plus™ has enabled the development of a model that can successfully simulate both industrial and pilot plant solvent capture processes employing MEA and K_2CO_3 as the capture solvent. This is a vital first step to simulating MEA-promoted potassium carbonate processes. The rate constants and process model presented in this study have important implications for designing large scale absorption for carbon capture processes employing MEA-promoted potassium carbonate solvents.

CHAPTER 7 - A KINETIC STUDY OF CO_2 CAPTURE WITH POTASSIUM CARBONATE SOLUTIONS PROMOTED WITH VARIOUS AMINO ACIDS: GLYCINE, SARCOSINE AND PROLINE

7.1 Introduction

This chapter focuses on the use of aqueous K_2CO_3 promoted with various primary and secondary deprotonated amino acids (see Table 7-1). A previous study by van Holst *et al.* [56] revealed that these amino acids exhibit a relatively high reaction rate towards CO_2 and possess a rather low pK_a. The rate of reaction is an important factor in reducing the size and therefore the capital costs of the absorber, while a low pK_a is necessary to reduce the energy requirement for CO_2 regeneration [56].

Aqueous amino acids such as glycine, sarcosine and proline exist in three states: acidic, zwitterionic and basic or deprotonated (see Table 7-1). The acidic state and zwitterionic state of the amino acids are much less reactive towards CO_2 than the deprotonated state [56, 119, 120].

Table 7-1 Structures and pK_a of amino acids studied in this work.

Amino acid	Structure			pK_a	Source
	Acidic	Zwitterionic	Basic		
Glycine	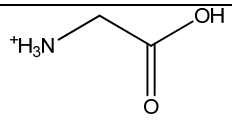	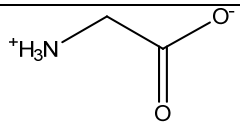	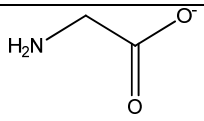	9.8	[100]
Sarcosine	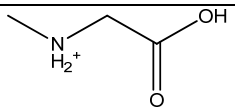	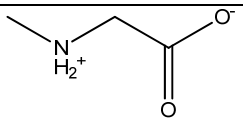	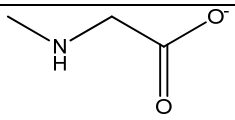	10.6	[56]
Proline	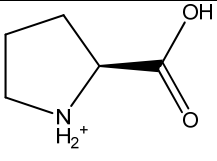	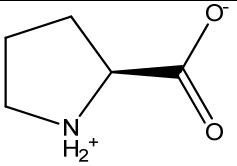	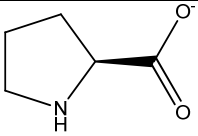	10.2	[89]

*Note that pK_a values indicated in this table were of the deprotonated form of the amino acids and obtained at 25 °C.

In this study, deprotonation of the zwitterionic amino acids is achieved by adding an equimolar amount of a strong base such as potassium hydroxide (KOH) which fully dissociates in water (Equation 7-1).

$$KOH\ (s) \leftrightarrow K^{+} + OH^{-}$$

Equation 7-1

The deprotonation of the zwitterions can then be written as:

$$^{+}NH_2R_1R_2COO^{-} + OH^{-} \rightleftharpoons NHR_1R_2COO^{-} + H_2O$$

Equation 7-2

A number of researchers [50, 56, 119, 121] have shown that the reaction between CO_2 and the deprotonated amino acids the proceeds via a zwitterionic carbamate intermediate (Equation 7.1-6), similar to that of Equation 2-11.

$$CO_2 + NHR_1R_2COO^{-} \underset{k_{-1}}{\overset{k_2}{\rightleftharpoons}} {}^{-}OOCNH^{+}R_1R_2COO^{-}$$

Equation 7-3

This reaction is followed by the removal of a proton from the zwitterionic carbamate by any base, B, to form a neutral carbamate as shown in Equation 7-4. In this work, water (H_2O), carbonate ions (CO_3^{2-}), bicarbonate ions (HCO_3^{-}) and the deprotonated amino acid (AA) itself can all act as bases.

$$^{-}OOCNH^{+}R_1R_2COO^{-} + B \underset{k_{-b}}{\overset{k_b}{\rightleftharpoons}} {}^{-}OOCNR_1R_2COO^{-} + BH^{+}$$

Equation 7-4

This two-step reaction mechanism was proposed by Caplow [17] and used previously by Danckwerts [122] to explain the reactions of CO_2 with alkanolamines. The overall reaction rate for the reaction of CO_2 with potassium salts of glycine, sarcosine and proline can then be expressed in a comparable equation to Equation 2-17.

$$r_{CO_2} = -\frac{k_2[CO_2][AA]}{1 + \frac{k_{-1}}{\sum k_b[B]}}$$

Equation 7-5

$$r_{CO_2} = -\frac{k_2[CO_2][AA]}{1 + \frac{k_{-1}}{k_{AA}[AA] + k_{H2O}[H_2O] + k_{CO3}[CO3^{2-}] + k_{HCO3}[HCO3^{-}]}}$$

Equation 7-6

If the formation of the zwitterionic carbamate (Equation 7-3) is the rate limiting step, then $1 >> k_{-1}/\sum k_b[B]$ and thus, Equation 7-6 reduces to a simple second order kinetic relationship as follows:

$$r_{CO_2} = -k_2[CO_2][AA]$$

Equation 7-7

When the pH of the solution is above 10, the contribution of the CO_2 + OH^- reaction to the overall consumption of carbon dioxide must also be taken into account (Equation 2-4 and Equation 2-5). Therefore Equation 7-7 becomes:

$$-r_{CO_2} = k_2[CO_2][AA] + k_{OH}[OH^-][CO_2]$$

Equation 7-8

However, if the proton removal from the zwitterionic carbamate is the rate limiting step (Equation 7-4), then the opposite is true (i.e. $1 << k_{-1}/\sum k_b[B]$) and thus Equation 7-6 becomes:

$$r_{CO_2} = \frac{-k_2[CO_2][AA](\sum k_b[B])}{k_{-1}}$$

Equation 7-9

$$k'obs = \frac{-k_2[AA](k_{AA}[AA] + k_{H2O}[H_2O] + k_{CO3}[CO3^{2-}] + k_{HCO3}[HCO3^{-}])}{k_{-1}}$$

Equation 7-10

In this latter case, the reaction order dependency on the amino acid concentration varies from 1.0 ($k_{AA}[AA] \ll k_{H2O}[H_2O]+k_{CO3}[CO_3^{2-}]+k_{HCO3}[HCO_3^-]$) to 2.0 ($k_{AA}[AA] \gg k_{H2O}[H_2O]+k_{CO3}[CO_3^{2-}]+k_{HCO3}[HCO_3^-]$). This phenomenon is commonly observed in the absorption of CO_2 into secondary alkanolamines and the aqueous potassium salt of taurine [22, 50, 122].

In the presence of potassium carbonate where the pH of the solution is above 10, Equation 7-9 becomes:

$$-r_{CO_2} = \frac{k_2[CO_2][AA](\sum k_b[B])}{k_{-1}} + k_{OH}[OH^-][CO_2]$$

Equation 7-11

Using a wetted wall column (WWC), the reactions between CO_2 and the amino acids glycine, sarcosine and proline in their deprotonated form have been studied and their activation energy is measured under temperatures, pH levels and ionic strengths relevant to industrial CO_2 capture systems employing carbonate solutions.

7.2 Results and Discussion

7.2.1 NMR Analysis

NMR spectroscopy was used to determine the ratio of carbamate to free amino acid in a 30 wt% potassium carbonate solution before and after CO_2 absorption. Figure 7-1 displays a typical ^1H NMR spectrum of glycine and sarcosine in a pre-loaded 30 wt% potassium carbonate solution. Due to the overlapping peaks occurring in the ^1H NMR spectra of proline, ^{13}C NMR analysis was necessary to calculate the concentration of deprotonated proline. Figure 7-2 displays a typical ^{13}C NMR spectrum of proline. The chemical shift of the internal references D_2O (for ^1H NMR spectroscopy) and 1,4-dioxane (for ^{13}C NMR spectrocopy) were assigned as 4.8 ppm and 66.5 ppm respectively [123]. In the ^{13}C NMR analysis, the chemical shift of carbonate and bicarbonate ions appeared at around 168 ppm [121, 124]. As the sample was mixed with a considerable amount of D_2O, the labile OH and NH protons exchanged rapidly

with the deuterium ions forming HDO. The signal of the OH and NH simply disappeared from the ^{1}H NMR spectrum or was replaced by a weak signal close to chemical shift (δ) 4.8 coming from suspended droplets of HDO [123].

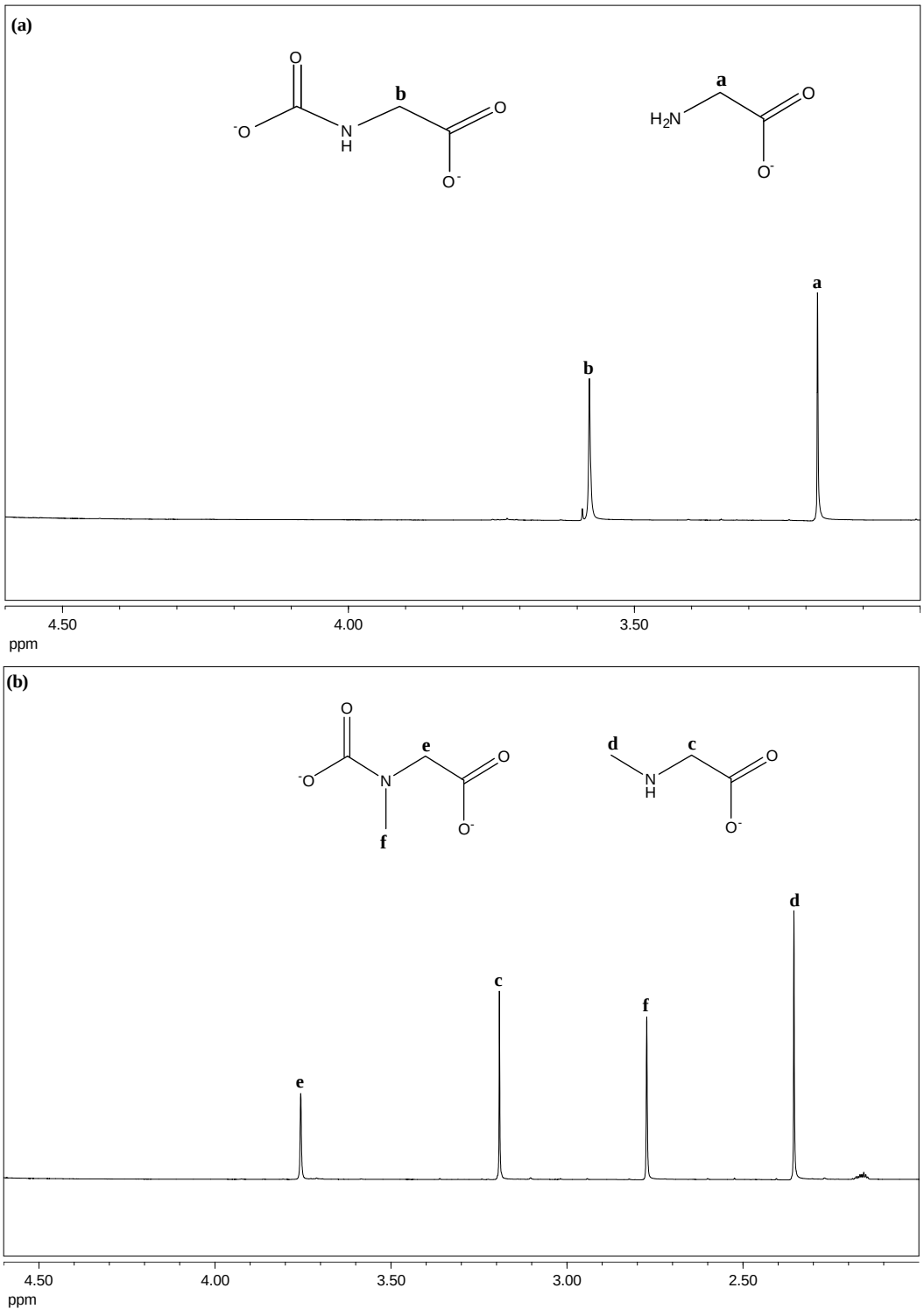

Figure 7-1 ^{1}H NMR spectra of **(A)** glycine and **(B)** sarcosine as well as their equivalent carbamate species in a 30 wt% potassium carbonate solution with 1 M added amino acid concentration. D_2O was used as an internal reference.

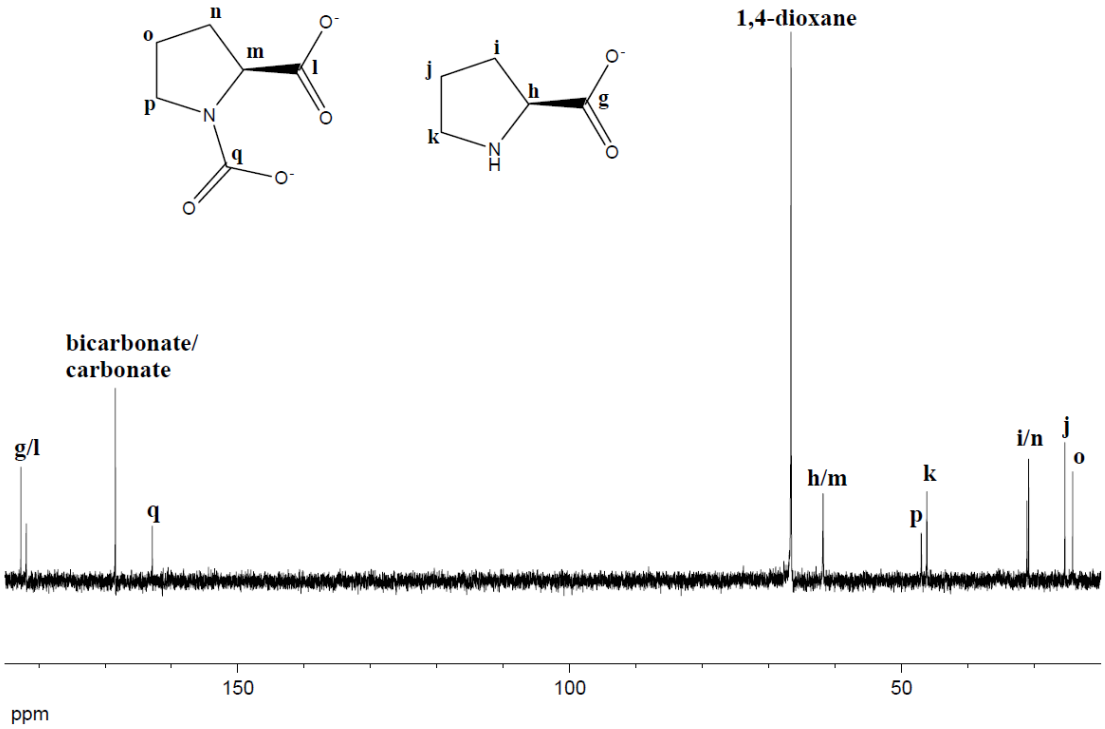

Figure 7-2 ^{13}C NMR spectra showing deprotonated proline and its carbamate in a 30 wt% potassium carbonate solution with 2 M added proline concentration. The chemical shift of 1,4-dioxane as an internal reference was assigned at 66.5 ppm.

The ratio of the concentration of the deprotonated amino acid to its carbamate is proportional to the ratio of the area under the peak of the corresponding species. For example, the ratio of glycine to its carbamate is proportional to the ratio of the area under peak 'a' to the area under peak 'b' (see Figure 7-1a). Table 7-2 summarizes the chemical shift (δ) of the species present in ^{1}H and ^{13}C NMR analysis as well as the concentration of deprotonated or active amino acid based on this ratio. It is important to note that for concentrations of 0.5 M proline, only a trace amount of active proline was found in the liquid sample leading to peak 'j' and peak 'k' being undetectable. In addition, sample dilution (by a factor of 3 to 18 in volume) and measurement temperature (25 °C - 80 °C) have a small effect (deviation < 14.7 % for sample dilution and < 13.5 % for measurement temperature) on the NMR results.

Table 7-2 Concentration of active or deprotonated amino acid (AA) and chemical shift (δ) of species present in ^{1}H NMR and ^{13}C NMR spectra at different added amino acid concentrations.

Deprotonated	Carbamate	$[AA]_{added}$ / M	δ* / ppm								$[AA]^{**}_{active}$ / M
Glycine			a	b							
		0.5	3.2	3.5							0.14
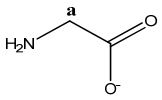	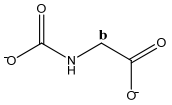	1.0	3.2	3.6							0.40
		1.5	3.1	3.5							0.67
		2.0	3.2	3.5							1.10
Sarcosine			d	f	c	e					
		0.5	2.4	2.7	3.3	3.7					0.17
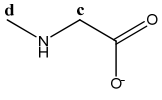	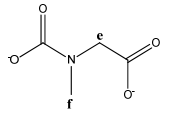	1.0	2.4	2.8	3.2	3.8					0.42
		1.5	2.3	2.8	3.1	3.7					0.67
		2.0	2.3	2.8	3.1	3.8					1.05
Proline			o	j	i/n	k	p	h/m	q	g/l	
		0.5	24.2	- †	31.1	- †	47.1	61.9	162.9	182.8	Trace
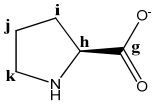	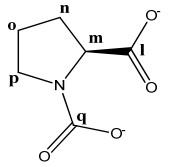	1.0	24.2	25.3	31.2	46.2	47.1	61.9	162.9	182.7	0.21
		1.5	24.1	25.3	31.0	46.1	46.9	61.7	162.8	182.6	0.86
		2.0	24.2	25.4	30.9	46.2	47.0	61.8	162.9	182.7	1.26

* Results presented here were obtained from ^{1}H NMR analysis for glycine and sarcosine and ^{13}C NMR analysis for proline.

** Ratio of the concentration of active or deprotonated amino acid to the concentration its carbamate is proportional to the ratio of the area under its corresponding peak in the ^{1}H and ^{13}C NMR spectrum.

† Intensity of 'j' and 'k' peaks at 0.5 M added proline concentration was very low indicating small amount of active or deprotonated proline.

7.2.2 Wetted Wall Column Kinetics

Figure 7-3 illustrates the effect of adding deprotonated glycine, sarcosine, and proline on the pH of a pre-loaded 30 wt% potassium carbonate solution at 60 °C. In all cases the addition of deprotonated amino acids results in a significant increase in the solution pH. The addition of glycinate and sarcosinate from 0 M to 2 M increases the pH in each solution by very similar amounts. The addition of deprotonated proline results in a greater increase in

solution pH than glycinate and sarcosinate. An increase in the solvent pH increases the rate of the CO_2 + OH^- reaction and hence improves the overall absorption rate of CO_2.

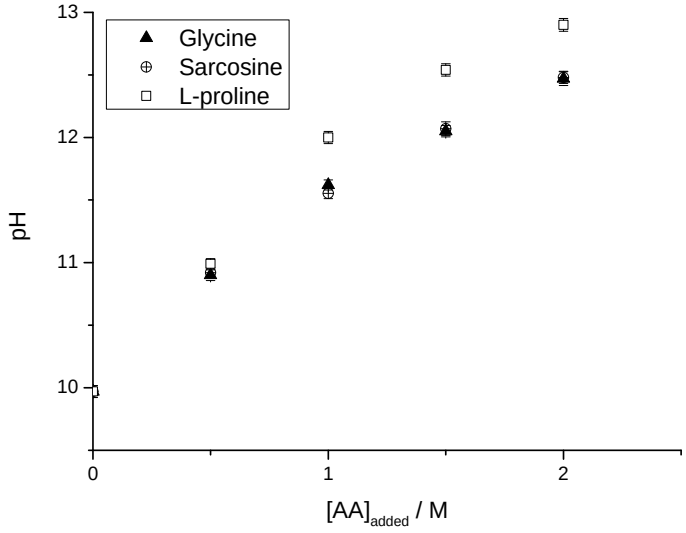

Figure 7-3 The pH of a pre-loaded 30 wt% potassium carbonate solution with different concentrations of glycinate, sarcosinate and prolinate at 60 °C.

Pseudo-first order rate constants (k_{obs}, s^{-1}) for CO_2 reacting in a K_2CO_3 solution promoted with glycine, sarcosine, and proline from 40 °C to 82 °C are shown in Figure 7-4a, Figure 7-5a and Figure 7-6a respectively.

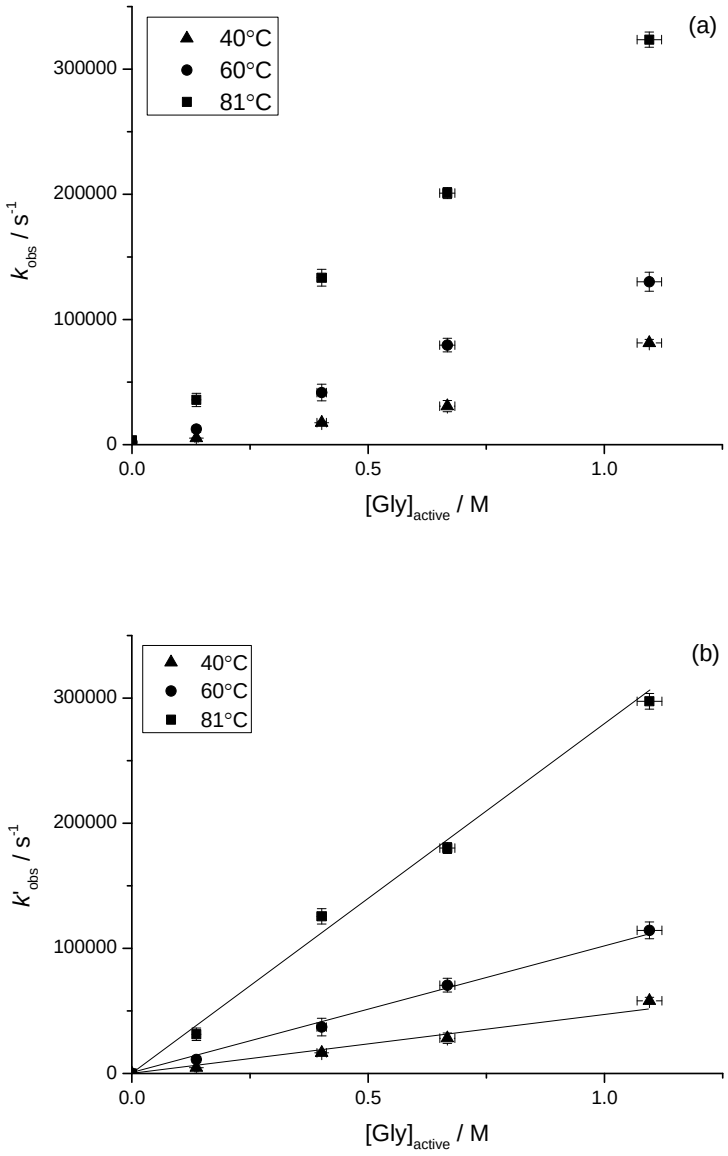

Figure 7-4 (A) Plot of the pseudo-first-order reaction rate constant k_{obs} versus the concentration of active or deprotonated glycine $[Gly]_{active}$ at 40 °C to 81 °C. **(B)** Plot of k'_{obs} (= $k_{2\text{-}Gly}$ $[Gly]_{active}$ = k_{obs} – k_{OH} $[OH^-]$) versus $[Gly]_{active}$ at 40 °C to 81 °C. The presence of deprotonated glycine increases the apparent rate constant (k_{obs}) especially at high temperatures. The reaction rate (k'_{obs}) increases linearly with $[Gly]_{active}$ indicating a first-order reaction rate. The slopes of these lines represent the rate constant $k_{2\text{-}Gly}$.

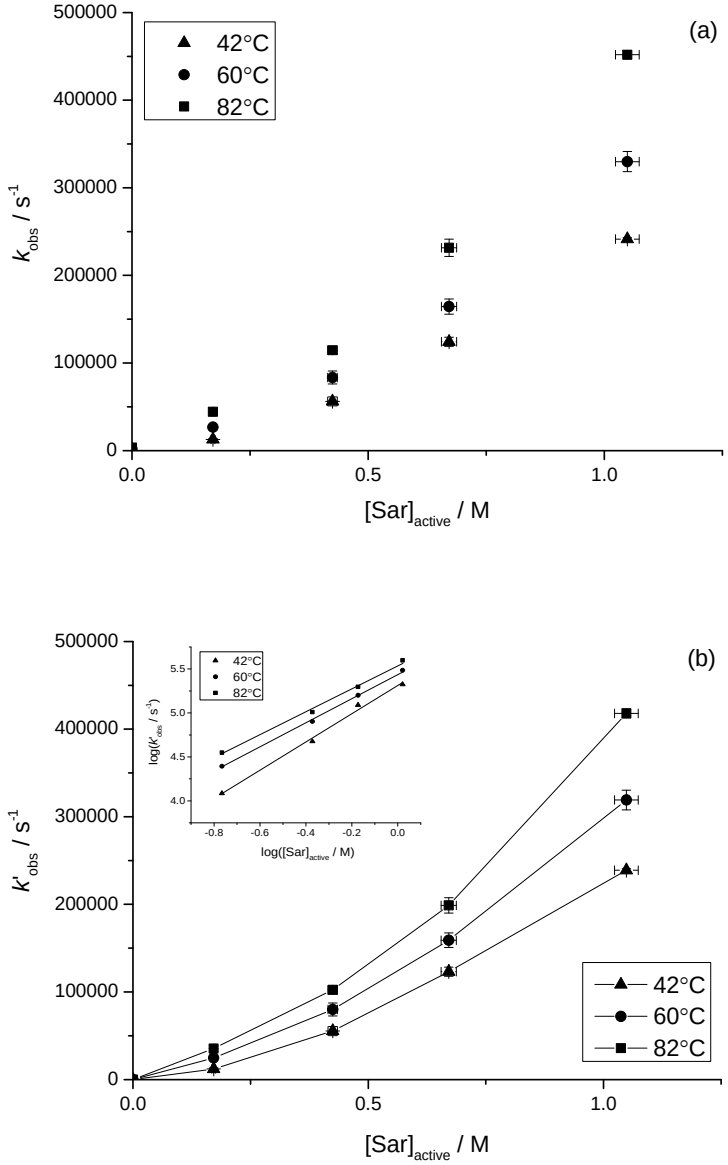

Figure 7-5 (A) Plot of the pseudo-first-order reaction rate constant k_{obs} versus the concentration of active or deprotonated sarcosine $[Sar]_{active}$ at 42 °C to 82 °C. **(B)** Plot of k'_{obs} (= $k_{obs} - k_{OH}$ $[OH^-]$) versus $[Sar]_{active}$ at 42 °C to 82 °C. The presence of deprotonated sarcosine increases the apparent rate constant (k_{obs}). The reaction rate (k'_{obs}) does not increase linearly with $[Sar]_{active}$ indicating a reaction rate greater than first order.

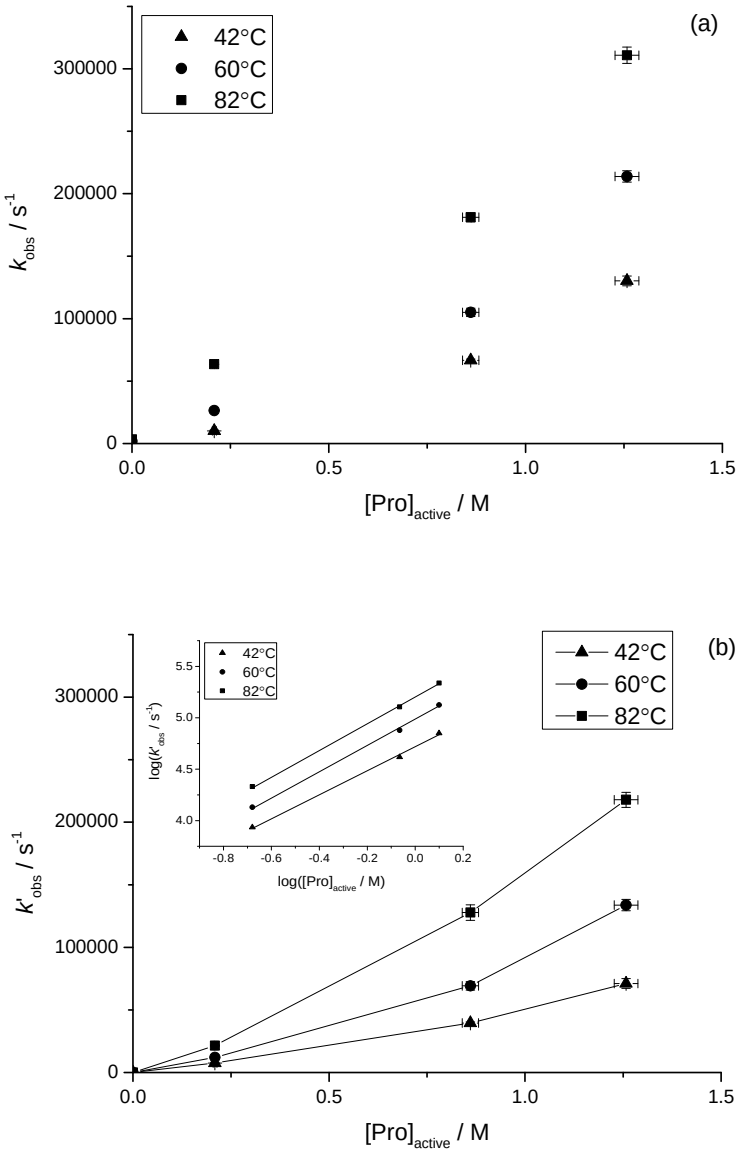

Figure 7-6 (A) Plot of the pseudo-first-order reaction rate constant k_{obs} versus concentration of active or deprotonated proline $[Pro]_{active}$ at 42 °C to 82 °C. **(B)** Plot of k'_{obs} (= $k_{obs} - k_{OH}$ $[OH^-]$) versus $[Pro]_{active}$ at 42 °C to 82 °C. The presence of deprotonated proline increases the apparent rate constant (k_{obs}). The reaction rate (k'_{obs}) does not increase linearly with $[Pro]_{active}$ indicating a reaction rate greater than first order.

Of the three amino acids tested, sarcosine is found to provide the greatest enhancement for the absorption of CO_2 into carbonate solutions. The addition of sarcosine accelerates the rate of absorption of CO_2 into pre-loaded

30 wt% potassium carbonate solvents by a factor of 45 for a 1.0 M (9.6 wt%) solution and 179 for a 2.0 M (18.6 wt%) solution at 60 °C. In comparison, the addition of glycine and proline in the same concentrations, 1.0 M and 2.0 M, and at the same temperature accelerates the rate of absorption of CO_2 by a factor of 23 and 70 for glycine, and 14 and 116 for proline. An increase in temperature from 42 °C to 60 °C and from 60 °C to 82 °C leads to an increase in the rate of absorption of CO_2 in a 30 wt% potassium carbonate solution added with 1.0 M deprotonated sarcosine by a factor of 1.5 and 1.4 respectively. The same effect of increasing temperature on k_{obs} was observed for proline, but is more pronounced for glycine. An increase in temperature from 40 °C to 60 °C and from 60 °C to 81 °C leads to an increase in the rate of absorption of CO_2 in the carbonate solution promoted with 1.0 M deprotonated glycine by a factor of 2.4 and 3.2 respectively.

Glycine

When the rate component due to $CO_2 + OH^-$ is excluded from the observed first order rate constant ($k'_{obs} = k_{obs} - k_{OH}[OH^-]$), non-zero values are observed, which signifies a reaction between the amino acid with dissolved CO_2. Figure 7-4b shows a linear relationship between k'_{obs} and deprotonated glycine concentration $[Gly]_{active}$ indicating a first-order reaction rate with respect to glycine (Equation 7-7). The slopes of these lines provide values of the rate constant $k_{2\text{-}Gly}$ (M^{-1} s^{-1}) for the reaction of CO_2 and deprotonated glycine.

Figure 7-7 shows that the rate constants measured in this study are similar to the extrapolated data from a previous study [120] which was completed using the stopped-flow technique and a WWC over a lower temperature range (25 °C – 62 °C) and different concentrations of deprotonated glycine (0.002 M – 0.005 M for stopped-flow experiments and 0 – 2 M for WWC experiments). For the deprotonated glycine + CO_2 reaction, the Arrhenius expression across the full temperature range of 25 to 81 °C is determined as $k_{2\text{-}Gly}$ [M^{-1} s^{-1}] = $1.22\times10^{12}\exp(-5434/T\,[K])$, where the activation energy is 45.2 kJ mol^{-1}. Good agreement is also found between results from this study and work done in a lower temperature range (5 °C – 30 °C) and concentration (0.009 M – 0.060 M) by Penny *et al.* [21]. The studies by Jensen *et al.* [125], Caplow *et al.*

[17] and Vaidya *et al.* [46] are also included in Figure 7-7 and found to be in good agreement with the Arrhenius fit of the present work. It is important to note that in all these literature references, experiments were conducted in the absence of potassium carbonate.

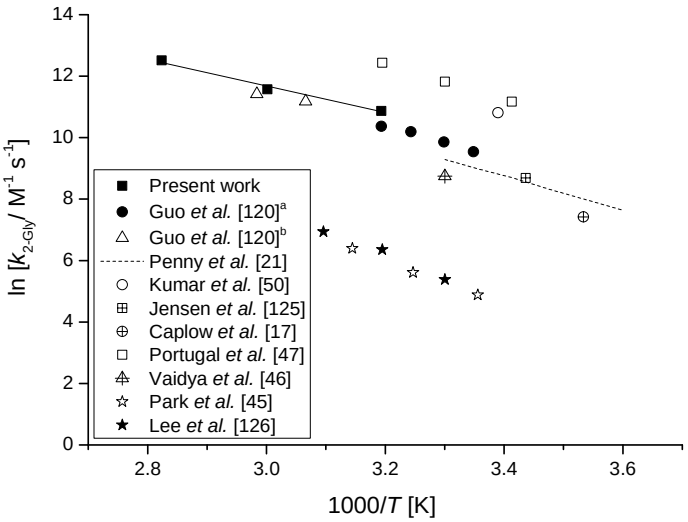

Figure 7-7 Arrhenius plot of $\ln k_{2\text{-Gly}}$ versus $1000/T$ for the reaction between potassium glycinate and CO_2 in the presence of potassium carbonate from this work compared with prior works ([a] stopped-flow device and [b] wetted walled column) [120], the Arrhenius fit (dashed line) of a work by Penny *et al.* [21], works by Kumar *et al.* [50], Jensen *et al.* [125], Caplow *et al.*[17], Portugal *et al.* [47], Vaidya *et al.* [46], and reaction of sodium glycinate and CO_2 obtained from works by Park *et al.* [45] and Lee *et al.* [126].

Despite good agreement with this literature data, experimental results from this work were somewhat lower than the data obtained by Portugal *et al.* [47] and Kumar *et al.* [50]. Both these groups conducted their experiments using a stirred cell reactor and across a broader glycine concentration range (0.1 to 3 M), again in the absence of any carbonate.

Results from the present work are also compared with the works done by Park *et al.* [45] and Lee *et al.* [126] who studied the kinetics of the reaction between sodium glycinate and CO_2, again over a broader concentration range (0.5 M – 3.5 M). At 40 °C, Figure 7-7 shows that the reaction rate constant $k_{2\text{-gly}}$ (M^{-1} s^{-1}) obtained from this work is approximately two orders of magnitude

larger than that of sodium glycinate. As also pointed out by Portugal *et al.* [47], the deviation could be due to the experiments of Park *et al.* [45] and Lee *et al.* [126] not being performed in the pseudo-first-order regime.

Sarcosine and Proline

Figure 7-5b shows a non-linear relationship between k'_{obs} and the deprotonated sarcosine concentration $[Sar]_{active}$ indicating a non-first-order reaction rate with respect to sarcosine. This would suggest that deprotonation of the zwitterionic carbamate (Equation 7-4) is the rate limiting step. Based on the similar trend seen in Figure 7-6b, the same applies for the reaction between CO_2 and proline. As opposed to glycine, the deviations between k'_{obs} and k_{obs} for sarcosine are quite large (< 20% for sarcosine and < 40% for proline) indicating a significant contribution from the reaction of CO_2 with OH^- ion to the overall reaction.

The partial reaction orders with respect to the concentration of the amino acid were determined by calculating the slope of the log-log plots of k'_{obs} shown in Figure 7-5b and Figure 7-6b. The partial reaction orders were obtained in the range of 1.3 – 1.6 (average = 1.4) for sarcosine and 1.2 – 1.3 (average = 1.2) for proline for the temperature range 42 °C – 82 °C. This reaction order suggests that the zwitterion deprotonation step (Equation 7-4) is not fast enough for the zwitterion formation step (Equation 7-3) to be rate controlling. This base-catalyzed behavior is typically observed in secondary alkanolamines such as diethanolamine (DEA), and the aqueous potassium salt of taurine [22, 50, 122].

Partial reaction orders deduced here are consistent with the values reported by Aronu *et al.* [119], Simons *et al.* [127], and Paul *et al.* [128]. Aronu *et al.* [119] reported an average partial order with respect to the concentration of sarcosine to be 1.58 over a range of sarcosine concentrations (1.0 M – 4.0 M) and temperatures (25 °C – 62 °C), while Simons *et al.* [127] observed a partial order of 1.66 over a range of sarcosine concentrations (0.5 M – 3.8 M) and temperatures (25 °C – 35 °C). Paul *et al.* [128] observed a partial reaction order with respect to the concentration of proline to be in the range of 1.36 – 1.40 for proline concentrations 0.5 M – 3.0 M and temperatures 30 °C – 50 °C. This implies that deprotonation by the weak bases HCO_3^- and CO_3^{2-}, which will be

present at higher concentrations in the experiments done in this work, is relatively unimportant.

Using the values of k'_{obs} presented in Figure 7-5b and Figure 7-6b, the kinetic parameters for sarcosine and proline were determined by non-linear regression of Equation 7-10. For both amino acids, it was found that the best fit to the data was obtained by setting k_{CO3} and k_{HCO3} equal to zero. This indicates that the role of carbonate ions (CO_3^{2-}) and bicarbonate ions (HCO_3^-) as bases in Equation 7-4 is limited, while that of water is significant, as expected. Given that k_{AA}/k_{-1} and k_{H2O}/k_{-1} were known from the literature [50, 119, 128], this allowed evaluation of the k_2 values for the two amino acids.

For the deprotonated sarcosine + CO_2 reaction, the Arrhenius expression is determined as:

$$k_{2\text{-Sar}}\ [\text{M}^{-1}\ \text{s}^{-1}] = 6.24\times10^{10}\exp(-1699/T\ [\text{K}])$$

Equation 7-12

For the deprotonated proline + CO_2 reaction, the Arrhenius expression is determined as:

$$k_{2\text{-Pro}}\ [\text{M}^{-1}\ \text{s}^{-1}] = 1.02\times10^{11}\exp(-2168/T\ [\text{K}])$$

Equation 7-13

The use of these parameters (Equation 7-12 and Equation 7-13) within Equation 7-10 adequately correlates with the experimental data. The average deviation between the model predictions and the experimental data were found to be 14.6 % for sarcosine and 14.1 % for proline.

The Arrhenius plot for the reaction between carbon dioxide and the potassium salt of sarcosine from this work compares well with work by Aronu *et al.* [119] (Figure 7-8). However, the available literature for the proline rate constant $k_{2\text{-Pro}}$ does not appear to agree well with the results obtained from this work. Paul *et al.* [128] reported a value of 2.0×10^5 M^{-1} s^{-1} at 40 °C, whereas a value of 1.0×10^8 M^{-1} s^{-1} was obtained in this work at the same temperature. A possible explanation for such discrepancy could be due to the experiments in

this work being carried out at much higher ionic strength conditions. However, this claim may require further investigation using alternate experimental techniques.

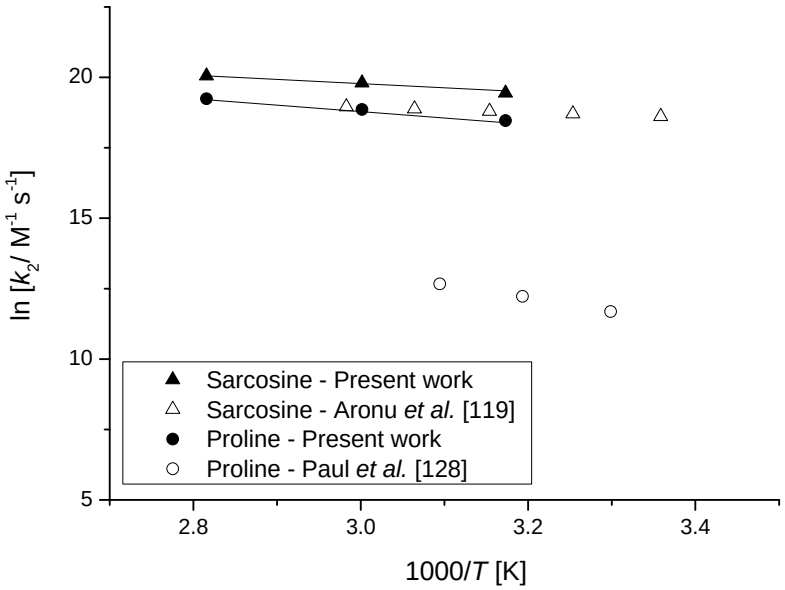

Figure 7-8 Arrhenius plot of lnk_2 of sarcosine and proline versus 1000/T for the reaction between carbon dioxide and potassium salt of sarcosine and proline at high ionic strength from this work compared with a work by Aronu *et al.* [119] and Paul *et al.* [128].

7.3 Conclusions

A detailed kinetic study on the absorption of CO_2 into primary and secondary amino acid promoted potassium carbonate solutions has been presented in this work under conditions similar to industrial CO_2 capture plants. Results show that the addition of glycine, sarcosine and proline has significantly accelerated the apparent pseudo-first-order rate constant, and thus, the overall absorption rate of CO_2 into potassium carbonate is greatly improved.

CHAPTER 8 - CARBONIC ANHYDRASE PROMOTED ABSORPTION OF CO_2 INTO POTASSIUM CARBONATE SOLUTIONS

8.1 Introduction

The enzyme carbonic anhydrase shows excellent potential for enhancing CO_2 capture from flue gas streams. A number of potential technologies for carbon capture have examined the potential to exploit carbonic anhydrase, including solvent technology [129-131], membrane technology [132, 133] and bio-sequestration [134, 135]. Carbonic anhydrase catalyses the hydration of CO_2 to HCO_3^-, and in aqueous carbonate solvents where CO_2 hydration via reaction with OH^- is the rate determining step, it has the potential to significantly increase reaction rates. Moreover, since carbonic anhydrase does not bind CO_2 (as amine solvents do) it should not impact the energy requirements for CO_2 desorption.

The purpose of this chapter is to study the reaction kinetics of CO_2 hydration catalyzed by carbonic anhydrase enzyme using stopped-flow UV/visible spectrophotometry and its performance as a promoter in carbonate solvents using a wetted wall column (WWC). The carbonic anhydrase enzyme tested was supplied by Novozymes Denmark (product code NS81239). The product contains approximately 3 g/L carbonic anhydrase enzyme protein and has an enzyme activity of 900 kWAU/mL and a molecular weight of approximately 27500 g/mol.

8.2 Results and Discussion

8.2.1 Stopped-flow Kinetics

An initial screening of Novozymes NS81239 Carbonic Anhydrase (NCA) has been performed using a stopped-flow apparatus to confirm the activity of the enzyme. The experiments at high enzyme concentrations (> 5 v/v%) are found to be influenced by the solution opacity such that it interferes with the indicator, but experiments carried out in lower concentrations (< 1 v/v%) appeared to provide little interference. Figure 8-1 shows a plot of the pseudo first order rate constant due to the reaction of NCA with CO_2 (k'_{obs}, s^{-1}) against the concentration of enzyme, [NCA]. It is apparent that the addition of NCA

dramatically increases the rate of CO_2 hydration, although the considerable non-linearity in the plot of k'_{obs} against [NCA] suggests that solution opacity at 1 v/v% continues to interfere with the measurements, at least to some extent.

From k'_{obs} the second order rate constant k_{NCA} is estimated to be 3.7×10^7 M^{-1} s^{-1} at 25 °C and pH 7. It is important to note that the contribution of the reaction of CO_2 with hydroxide ions at these conditions is very low such that k'_{obs} roughly equals k_{obs}. Here k_{enzyme} is obtained by calculating the slope of k'_{obs} against the molar concentration of the enzyme. The uncertainty of the calculated rate constant is relatively large (estimated to be within an order of magnitude) as the molecular weight of the enzyme is unknown and estimated based on the molecular weight of common carbonic anhydrase enzyme, approximately 27500 g/mol.

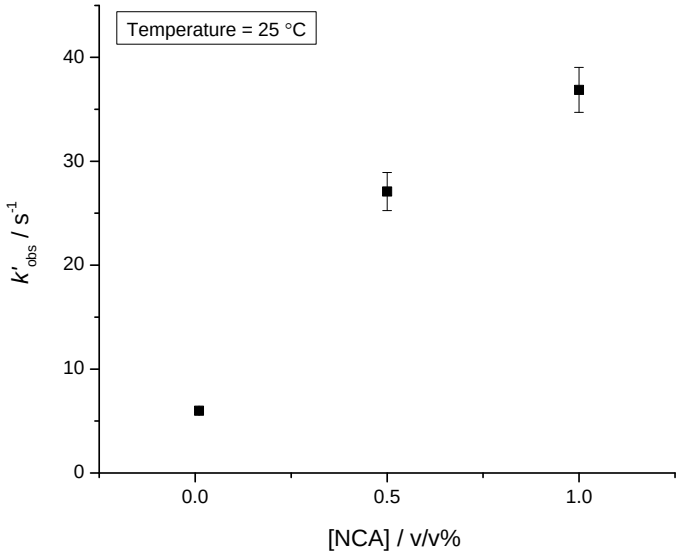

Figure 8-1 Plot of k'_{obs} (= k_{obs} – $k_{OH}[OH^-]$) versus [NCA] at standard temperature, from stopped-flow measurements.

8.2.2 WWC Kinetics

An experimental study on the performance of carbonic anhydrase enzyme NCA as a promoter in the absorption process of CO_2 into a 30 wt% potassium carbonate solvent has been performed from 40 °C to 80 °C and at a

partial pressure of CO_2 of 90 kPa. Using a wetted wall column (WWC), the kinetics of CO_2 reacting with NCA has been characterized under conditions relevant to industrial absorption columns. Three repeat runs were carried out for each set of conditions and values reported here represent averages.

Typical experimental absorption data of CO_2 in an unpromoted 30 wt% potassium carbonate solution and with an addition of 0.1 v/v% (1300 mg mL^{-1}) NCA at 40 °C are plotted in Figure 8-2. This demonstrates that NCA addition has a dramatic effect on the rate of CO_2 uptake by the potassium carbonate solvent, under conditions that are relatively representative of industrial absorber columns (30 wt% K_2CO_3 at 40 °C).

In contrast to some promoters (such as boric acid and amines), addition of small amounts of NCA does not significantly alter the pH of carbonate solvents (*i.e.,* pH ≈ 9.8 – 10.2 for a 30 wt% potassium carbonate solution with 0.15 CO_2 loading) and therefore, results in an unaffected rate of $CO_2 + OH^-$ reaction. Experimental data presented in Figure 8-3 and Figure 8-4 demonstrate that, at 40 °C, addition of NCA (300 mg L^{-1}, 600 mg L^{-1} and 1300 mg L^{-1}) enhances the pseudo-first-order rate constant (k_{obs}, s^{-1}) and thus, the overall absorption process of CO_2 in carbonate solvents by 14 %, 20 % and 34 %, respectively. However, a further increase in [NCA] to 6600 mg L^{-1} is ineffective and presents no greater catalytic effect than that from 1300 mg L^{-1} [NCA]. It is observed that an addition of a relatively large amount of NCA (*i.e.,* [NCA] = 6600 mg L^{-1}) results in flocculation of the NCA in a carbonate solvent which is likely responsible for the plateau in CO_2 flux at high [NCA].

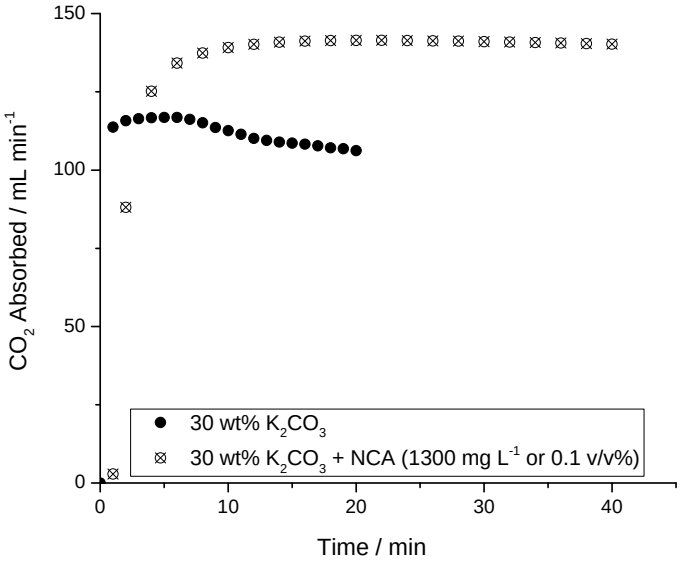

Figure 8-2 Typical absorption rate of unpromoted 30 wt% potassium carbonate and that with an addition of 0.1 v/v% or 1300 mg mL^{-1} NCA in WWC at 40 °C.

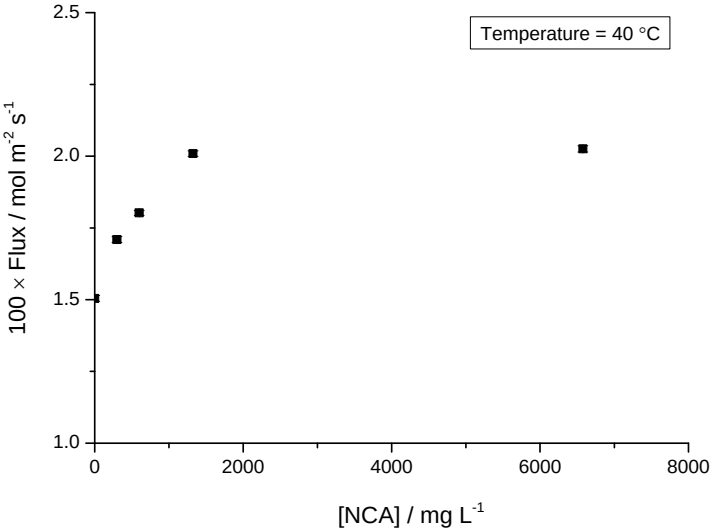

Figure 8-3 CO_2 flux into an enzyme-promoted potassium carbonate solution versus the concentration of enzyme [NCA] at 40 °C.

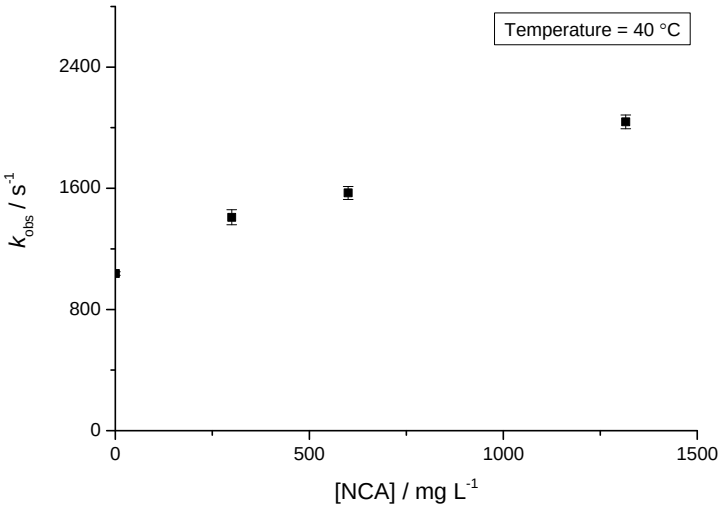

Figure 8-4 Pseudo-first-order rate constant k_{obs} versus the concentration of enzyme [NCA] at 40 °C.

The effect of temperature on performance of NCA in a 30 wt% potassium carbonate solution has also been investigated. As revealed in Figure 8-5, when a concentration of 1300 mg L^{-1} NCA is used, the pseudo-first-order rate constant (k_{obs}, s^{-1}) increases with temperature. An increase in k_{obs} over the temperature range from 40 °C to 80 °C is due to the addition of NCA. This can be confirmed by the non-zero rate component attributed to the reaction with NCA when the contribution of the reaction $CO_2 + OH^-$ ($k'_{obs} = k_{obs} - k_{OH}[OH^-]$) is excluded.

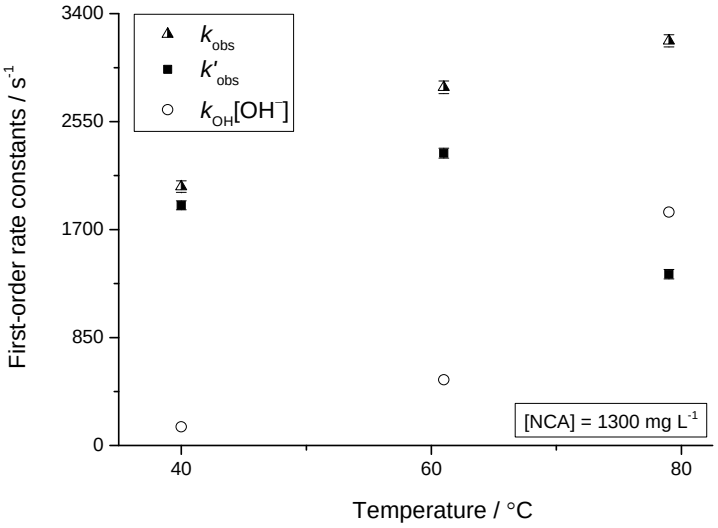

Figure 8-5 Plot of first-order reaction rate constants (k_{obs}, k'_{obs} and $k_{OH}[OH^-]$) versus temperature at a constant concentration of promoter ([NCA] = 1300 mg L^{-1}).

Results shown in Figure 8-5 demonstrate a significant decrease in the rate enhancement by NCA (as shown by k'_{obs}) at 80 °C. The literature indicates that conventional carbonic anhydrase strains can be denatured at temperatures as low as 70 °C [136]. Figure 8-5 also shows that the rate contribution ($k_{OH}[OH^-]$) from the reaction shown in Equation 2-4 increases exponentially with temperature.

The rate constant for NCA ($k_{enzyme} = k'_{obs}$ / [NCA]) was compared with other types of carbonic anhydrase and some zinc complexes which catalyze the conversion of CO_2 to HCO_3^- through the same reaction mechanism as the carbonic anhydrase enzyme. The comparison is summarized in Table 8-1. NCA appears to possess the highest catalytic activity although the data were measured at a higher temperature and pH. The result from the WWC experiments (1.5×10^7 M^{-1} s^{-1} at 40 °C) is comparable with the result obtained from stopped-flow experiments (3.7×10^7 M^{-1} s^{-1} at 25 °C).

Table 8-1 Comparison of the reactivity towards CO_2 of NCA with other carbonic anhydrase enzymes at various pH levels and temperatures.

Complex/Enzyme*	pH	T (°C)	k_{enzyme} (M^{-1} s^{-1})	Source
HCA* I	7	25	2.0×10^5	[137]
HCA II	7	25	1.1×10^6	[137]
Co^{2+}-HCA II	7	25	3.1×10^5	[137]
Zn(II) Complex of 1,5,9-Triazacyclododecane	8 – 10	25	6.0×10^2	[138]
Tripod ZnL1S	9.5	15	3.3×10^3	[139]
NCA	9.8 – 10.2	40	1.5×10^7	This work

* Refer to the source cited for the actual structures of the complex/enzyme

** HCA is the abbreviation of human carbonic anhydrase

The contribution of NCA catalysis in the pseudo-first-order rate constant, defined as k'_{obs} / k_{obs}, over a range of [NCA] and temperatures is demonstrated in Figure 8-6. NCA is estimated to have contributed up to 95 % of the overall absorption of CO_2 into a 30 wt% potassium carbonate solvent at 40 °C. This indicates that the addition of small amount of NCA proves to be useful for CO_2 absorption in carbonate solvents, especially at low temperatures. However, further study needs to be undertaken to understand how carbonic anhydrase enzyme would survive in the regeneration process which is often run at high temperatures.

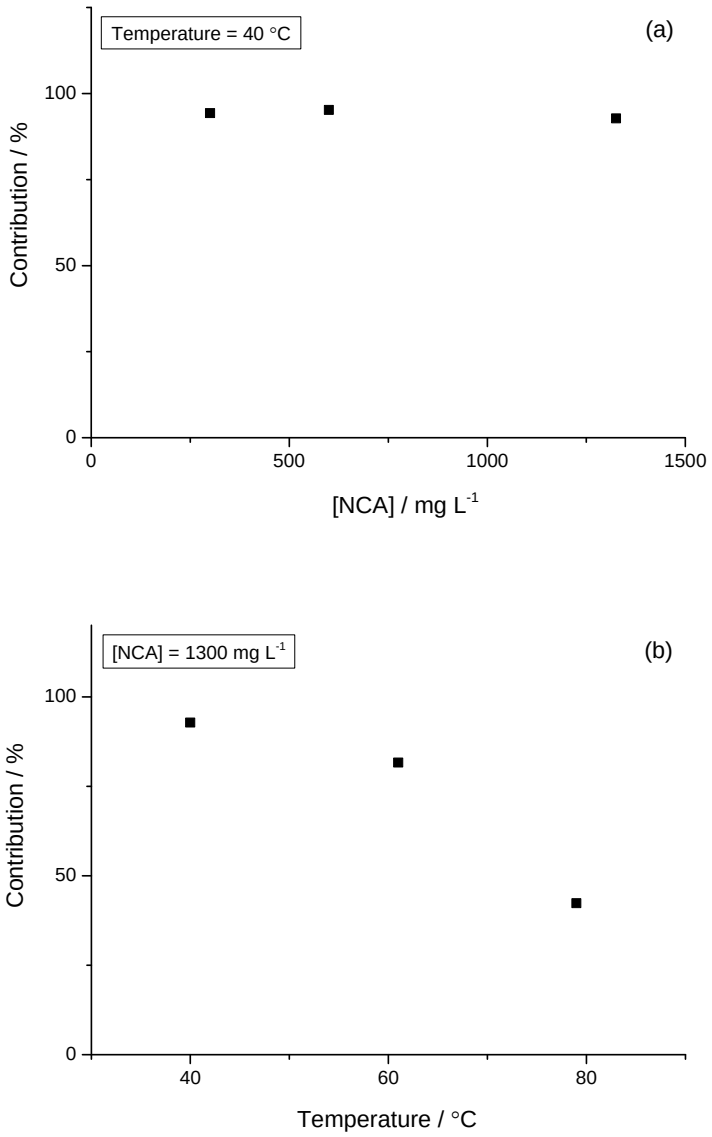

Figure 8-6 Contribution of NCA catalysis in the pseudo-first-order rate constant (k_{obs}, s^{-1}) over: **(A)** various concentration of NCA ([NCA] = 300 mg L^{-1}, 600 mg L^{-1} and 1300 mg L^{-1}) and **(B)** 40 °C to 80 °C.

8.3 Conclusions

An experimental study on the performance of Novozymes NS81239 Carbonic Anhydrase (NCA) as a promoter in the absorption process of CO_2 into potassium carbonate solvents has been presented. Results demonstrate that the addition of NCA (300 mg L^{-1}, 600 mg L^{-1} and 1300 mg L^{-1}) enhances the pseudo-first-order rate constant (k_{obs}, s^{-1}) and thus, the overall absorption process of CO_2 in carbonate solvents by 14 %, 20% and 34 % at 40 °C. It is also found that an addition of a relatively large amount of NCA (*i.e.* [NCA] = 6600 mg L^{-1}) results in flocculation of the NCA in a carbonate solvent which seems to have an adverse effect on the catalytic activity of NCA. Similarly, experimental data indicate that an increase in the temperature to more than 60 °C results in a significant decrease in the rate enhancement by NCA.

CHAPTER 9 - CONCLUSIONS AND RECOMMENDATIONS

9.1 Comparison of the Promoters Studied

A comparison of the partial reaction order, activation energy (E_a), pre-exponential factor (A) and rate constant (k'_{obs}) of a range of amino acid promoters (potassium salts of glycine, sarcosine and proline and sodium salt of glycine), amine-based promoters and boric acid at 1.0 M and 40 °C is presented in Table 9-1. The reactivity of all primary amine promoters under these conditions is comparable, with potassium taurate and ethylenediamine giving slightly better results and sodium glycinate a poorer result. The reactivity of the secondary promoters sarcosine and prolinate is clearly greater, but diethanolamine (DEA) provides a slower rate than most of the primary promoters.

The pre-exponential factor for the CO_2 + MEA reaction, 4.2×10^9 M^{-1} s^{-1}, obtained in this work is relatively small for a primary amine when compared to that of cyclic and secondary amine-based promoters, but is larger than a tertiary amine *N*-methyldiethanolamine (MDEA). The activation energy 31.8 kJ mol^{-1} is somewhat smaller than that of other amine-based promoters indicating that the reaction CO_2 + MEA possesses a larger positive change in reaction rate at an elevated temperature. Additionally, MEA exhibits a comparable rate constant to that of ethylenediamine and a larger rate constant than that of other amines from secondary and tertiary class, although it is approximately 10 times smaller than that of piperazine at 40 °C.

The activation energy of the reaction CO_2 + $B(OH)_4^-$ obtained in this study is larger than most of the other promoters, and is comparable to that of ethylenediamine, sodium glycinate and DEA. $B(OH)_4^-$ also exhibits a comparable rate constant to that of tertiary and hindered amine-promoters and possesses a higher rate constant than that of MDEA. Despite borate offering less rate promotion when compared to piperazine and MEA, borate is environmentally friendly and less toxic and therefore may be regarded as an alternative promoter for carbonate based solvents. Unlike amine solvents, borate does not form a rather stable intermediate such as carbamate when reacting with CO_2 which allows easier regeneration of promoter.

A carbonic anhydrase enzyme NCA exhibits a comparable rate constant to that of a DEA and TEA and a higher rate constant when compared to that of boric acid and MDEA despite a much lower quantity (1300 mg L-1 or around 0.1 wt%) of the enzyme added to carbonate solvents.

Table 9-1 Activation energy, pre-exponential factor and rate constant k'_{obs} (s^{-1}) comparison of 1.0 M amine, amino acid and other promoters.

Class	Promoter	k'_{obs} (s^{-1}) (40 °C)	pK_a (25 °C)	Order[a]	A[b] (M^{-1} s^{-1})	E_a (kJ mol^{-1})	Temp range (°C)	Source
Primary	Potassium taurate	35.6×10^3	9.1	1-1.50	3.2×10^{12}	47.4	12 - 32	[50, 89]
	Potassium glycinate	19.6×10^3	9.8	-	8.5×10^{11}	45.8	5 - 30	[21]
		252×10^3		-	2.8×10^{13}	48.2	20 - 30	[47]
		52.6×10^3		1	1.2×10^{12}	45.2	25 - 81	This work[e]
	Sodium glycinate	0.5×10^3	-	-	2.0×10^{13}	63.8	30 - 50	[126]
		0.4×10^3		1	3.8×10^{12}	59.8	25 - 45	[45]
	Ethylenediamine	35.6×10^3	10.0	1	3.1×10^{13}	53.6	5.5 - 40.4	[100, 140]
	MEA	13.1×10^3	9.5	1	4.4×10^{11}	44.9	5 - 40	[22]
		-			9.8×10^{10}	41.2	5.6 - 35.4	[20]
		-			1.2×10^{11}	42.2	5 - 30	[21]
		-			8.5×10^{11}	46.7	5 - 25	[42]
		11.7×10^3			8.3×10^{15}	71.0	30 - 40	[115]
		10.5×10^3			3.0×10^{11}	44.7	30 - 40	[116]
		21.0×10^3			4.2×10^9	31.8	43 - 83	This work[e]
Secondary	Potassium sarcosinate	38.3×10^3	10.6	1.66	8.7×10^8	26.2	25 - 35	[127]
		14.1×10^7		1.58	2.6×10^9	7.6	25 - 62	[119]
		16.9×10^7		1.39	6.2×10^{10}	14.1	42 - 82	This work[e]
	Potassium prolinate	20.4×10^4	10.2	1.36-1.40	2.4×10^{11}	36.5	30 - 50	[128]
		42.4×10^5		1.17	1.0×10^{11}	18.0	42 - 82	This work[e]
	Diethanolamine (DEA)	3.5×10^3	8.9	2	2.6×10^{12}	53.1	5.8 - 40.3	[20, 100]
Tertiary	Triethanolamine (TEA)	1.4×10^2	7.8	1	5.2×10^{10}	51.5	20 - 40	[20, 100]
	N-methyldiethanolamine (MDEA)	2.8×10	8.5	1	3.1×10^8	42.4	12 - 85	[33, 141]
		1.3×10			4.0×10^8	44.9	30 - 40	[142]
Hindered	Isobutanolamine (AMP)	1.2×10^3	9.7	1	1.1×10^{10}	41.7	25 - 40	[40, 42]
Cyclic	Piperazine	10.3×10^4	9.7	1	4.1×10^{10}	33.6	25 - 60	[68, 100]
Other	Boric acid[c]	1.4×10^2	9.2	1	5.5×10^{11}	57.6	40 - 80	This work[e]
	NCA[d]	1.9×10^3	-	-	-	-	40 - 80	This work[e]

a. The number represents the order of reaction with respect to the promoter.
b. All the reactions (except for DEA) mentioned in this table have an overall order of reaction of 2 and therefore, the pre-exponential factor, A, has the unit M^{-1} s^{-1}. The unit of A for DEA was reported to be M^{-2} s^{-1}.
c. This refers to the active form of boron, $B(OH)_4^-$.
d. The concentration of the carbonic anhydrase enzyme [NCA] is 1300 mg L^{-1} or around 0.1 wt%.
e. These data were measured in a 30 wt% potassium carbonate solution.

Figure 9-1 compares the performance of promoted carbonate solvents studied in this work against the current industrial benchmark solvent (7 M MEA). The literature rate absorption data for pure MEA solvent at high temperatures (> 40 °C) are rare, and thus not shown in Figure 9-1. Of all promoters studied in this work, sarcosine shows the most promising results. At 40 °C, sarcosine-promoted potassium carbonate solvents have a twofold increase in overall rate absorption of CO_2 than pure MEA solvent at 7 M. That being said, the performance of MEA-promoted carbonate solvents and carbonate solvents promoted with glycine and proline has a comparable overall rate of CO_2 absorption as the benchmark solvent.

In comparison to other promoters studied in this work, borate and carbonic anhydrase enzyme performed poorly despite their environmental benignity and affordability. At 40 °C, the overall absorption rate of an unpromoted 30 wt% potassium carbonate is around 1060 s^{-1}. With an addition of 1M borate ($B(OH)_4^-$) and 0.1 v/v% carbonic anhydrase enzyme this number increases to 1200 s^{-1} and 1985 s^{-1} respectively.

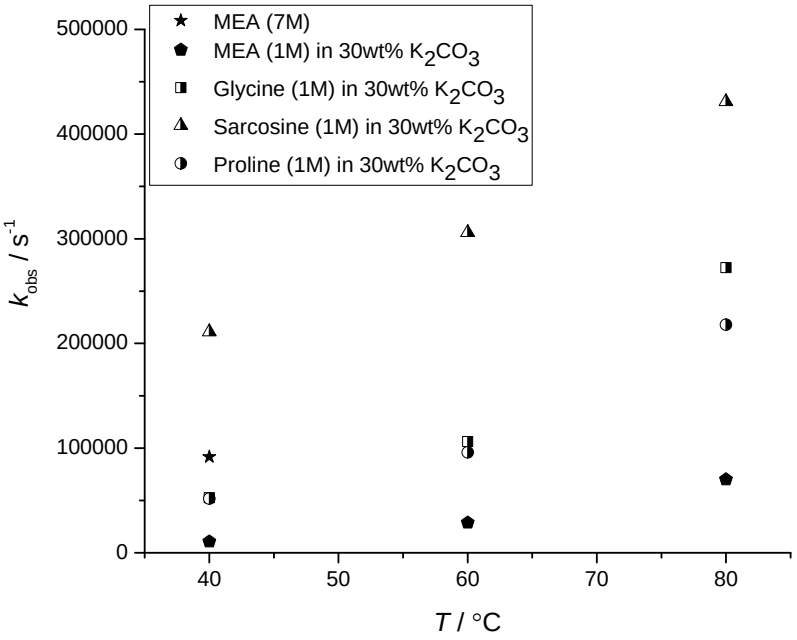

Figure 9-1 Comparison between promoted carbonate solvents studied in this work and industrial benchmark solvent (7 M MEA).

9.2 Conclusions

To date, solvent absorption is unarguably the most mature technology for carbon capture systems. Developing an affordable, readily available and non-toxic solvent is critical to the commercialisation of CCS. Potassium carbonate is one of a few solvents that possess the aforementioned properties. The commercial use of potassium carbonate as absorption solvents has existed since 1904. It is known that potassium carbonate solvents have slow reaction kinetics, and thus, require rate promotion to remain competitive.

A comprehensive kinetic study on the absorption of CO_2 into unpromoted and borate-promoted potassium carbonate solutions is presented in Chapter 5. Results indicate that an addition of a small amount of boric acid has accelerated the apparent pseudo-first-order rate constant, and thus, the overall absorption of CO_2 into potassium carbonate solutions. $B(OH)_4^-$ is found to exhibit a comparable catalytic activity to that of tertiary and hindered amine-promoters.

Chapter 6 presents a comprehensive kinetic and process modeling study on the absorption of CO_2 into MEA-promoted potassium carbonate solutions. Results show that the addition of MEA has significantly accelerated the apparent pseudo-first-order rate constant, and therefore, the overall absorption of CO_2 into potassium carbonate solutions is improved. MEA in carbonate is found to exhibit a comparable catalytic activity to that of ethylenediamine and a larger catalytic activity than that of other secondary and tertiary amines. Incorporating those experimental results into Aspen Plus™ has enabled the development of a model that can successfully simulate both industrial and pilot plant solvent capture processes employing MEA and K_2CO_3 as the capture solvent. This is a vital first step to simulating MEA-promoted potassium carbonate processes.

Chapter 7 presents a detailed kinetic study on the absorption of CO_2 into primary and secondary amino acid promoted potassium carbonate solutions under conditions similar to industrial CO_2 capture plants. Results show that the addition of glycine, sarcosine and proline has significantly accelerated the apparent pseudo-first-order rate constant, and thus, the overall absorption rate of CO_2 into potassium carbonate is improved. Glycine is found to exhibit a

comparable, if not larger, catalytic activity than that of a primary amine-based promoter, MEA. Sarcosine and proline are found to possess a larger catalytic activity than that of a secondary amine-based promoter, DEA.

An experimental study on the performance of Novozymes NS81239 Carbonic Anhydrase (NCA) as a promoter in the absorption process of CO_2 into potassium carbonate solvents has been performed and presented in Chapter 8. Results demonstrate that the addition of NCA (300 to 1300 mg L^{-1}) enhances the pseudo-first-order rate constant (k_{obs}, s^{-1}) and thus, the overall absorption process of CO_2 in carbonate solvents by 14 %, 20% and 34 % at 40 °C. It is also found that an addition of a relatively large amount of NCA (*i.e.* [NCA] = 6600 mg L^{-1}) results in flocculation of the NCA in a carbonate solvent which seems to have an adverse effect on the catalytic activity of NCA. Similarly, experimental data indicate that an increase in the temperature to more than 60 °C results in a significant decrease in the rate enhancement by NCA.

The rate constants determined in this study provide valuable information for determination of the operating conditions and the design of absorber units for carbon capture systems employing amino acid promoted potassium carbonate solvents.

9.3 Recommendations and Suggestions for Future Development

It is without a doubt that the understanding of the reaction kinetics of carbonate solvents has improved through this work. That being said, further studies aimed to verifying the reaction order are important. This could be done by carrying a kinetic study in a non-water-based solvent such as ethanol or methanol. The purpose of this specific experiment is to eliminate kinetic contributions of water to the partial reaction order which are quite significant in the case of secondary amino acid based promoters.

In industrial carbon capture plants, the flue gas comes with a relatively low concentration of CO_2. Therefore, to mimic this condition, the gas inlet to the wetted wall column (WWC) must contain a low concentration of CO_2 (< 10 vol%). Experiments in this work are designed to run the absorption of CO_2 using a higher bulk pressure of CO_2 for two reasons. The first was to reduce the gas phase resistance and therefore ensure the transfer of CO_2 from the gas to the

liquid is governed by the liquid film only. The second reason was to reduce the effect of the change in the equilibrium partial pressure of CO_2. Further research must incorporate better ways to quantify the gas phase resistance and thorough VLE data of promoted potassium carbonate. Also, knowledge on the effect of the addition of promoters in the carbonate solvents on the volatility of the solvents is important to estimate the amount of solvent losses in the absorber and the regenerator and to design a process that limits the release of solvent to the atmosphere.

The effect of ionic strength on the kinetics of promoted potassium carbonate should be further studied. CO_2 absorption experiments with various ionic strength conditions should be performed.

The experiments in this study are performed in controlled clean conditions. In industrial carbon capture plants, impurities and corrosion inhibitor such as vanadium may alter the performance of the solvents, and therefore, further research should take into account the effects of impurities and corrosion inhibitor if any is present. Important gas impurities include SO_x, NO_x, while impurities from corrosion include iron and copper. Furthermore, the rate of absorption and vapour liquid equilibrium of H_2S into carbonate solvents should be investigated as the absorption of H_2S is desirable for natural gas treating.

Solvent/promoter degradation and equipment corrosion are significant performance-hindering characteristics that are encountered during industrial application. These characteristics dictate the amount of solvent regularly added to the system to compensate solvent losses and the construction material for the process. The solvent degradation rate in the presence of promoter should be taken into account when designing a capture process and corrosion due to added promoter should be investigated to determine process constraints.

Further study should also look at long-term operation and cyclic operation as well as the performance of the promoters in the regeneration process. This includes carbamate stability for amine and amino acid promoters and survivability of enzyme promoters at high temperatures (*i.e.* carbonic anhydrase).

CHAPTER 10 - REFERENCES

1. International Energy Agency, *CO_2 Emissions from Fuel Combustion Highlights*. 2009.
2. Metz, B., et al., eds. *Carbon Dioxide Capture and Storage*. 2005, Cambridge University Press: Canada. 380.
3. Coutts, A.M., J. Beringer, and N.J. Tapper, *Characteristics Influencing the Variability of Urban CO_2 Fluxes in Melbourne, Australia.* Atmospheric Environment, 2007. **41**(1): p. 51-62.
4. International Energy Agency, *World Energy Outlook*. 2000.
5. IPCC, *Second Assessment Report 1995*, 1996, UNEP: Geneva, Switzerland.
6. IEA Greenhouse Gas R&D Programme, *Ocean Storage of CO_2*. 2002.
7. Narayan, P.K. and R. Smyth, *Electricity consumption, employment and real income in Australia evidence from multivariate Granger causality tests.* Energy Policy, 2005. **33**(9): p. 1109-1116.
8. International Energy Agency Greenhouse Gas R&D Programme, *Putting Carbon back into the Ground*. 2001.
9. Cullinane, J.T., *Thermodynamics and Kinetics of Aqueous Piperazine with Potassium Carbonate for Carbon Dioxide Absorption*, 2005, University of Texas: Austin.
10. Strazisar, B.R., R.R. Anderson, and C.M. White, *Degradation of MEA used in CO_2 Capture from Flue Gas of Coal-fired Electric Power Generating Station*, in *Clean Air Technology Division, National Energy Laboratory, U.S. Department of Energy*2003: Pittsburgh. p. 1-80.
11. Rubin E. A., Rao A. B., and Chen C., *Comparative Assessments of Fossil Fuel Power Plants with CO_2 Capture and Storage*. 7th International Conference on Greenhouse Gas Control Technologies, 2004.
12. Rao A. B. and Rubin E. S., *A Technical, Economic, and Environmental Assessment of Amine-Based CO_2 Capture Technology for Power Plant Greenhouse Gas Control*, 2002, Carnegie Mellon University.
13. Levenspiel, O., *Chemical Reaction Engineering*. Third Edition ed, ed. W. Anderson1999, New York: John Wiley & Sons.
14. Danckwerts, P., *Absorption by simultaneous diffusion and chemical reaction.* Transactions of the Faraday Society, 1950. **46**: p. 300-304.
15. Tseng, P.C., W.S. Ho, and D.W. Savage, *Carbon dioxide absorption into promoted carbonate solutions.* AIChE Journal, 1988. **34**(6): p. 922-931.
16. Astarita, G., D.W. Savage, and A. Bisio, *Gas Treating with Chemical Solvents*1983, New York: John Wiley & Sons, Inc. 493.
17. Caplow, M., *Kinetics of carbamate formation and breakdown.* Journal of the American Chemical Society, 1968. **90**(24): p. 6795-6803.
18. P.V, D., *The reaction of CO2 with ethanolamines.* Chemical Engineering Science, 1979. **34**(4): p. 443-446.
19. Thee, H., et al., *A kinetic and process modeling study of CO2 capture with MEA-promoted potassium carbonate solutions.* Chemical Engineering Journal, 2012. **210**(0): p. 271-279.
20. Hikita, H., et al., *The kinetics of reactions of carbon dioxide with monoethanolamine, diethanolamine and triethanolamine by a rapid mixing method.* The Chemical Engineering Journal, 1977. **13**(1): p. 7-12.
21. Penny, D.E. and T.J. Ritter, *Kinetic study of the reaction between carbon dioxide and primary amines.* Journal of the Chemical Society, Faraday Transactions 1: Physical Chemistry in Condensed Phases, 1983. **79**(9): p. 2103-2109.
22. Versteeg, G.F., L.A.J. Van Dijck, and W.P.M. Van Swaaij, *ON THE KINETICS BETWEEN CO2 AND ALKANOLAMINES BOTH IN AQUEOUS AND NON-AQUEOUS SOLUTIONS. AN OVERVIEW*. Chemical Engineering Communications, 1996. **144**(1): p. 113-158.
23. Yeh, J.T., H.W. Pennline, and K.P. Resnik, *Study of CO_2 Absorption and Desorption in a Packed Column.* Energy and Fuels, 2001. **15**(2): p. 274-278.
24. Simioni, M., *Membrane stripping : desorption of carbon dioxide from alkali solvents*, in *Chemical and Biomolecular Engineering*2010, The University of Melbourne: Australia.
25. Ramachandran, N., et al., *Kinetics of the Absorption of CO_2 into Mixed Aqueous Loaded Solutions of Monoethanolamine and Methyldiethanolamine.* Industrial & Engineering Chemistry Research, 2006. **45**(8): p. 2608-2616.
26. Bosch, H., G.F. Versteeg, and W.P.M. van Swaaij, *Gas-Liquid Mass Transfer with Parallel Reversible Reactions-III. Absorption of CO_2 into Solutions of Blends of Amines.* Chemical Engineering Science, 1989. **44**(11): p. 2745-2750.
27. Oyenekan, B.A. and G.T. Rochelle, *Alternative Stripper Configurations for CO_2 Capture by Aqueous Amines.* AIChE Journal, 2007. **53**(12): p. 3144 - 3154.

28. Horng, S.-Y. and M.-H. Li, *Kinetics of Absorption of Carbon Dioxide into Aqueous Solutions of Monoethanolamine and Triethanolamine.* Industrial & Engineering Chemistry Research, 2002. **41**(2): p. 257-266.
29. Kohl, A.L. and R.B. Nielson, *Gas Purification*1997, Houston, Texas: Gulf Publishing.
30. Bello, A. and R. Idem, *Pathways for the Formation of Products of the Oxidative Degradation of CO_2-Loaded Concentrated Aqueous Monoethanolamine Solutions during CO_2 Absorption from Flue Gases.* Industrial & Engineering Chemistry Research, 2005. **44**(4): p. 945-969.
31. Epp, B., et al., *Tail-end CO_2 Capture as Convincing Opportunity for Retrofitting of Coal-fired Power Stations and Related R&D Objectives.* VGB PowerTech, 2007. **87**(5): p. 106-116.
32. van Gijlswijk, R., P.H.M. Feron, and J. Davison. *Environmental Impact of Solvent Processes for CO_2 Capture.* in *8th International Conference on Greenhouse Gas Control Technologies*. 2006. Trondheim, Norway: CO2CRC.
33. Versteeg, G.F. and W.P.M. van Swaaij, *On the kinetics between CO2 and alkanolamines both in aqueous and non-aqueous solutions—II. Tertiary amines.* Chemical Engineering Science, 1988. **43**(3): p. 587-591.
34. Blauwhoff, P.M.M., G.F. Versteeg, and W.P.M. Van Swaaij, *A study on the reaction between CO2 and alkanolamines in aqueous solutions.* Chemical Engineering Science, 1984. **39**(2): p. 207-225.
35. Rinker, E.B., S.S. Ashour, and O.C. Sandall, *Kinetics and Modeling of Carbon Dioxide Absorption into Aqueous Solutions of Diethanolamine.* Industrial & Engineering Chemistry Research, 1996. **35**(4): p. 1107-1114.
36. Sada, E., H. Kumazawa, and M.A. Butt, *Gas absorption with consecutive chemical reaction: Absorption of carbon dioxide into aqueous amine solutions.* The Canadian Journal of Chemical Engineering, 1976. **54**(5): p. 421-424.
37. Donaldson, T.L. and Y.N. Nguyen, *Carbon Dioxide Reaction Kinetics and Transport in Aqueous Amine Membranes.* Industrial & Engineering Chemistry Fundamentals, 1980. **19**(3): p. 260-266.
38. Crooks, J.E. and J.P. Donnellan, *Kinetics of the reaction between carbon dioxide and tertiary amines.* The Journal of Organic Chemistry, 1990. **55**(4): p. 1372-1374.
39. Littel, R.J., W.P.M. Van Swaaij, and G.F. Versteeg, *Kinetics of Carbon Dioxide with tertiary Amines in aqueous solution.* AIChE Journal, 1990. **36**(11): p. 1633-1640.
40. Sartori, G. and D.W. Savage, *Sterically hindered amines for carbon dioxide removal from gases.* Industrial & Engineering Chemistry Fundamentals, 1983. **22**(2): p. 239-249.
41. Yih, S.M. and K.P. Shen, *Kinetics of carbon dioxide reaction with sterically hindered 2-amino-2-methyl-1-propanol aqueous solutions.* Industrial & Engineering Chemistry Research, 1988. **27**(12): p. 2237-2241.
42. Alper, E., *Reaction mechanism and kinetics of aqueous solutions of 2-amino-2-methyl-1-propanol and carbon dioxide.* Industrial & Engineering Chemistry Research, 1990. **29**(8): p. 1725-1728.
43. Sharma, M.M., *Kinetics of reactions of carbonyl sulphide and carbon dioxide with amines and catalysis by Bronsted bases of the hydrolysis of COS.* Transactions of the Faraday Society, 1965. **61**(0): p. 681-688.
44. Hook, R.J., *An Investigation of Some Sterically Hindered Amines as Potential Carbon Dioxide Scrubbing Compounds.* Industrial & Engineering Chemistry Research, 1997. **36**(5): p. 1779-1790.
45. Park, S.-W., et al., *Absorption of Carbon Dioxide into Aqueous Solution of Sodium Glycinate.* Separation Science and Technology, 2008. **43**(11-12): p. 3003-3019.
46. Vaidya, P.D., et al., *Kinetics of Carbon Dioxide Removal by Aqueous Alkaline Amino Acid Salts.* Industrial & Engineering Chemistry Research, 2010. **49**(21): p. 11067-11072.
47. Portugal, A.F., et al., *Characterization of potassium glycinate for carbon dioxide absorption purposes.* Chemical Engineering Science, 2007. **62**(23): p. 6534-6547.
48. Kohl, A.L. and R.B. Nielsen, *Alkanolamines for Hydrogen Sulfide and Carbon Dioxide Removal*, in *Gas Purification (Fifth Edition)*1997, Gulf Professional Publishing: Houston. p. 40-186.
49. Fernandez, E.S. and E.L.V. Goetheer, *DECAB: Process development of a phase change absorption process.* Energy Procedia, 2011. **4**(0): p. 868-875.
50. Kumar, P.S., et al., *Kinetics of the reaction of CO2 with aqueous potassium salt of taurine and glycine.* AIChE Journal, 2003. **49**(1): p. 203-213.
51. van Holst, J., G.F. Versteeg, and D.W.F. Brilman, *Kinetic Study of CO_2 with Various Amino Acid Salts in Aqueous Solution.* Chemical Engineering Science, 2009. **64**(1): p. 59-68.
52. Portugal, A.F., et al., *Solubility of Carbon Dioxide in Aqueous Solutions of Amino Acid Salts.* Chemical Engineering Science, 2009. **64**(9): p. 1993-2002.
53. Portugal, A.F., F.D. Magalhães, and A. Mendes, *Carbon Dioxide Removal from Anaesthetic Gas Circuits Using Hollow Fiber Membrane Contactors with Amino Acid Salt Solutions.* Journal of Membrane Science, 2009. **339**(1-2): p. 275.

54. Kumar, P.S., et al., *Equilibrium Solubility of CO_2 in Aqueous Potassium Taurate Solutions: Part 2. Experimental VLE Data and Model.* Industrial & Engineering Chemistry Research, 2003. **42**(12): p. 2841-2852.
55. Kumar, P.S., et al., *Equilibrium Solubility of CO_2 in Aqueous Potassium Taurate Solutions: Part 1. Crystallization in Carbon Dioxide Loaded Aqueous Salt Solutions of Amino Acids.* Industrial & Engineering Chemistry Research, 2003. **42**(12): p. 2832-2840.
56. Holst, J.v., et al., *Kinetic study of CO2 with various amino acid salts in aqueous solution.* Chemical Engineering Science, 2009. **64**(1): p. 59-68.
57. Song, H.-J., et al., *Solubilities of Carbon Dioxide in Aqueous Solutions of Sodium Glycinate.* Fluid Phase Equilibria, 2006. **246**(1-2): p. 1-5.
58. Supap, T., et al., *Analysis of Monoethanolamine and Its Oxidative Degradation Products during CO2 Absorption from Flue Gases: A Comparative Study of GC-MS, HPLC-RID, and CE-DAD Analytical Techniques and Possible Optimum Combinations.* Industrial & Engineering Chemistry Research, 2005. **45**(8): p. 2437-2451.
59. Bello, A. and R.O. Idem, *Pathways for the Formation of Products of the Oxidative Degradation of CO2-Loaded Concentrated Aqueous Monoethanolamine Solutions during CO2 Absorption from Flue Gases.* Industrial & Engineering Chemistry Research, 2005. **44**(4): p. 945-969.
60. Strazisar, B.R., R.R. Anderson, and C.M. White, *Degradation Pathways for Monoethanolamine in a CO2 Capture Facility.* Energy & Fuels, 2003. **17**(4): p. 1034-1039.
61. Kohl, A.L. and F.C. Riesenfeld, *Alkaline Salt Solutions for Hydrogen Sulfide and Carbon Dioxide Absorption*, in *Gas Purification*1985, Gulf Publishing Company: Houston, Texas. p. 211-246.
62. Benson, H.E., J.H. Field, and R.M. Jimeson, *CO_2 Absorption: Employing Hot Potassium Carbonate Solutions.* Chemical Engineering Progress, 1954. **50**(7): p. 356-364.
63. Benson, H.E., J.H. Field, and W.P. Haynes, *Improved Process for Carbon Dioxide Absorption uses Hot Carbonate Solutions.* Chemical Engineering Progress, 1956. **52**(10): p. 433-438.
64. Tosh, J.S., et al., *Equilibrium Study of the System Potassium Carbonate Potassium Bicarbonate, Carbon Dioxide and Water.* Bureau of Mines Report of Investigations, 1959. **5484**: p. 23.
65. Astarita, G., D.W. Savage, and J.M. Longo, *Promotion of Carbon Dioxide Mass Transfer in Carbonate Solutions.* Chemical Engineering Science, 1981. **36**(3): p. 581-588.
66. Shen, S. and G. Stevens, *Recent Progress in Carbon Dioxide Absorption with Aqueous Potassium Carbonate Promoted by Borates.* 2010.
67. Cullinane, J.T. and G.T. Rochelle, *Carbon Dioxide Absorption with Aqueous Potassium Carbonate Promoted by Piperazine.* Chemical Engineering Science, 2004. **59**(17): p. 3619-3630.
68. Bishnoi, S. and G.T. Rochelle, *Absorption of carbon dioxide into aqueous piperazine: reaction kinetics, mass transfer and solubility.* Chemical engineering science, 2000. **55**(22): p. 5531-5543.
69. Mahajani, V.V. and P.V. Danckwerts, *The Stripping of CO_2 from Amine-Promoted Potash Solutions at 100°C.* Chemical Engineering Science, 1983. **38**(2): p. 321-327.
70. Danckwerts, P.V. and K.M. McNeil, *The Effects of Catalysis on Rates of Absorption of CO_2 into Aqueous Amine-Potash Solutions.* Chemical Engineering Science, 1967. **22**(7): p. 925-930.
71. Cullinane, J.T. and G.T. Rochelle, *Kinetics of Carbon Dioxide Absorption into Aqueous Potassium Carbonate and Piperzine.* Industrial & Engineering Chemistry Research, 2006. **45**(8): p. 2531-2545.
72. Bosch, H., G.F. Versteeg, and W.P.M. van Swaaij, *Gas-Liquid Mass Transfer with Parallel Reversible Reactions-II. Absorption of CO_2 into Amine-Promoted Carbonate Solutions.* Chemical Engineering Science, 1989. **44**(11): p. 2735-2743.
73. Ghosh, U.K., S.E. Kentish, and G.W. Stevens, *Absorption of carbon dioxide into aqueous potassium carbonate promoted by boric acid.* Energy Procedia, 2009. **1**(1): p. 1075-1081.
74. Thee, H., et al., *Carbon dioxide absorption into unpromoted and borate-catalyzed potassium carbonate solutions.* Chemical Engineering Journal, 2012. **181–182**(0): p. 694-701.
75. Savage, D.W., G. Sartori, and G. Astarita, *Amines as Rate Promoters for Carbon Dioxide Hydrolysis.* Faraday Discussions of the Chemical Society, 1984. **77**: p. 17-31.
76. Mesmer, R.E., C.F. Baes Jr, and F.H. Sweeton, *Acidity Measurements at Elevated Temperatures.* Inorganic Chemistry, 1971. **11**(3).
77. Guo, D., et al., *Borate-Catalyzed Carbon Dioxide Hydration via the Carbonic Anhydrase Mechanism.* Environmental Science & Technology, 2011. **45**(11): p. 4802-4807.
78. Eickmeyer, A.G., *METHOD FOR REMOVING ACID GASES FROM GASEOUS MIXTURES*, 1974, Google Patents.
79. Ahmadi, M., V.G. Gomes, and K. Ngian, *Advanced modelling in performance optimization for reactive separation in industrial CO2 removal.* Separation and Purification Technology, 2008. **63**(1): p. 107-115.

80. Endo, K., et al., *The effect of boric acid on the vapour liquid equilibrium of aqueous potassium carbonate.* Fluid Phase Equilibria, 2011. **309**(2): p. 109-113.
81. Kierzkowska-Pawlak, H., *Determination of Kinetics in Gas-Liquid Reaction Systems.* Ecological Chemistry and Engineering S, 2012. **19**(2): p. 133-279.
82. Kumar, P.S., et al., *Density, Viscosity, Solubility, and Diffusivity of N2O in Aqueous Amino Acid Salt Solutions.* Journal of Chemical & Engineering Data, 2001. **46**(6): p. 1357-1361.
83. Knuutila, H., O. Juliussen, and H.F. Svendsen, *Density and N2O solubility of sodium and potassium carbonate solutions in the temperature range 25 to 80 °C.* Chemical Engineering Science, 2010. **65**(6): p. 2177-2182.
84. Joosten, G.E.H. and P.V. Danckwerts, *Solubility and Diffusivity of Nitrous Oxide in Equimolar Potassium Carbonate-Potassium Bicarbonate Solutions at 25°C and 1 atm.* Journal of Chemical and Engineering Data, 1972. **17**(4): p. 452-454.
85. Versteeg, G.F., *Solubility and diffusivity of acid gases (carbon dioxide, nitrous oxide) in aqueous alkanolamine solutions.* Journal of chemical & engineering data, 1988. **33**(1): p. 29.
86. Ratcliff, G.A. and J.G. Holdcroft, *Diffusivities of Gases in Aqueous Electrolyte Solutions.* Transactions of the Institution of Chemical Engineers, 1963. **41**(10): p. 315-319.
87. Versteeg, G.F., P.M.M. Blauwhoff, and W.P.M. van Swaaij, *The effect of diffusivity on gas-liquid mass transfer in stirred vessels. Experiments at atmospheric and elevated pressures.* Chemical Engineering Science, 1987. **42**(5): p. 1103-1119.
88. Pröll, T., et al., *Acid gas absorption in trickle flow columns—Modelling of the residence time distribution of a pilot plant.* Chemical Engineering and Processing: Process Intensification, 2007. **46**(3): p. 262-270.
89. Hamborg, E.S., J.P.M. Niederer, and G.F. Versteeg, *Dissociation Constants and Thermodynamic Properties of Amino Acids Used in CO2 Absorption from (293 to 353) K.* Journal of Chemical & Engineering Data, 2007. **52**(6): p. 2491-2502.
90. Versteeg, G.F., W.P.M. Van Swaaij, and E.S. Hamborg, *Diffusivities in aqueous solutions of the potassium salt of amino acids*, 2008.
91. Pacheco, M.A., *CO2 absorption into aqueous mixtures of diglycolamine® and methyldiethanolamine.* Chemical engineering science, 2000. **55**(21): p. 5125.
92. Treybal, R.E., *Mass-Transfer Operations*. Third ed1981: McGraw-Hill.
93. Hobler, T., *Mass transfer and absorbers*1966.
94. Vivian, J.E., *Liquid-side resistance in gas absorption.* AIChE journal, 1956. **2**(4): p. 437.
95. Emmert, R.E., *A study of gas absorption in falling liquid films.* Chemical engineering progress, 1954. **50**(2): p. 87.
96. Harned, H.S. and R. Davis, *The Ionization Constant of Carbonic Acid in Water and the Solubility of Carbon Dioxide in Water and Aqueous Salt Solutions from 0 to 50°.* Journal of the American Chemical Society, 1943. **65**(10): p. 2030-2037.
97. Schmidt, C., R. Thomas, and W. Heinrich, *Boron speciation in aqueous fluids at 22 to 600°C and 0.1 MPa to 2 GPa.* Geochimica et Cosmochimica Acta, 2005. **69**(2): p. 275-281.
98. Ahmadi, M., V.G. Gomes, and K. Ngian, *Advanced modelling in performance optimization for reactive separation in industrial CO2 removal.* Sep. Purif. Technol., 2008. **63**(1): p. 107-115.
99. Knuutila, H., O. Juliussen, and H.F. Svendsen, *Kinetics of the reaction of carbon dioxide with aqueous sodium and potassium carbonate solutions.* Chemical Engineering Science, 2010. **65**(23): p. 6077-6088.
100. Goldberg, R.N., *Thermodynamic quantities for the ionization reactions of buffers.* Journal of physical and chemical reference data, 2002. **31**(2): p. 231.
101. Anderson, C., et al., *Novel pre-combustion capture technologies in action-Results of the CO2CRC/HRL Mulgrave capture project.* Energy Procedia, 2011. **4**: p. 1192-1198.
102. Qader, A., et al., *Novel post-combustion capture technologies on a lignite fired power plant - results of the CO2CRC/H3 capture project.* Energy Procedia, 2011. **4**: p. 1668-1675.
103. Goff, G.S. and G.T. Rochelle, *Monoethanolamine Degradation: O2 Mass Transfer Effects under CO2 Capture Conditions.* Industrial & Engineering Chemistry Research, 2004. **43**(20): p. 6400-6408.
104. Zhang, Y., et al., *Rate-Based Process Modeling Study of CO2 Capture with Aqueous Monoethanolamine Solution.* Industrial & Engineering Chemistry Research, 2009. **48**(20): p. 9233-9246.
105. Abu-Zahra, M.R.M., et al., *CO2 capture from power plants: Part I. A parametric study of the technical performance based on monoethanolamine.* International Journal of Greenhouse Gas Control, 2007. **1**(1): p. 37-46.
106. Austgen, D.M., et al., *Model of vapor-liquid equilibria for aqueous acid gas-alkanolamine systems using the electrolyte-NRTL equation.* Industrial & Engineering Chemistry Research, 1989. **28**(7): p. 1060-1073.

107. Kent, R.L. and B. Eisenberg, *BETTER DATA FOR AMINE TREATING*. Hydrocarbon processing, 1976. **55**(2): p. 87-90.
108. Edwards, T.J., et al., *Vapor-liquid equilibria in multicomponent aqueous solutions of volatile weak electrolytes*. AIChE Journal, 1978. **24**(6): p. 966-976.
109. Pinsent, B.R.W., L. Pearson, and F.J.W. Roughton, *The kinetics of combination of carbon dioxide with hydroxide ions*. Transactions of the Faraday Society, 1956. **52**: p. 1512-1520.
110. Lee, J.I., F.D. Otto, and A.E. Mather, *Equilibrium between carbon dioxide and aqueous monoethanolamine solutions*. Journal of Applied Chemistry and Biotechnology, 1976. **26**(1): p. 541-549.
111. Jou, F.-Y., A.E. Mather, and F.D. Otto, *The solubility of CO2 in a 30 mass percent monoethanolamine solution*. The Canadian Journal of Chemical Engineering, 1995. **73**(1): p. 140-147.
112. Cullinane, J.T. and G.T. Rochelle, *Thermodynamics of Aqueous Potassium Carbonate, Piperazine and Carbon Dioxide*. Fluid Phase Equilibria, 2005. **227**(2): p. 197-213.
113. Aboudheir, A., et al., *Kinetics of the reactive absorption of carbon dioxide in high CO2-loaded, concentrated aqueous monoethanolamine solutions*. Chemical Engineering Science, 2003. **58**(23–24): p. 5195-5210.
114. Leder, F., *The absorption of CO2 into chemically reactive solutions at high temperatures*. Chemical Engineering Science, 1971. **26**(9): p. 1381-1390.
115. Xiao, J., C.-W. Li, and M.-H. Li, *Kinetics of absorption of carbon dioxide into aqueous solutions of 2-amino-2-methyl-1-propanol+monoethanolamine*. Chemical Engineering Science, 2000. **55**(1): p. 161-175.
116. Horng, S.-Y. and M.-H. Li, *Kinetics of Absorption of Carbon Dioxide into Aqueous Solutions of Monoethanolamine + Triethanolamine*. Industrial & Engineering Chemistry Research, 2001. **41**(2): p. 257-266.
117. Onda, K., *Mass transfer coefficients between gas and liquid phases in packed columns*. Journal of chemical engineering of Japan, 1968. **1**(1): p. 56.
118. Mumford, K.A., et al., *Post-combustion Capture of CO2: Results from the Solvent Absorption Capture Plant at Hazelwood Power Station Using Potassium Carbonate Solvent*. Energy & Fuels, 2011. **26**(1): p. 138-146.
119. Aronu, U.E., et al., *Kinetics of Carbon Dioxide Absorption into Aqueous Amino Acid Salt: Potassium Salt of Sarcosine Solution*. Industrial & Engineering Chemistry Research, 2011. **50**(18): p. 10465-10475.
120. Guo, D., et al., *Amino Acids as Carbon Capture Solvents: Chemical Kinetics and Mechanism of the Glycine + CO2 Reaction*. Energy & Fuels, 2013. **27**(7): p. 3898-3904.
121. Lim, J.-a., et al., *Absorption of CO2 into Aqueous Potassium Salt Solutions of l-Alanine and l-Proline*. Energy & Fuels, 2012. **26**(6): p. 3910-3918.
122. Danckwerts, P.V., *The reaction of CO2 with ethanolamines*. Chemical Engineering Science, 1979. **34**(4): p. 443-446.
123. Pouchert, C.J. and J. Behnke, *The aldrich library of 13C and 1H FT NMR spectra / Charles J. Pouchert, Jacqlynn Behnke*, 1993, Milwaukee : Aldrich Chemical Company.
124. Mani, F., M. Peruzzini, and P. Stoppioni, *CO2 absorption by aqueous NH3 solutions: speciation of ammonium carbamate, bicarbonate and carbonate by a 13C NMR study*. Green Chemistry, 2006. **8**(11): p. 995-1000.
125. Jensen, A., J.B. Jensen, and C. Faurholt, *STUDIES ON CARBAMATES .6. THE CARBAMATE OF GLYCINE*. Acta Chemica Scandinavica, 1952. **6**(3): p. 395-397.
126. Lee, S., et al., *Kinetics of CO2 Absorption in Aqueous Sodium Glycinate Solutions*. Industrial & Engineering Chemistry Research, 2007. **46**(5): p. 1578-1583.
127. Simons, K., et al., *Kinetics of CO2 Absorption in Aqueous Sarcosine Salt Solutions: Influence of Concentration, Temperature, and CO2 Loading*. Industrial & Engineering Chemistry Research, 2010. **49**(20): p. 9693-9702.
128. Paul, S. and K. Thomsen, *Kinetics of absorption of carbon dioxide into aqueous potassium salt of proline*. International Journal of Greenhouse Gas Control, 2012. **8**(0): p. 169-179.
129. Mirjafari, P., K. Asghari, and N. Mahinpey, *Investigating the Application of Enzyme Carbonic Anhydrase for CO2 Sequestration Purposes*. Industrial & Engineering Chemistry Research, 2007. **46**(3): p. 921-926.
130. Lu, Y., et al., *Development of a carbonate absorption-based process for post-combustion CO2 capture: The role of biocatalyst to promote CO2 absorption rate*. Energy Procedia, 2011. **4**: p. 1286-1293.
131. Davy, R., *Development of catalysts for fast, energy efficient post combustion capture of CO2 into water; an alternative to monoethanolamine (MEA) solvents*. Energy Procedia, 2009. **1**(1): p. 885-892.
132. Trachtenberg, M.C., et al., *Membrane-based, enzyme-facilitated, efficient carbon dioxide capture*. Energy Procedia, 2009. **1**(1): p. 353-360.
133. Bao, L. and M.C. Trachtenberg, *Facilitated transport of CO2 across a liquid membrane: Comparing enzyme, amine, and alkaline*. Journal of Membrane Science, 2006. **280**(1-2): p. 330-334.

134. Bond, G.M., et al., *Development of Integrated System for Biomimetic CO2 Sequestration Using the Enzyme Carbonic Anhydrase.* Energy & Fuels, 2001. **15**(2): p. 309-316.
135. Ramanan, R., et al., *Bio-sequestration of carbon dioxide using carbonic anhydrase enzyme purified from Citrobacter freundii.* World Journal of Microbiology and Biotechnology, 2009. **25**(6): p. 981-987.
136. Lavecchia, R. and M. Zugaro, *Thermal denaturation of erythrocyte carbonic anhydrase.* FEBS Letters, 1991. **292**(1-2): p. 162-164.
137. Zhang, X. and R. van Eldik, *A functional model for carbonic anhydrase: thermodynamic and kinetic study of a tetraazacyclododecane complex of zinc(II).* Inorganic Chemistry, 1995. **34**(22): p. 5606-5614.
138. Zhang, X., et al., *Kinetics and mechanism of the hydration of carbon dioxide and dehydration of bicarbonate catalyzed by a zinc (II) complex of 1,5,9-triazacyclododecane as a model for carbonic anhydrase.* Inorganic Chemistry, 1993. **32**(25): p. 5749-5755.
139. Nakata, K., et al., *Kinetic study of catalytic CO2 hydration by water-soluble model compound of carbonic anhydrase and anion inhibition effect on CO2 hydration.* Journal of Inorganic Biochemistry, 2002. **89**(3-4): p. 255-266.
140. Hikita, H., et al., *The kinetics of reactions of carbon dioxide with monoisopropanolamine, diglycolamine and ethylenediamine by a rapid mixing method.* The Chemical Engineering Journal, 1977. **14**(1): p. 27-30.
141. Barth, D., C. Tondre, and J.J. Delpuech, *Kinetics and mechanisms of the reactions of carbon dioxide with alkanolamines: a discussion concerning the cases of MDEA and DEA.* Chemical Engineering Science, 1984. **39**(12): p. 1753-1757.
142. Ko, J.-J. and M.-H. Li, *Kinetics of absorption of carbon dioxide into solutions of N-methyldiethanolamine+water.* Chemical Engineering Science, 2000. **55**(19): p. 4139-4147.
143. Palaty, Z., *Viscosity of Aqueous Solutions of Potassium Carbonate/Potassium Bicarbonate (K_2CO_3/$KHCO_3$).* Chemical and Biochemical Engineering Quarterly, 1993. **7**(3): p. 155-159.
144. Pohorecki, R. and W. Moniuk, *Calculation of Densities, Viscosities and Surface Tensions of Aqueous Solutions of Potassium and Sodium Hydroxides and Carbonates.* Prace Instytutu Inzynierii Chemicznej Politechniki Warszawskiej, 1982. **11**(3-4): p. 127-140.

CHAPTER 11 - APPENDIX A

This chapter summarizes the measurements of density, viscosity, physical CO_2 solubility of potassium carbonate solvents which were taken from the work undertaken by Simioni [24] and are used in this study.

11.1 Viscosity

Figure 11-1 summarizes the measurements of the viscosity of potassium carbonate solutions at different carbonate concentrations and temperatures. Simioni [24] notes that the results follow similar trends to experimental values taken from Palaty *et al.* [143] At 20 °C. It can be observed that the increase in temperature causes a reduction in the solvent viscosities.

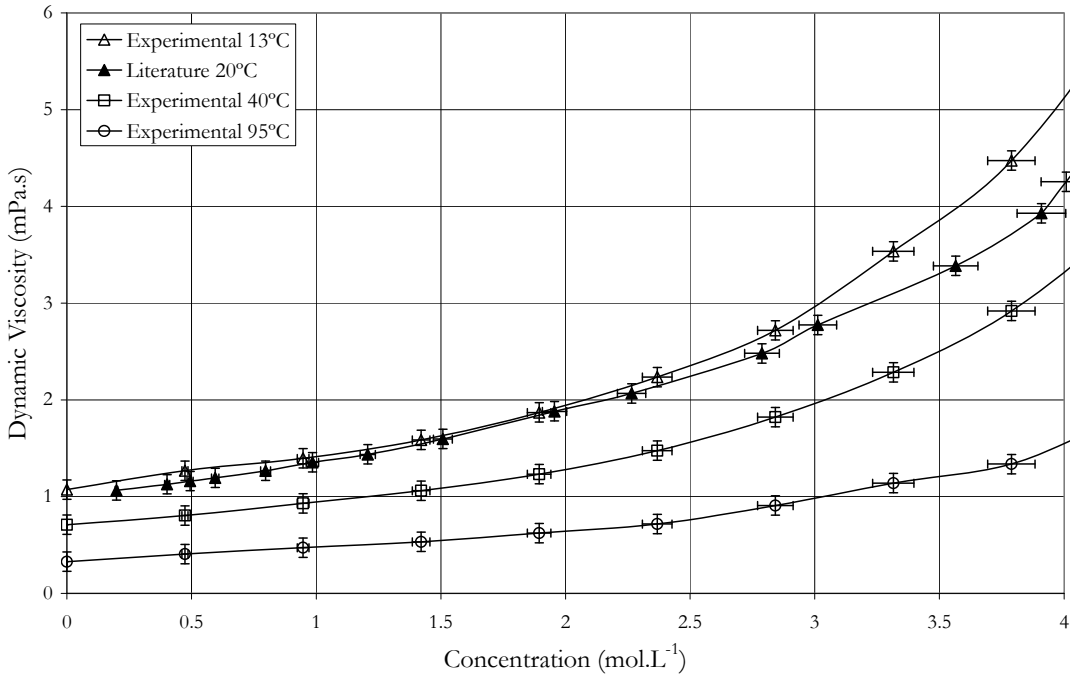

Figure 11-1 Measurements of viscosity of potassium carbonate solvents. Reprinted from Simioni [24] where literature results refer to the work undertaken by Palaty *et al.* [143].

11.2 Density

The measurements of density of potassium carbonate solvents were performed by Simioni [24] using a weighed volume method at a constant temperature (25 °C). Figure 11-2 shows the comparison between density measurements performed by Simioni [24] and a linear prediction developed by Pohorecki *et al.* [144]. Simioni [24] notes that the results of both studies follow a similar trend over the range of concentrations used.

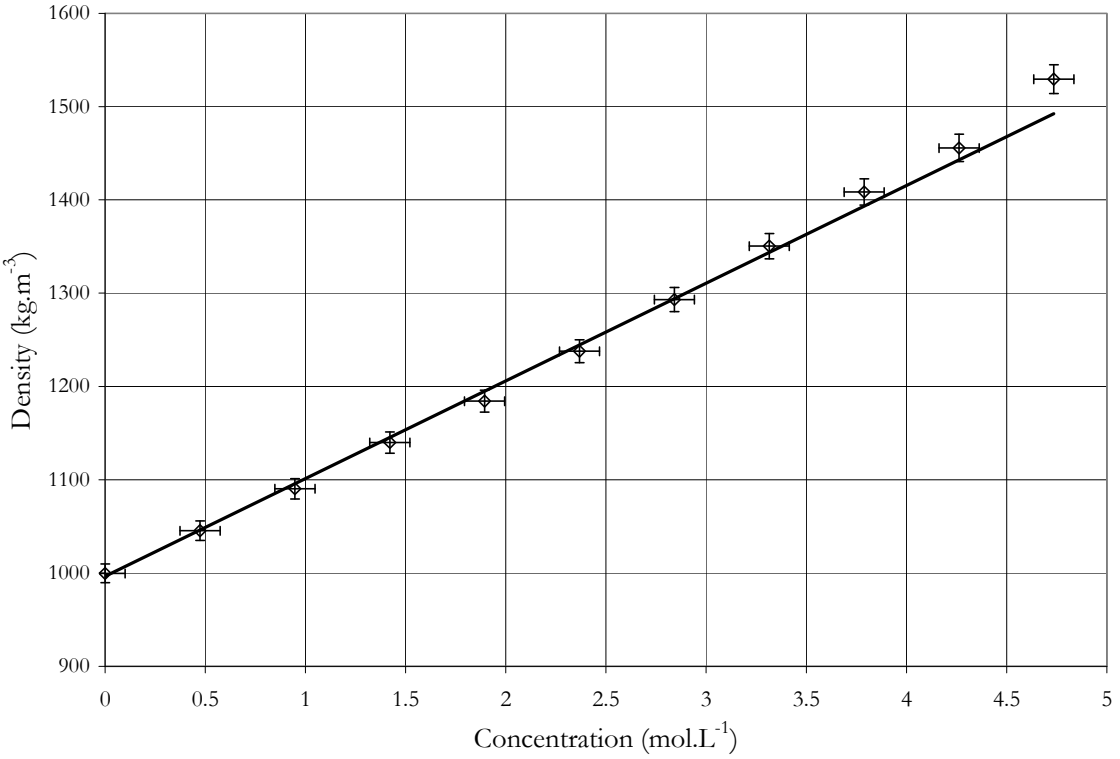

Figure 11-2 Measurements of density of various concentrations of potassium carbonate solutions at 25 °C. Reprinted from Simioni [24] where the experimental data is taken from his work and the linear prediction is that developed by Pohorecki *et al.* [144].

11.3 Vapour Pressure

Using ASPEN Plus™ simulations, Simioni [24] determined the vapour pressure of carbon dioxide above potassium carbonate solutions at different temperatures, solution loadings and potassium carbonate concentrations. Liquid phase activity was determined using the Electrolyte Non-Random Two

Liquid (E-NRTL) model with interaction parameters obtained from Cullinane [67, 71, 112]. Figure 11-3 shows the vapour pressure of 30 wt% potassium carbonate solutions as a function of temperature and solvent loading. The simulation was also compared with experimental data taken from the work done by Tosh *et al.* [64].

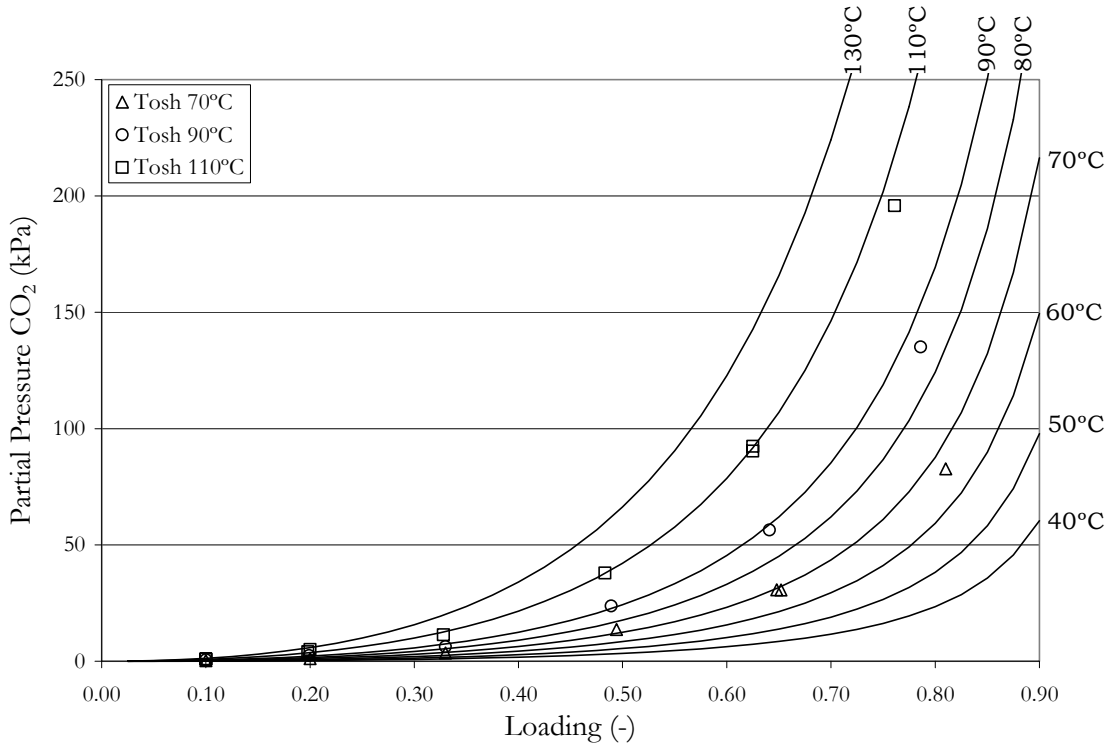

Figure 11-3 Partial pressure of carbon dioxide above a 30 wt% solution of aqueous potassium carbonate at various temperatures and solvent loadings based on an ASPEN Plus E-NTRL model. Experimental data points are taken from work completed by Tosh *et al.* [64] (taken from Simioni [24]).

11.4 Surface Tension

The surface tension measurements of potassium carbonate solutions were taken the work completed by Simioni [24] who employed the pendant drop technique. Figure 11-4 shows a comparison between the surface tension obtained from Simioni [24] and used in this study, and those found in work by Pohorecki [144].

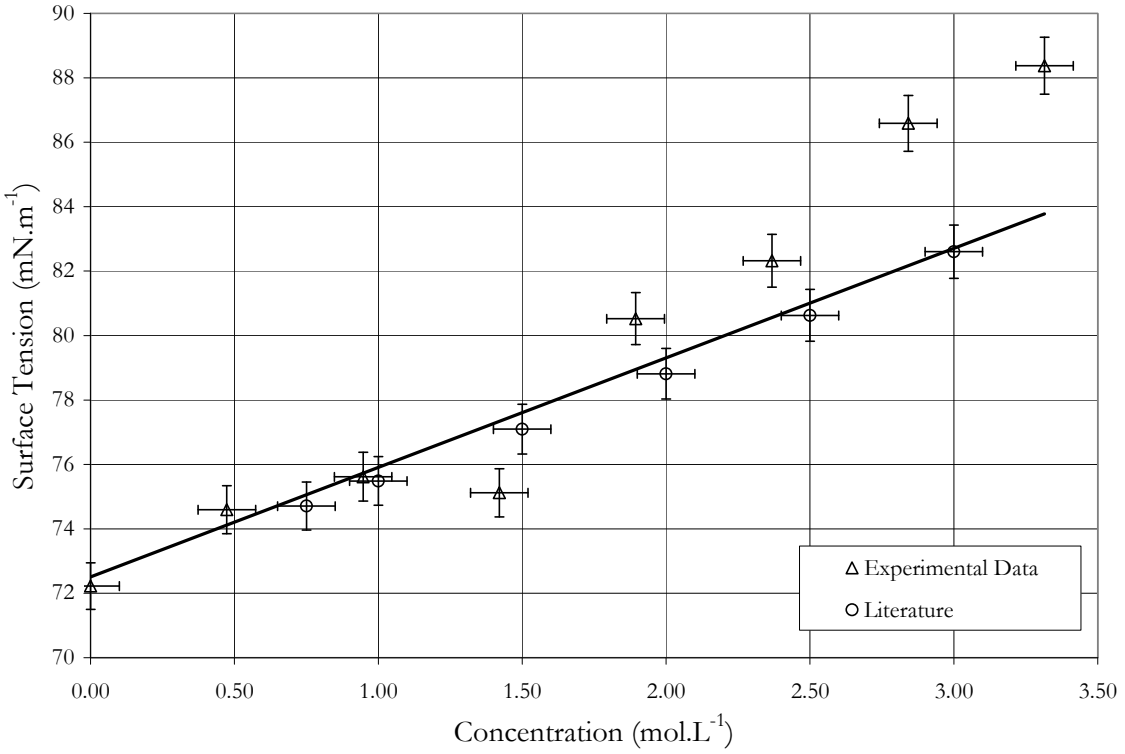

Figure 11-4 A comparison of surface tension of various concentration potassium carbonate solutions at 298 K. Reprinted from Simioni [24] where the literature refers to Pohorecki et al [144].